# METHAMPHETAMINE-INDUCED NEUROTOXICITY IN CULTURED ASTROCYTES

By

Josephine Wing Sze Lau

B.Sc. (Hon.), CUHK

A thesis submitted in partial fulfilment of the requirements for the degree of Master of Philosophy in Anatomy

June 1999

Department of Anatomy

The Chinese University of Hong Kong

Shatin, N.T., Hong Kong

UL


香港中文大學
大學
統系館書圖
0 2 MAR 2000
UNIVERSITY
LIBRARY SYSTEM
THE CHINESE UNIVERSITY OF HONG KONG

# METHAMPHETAMINE-INDUCED NEUROTOXICITY IN CULTURED ASTROCYTES

M.Phil

JOSEPHINE WING SZE, LAU

THE CHINESE UNIVERSITY OF HONG KONG

1999

**TABLE OF CONTENT**

## Acknowledgement

I would like to express my deepest gratitude to my supervisor Dr Alfreda Stadlin, who introduced me into the field of drug abuse. Her sincere and patient guidance and helpful advice offer me insight in my study as well as my life.

I am indebted to Mr Raymond H.Y. Li for his expert advice in computing.

Special thanks should go to Miss H.L. Choi and Mr Gary H.F. Yam for their technical support throughout the year and Ms Jenny Hou.

Last but not least, many thanks should be given to Ms Circle W. Yuen, Ms Carol Y.K. Szeto and Mr J.H. Zhu for their technical and spiritual support.

## Abstract

Methamphetamine (METH) is a common drug of abuse. METH induces the release of dopamine (DA) from presynaptic terminals and causes the decrease in the number of DA transporters (DAT) in human brains. Animal studies showed that chronic use of METH results in long-lasting depletion of DA, serotonin (5-HT) and their uptake sites as well as decreased in tyrosine hydroxylase (TH) activity in the striatum. Although the mechanism of METH-induced neurotoxicity is far from clear, so far, direct evidence showed that toxicity occurred mostly at the DA terminals where degenerating fibres and astrogliosis were observed. However, the reason for this regional selectivity is unknown. At present, it is unclear whether astrogliosis is a consequence of the degenerating dopaminergic terminals or that astrocytes actually act as a mediator of this toxicity. The present study therefore aims to clarify whether METH itself has a direct action on astrocytes, thus establishing a role for astrocytes in METH-induced neurotoxicity.

There are several established hypotheses that explain METH-induced toxicity; they include oxidative stress, metabolic stress and hyperthermia. Since astrocytes have a high content of antioxidants to protect neurons from oxidative stress, and are the main sites of energy metabolism in the CNS, their role in mediating METH-induced toxicity therefore cannot be overlooked.

To achieve this goal, primary astrocyte cultures from the striatum, mesencephalon (dopaminergic area) and cortex (non-dopaminergic area) were used. Cells were treated with 4 mM METH and were examined at different time points during 0 – 48 h treatment. The rationale for examining astrocytes from three different brain regions is to clarify whether astrocytes may be an important element governing the selective vulnerability of the striatum to METH treatment.

After METH treatment, phase contrast photomicrographs were taken to examine if astrogliosis occurred. In order to determine whether METH caused oxidative stress in astrocytes, reactive oxygen species (ROS) as well as nitric oxide (NO) production were examined. This was achieved using the dye '2,7'-dichlorofluorescin diacetate, and Griess reaction respectively. In order to ascertain the level of metabolic stress resulting from METH treatment, mitochondrial membrane potential ($\Delta\Psi m$) and ATP levels were measured using the dual emission dye JC-1 and firefly luciferase assay respectively. Cyclooxygenase-2 (COX-2) and heme-oxygenase-1 (HO-1) protein expression was examined in order to determine the hyperthermic response of astrocytes after METH treatment. Finally, CATH.a-astrocyte cocultures were established to clarify whether astrocytic-neuronal interaction may play a role in the enhancement of neuronal injury.

The present study showed that METH could directly cause astrogliosis in the absence of neurons. There was an increase in ROS level in astrocytes after METH treatment. However, there was a differential response in ROS production with striatal astrocytes showing the earliest and greatest response followed by mesencephalic astrocytes and cortical astrocytes. Moreover, the rate of change in ROS production in the control as well as METH-treated striatal astrocytes was significantly greater when compared to that of mesencephalic and cortical astrocytes. This suggested that striatal astrocytes are more vulnerable to METH-induced oxidative stress.

When ATP content was examined, astrocytes from all 3 regions showed a similar pattern of an initial increase followed by a decrease in ATP content. However, striatal astrocytes resulted in the maximum depletion (39% of control value) in ATP content at 48 h when compared to the astrocytes from the other two regions. When $\Delta\Psi m$ was examined, both striatal and mesencephalic astrocytes showed a decrease in

$\Delta\Psi m$ as early as 8 h post treatment while this decrease was only observed in cortical astrocytes after 12 h METH treatment.

Significant increase in NO level in astrocytes was observed as early as 1 h post-treatment. When aminoguanidine (AG) was added to METH-treated astrocytes, there were significant reductions (40 – 70 %) in NO levels when compared with their respective METH-treated groups. This suggested that NO production in astrocytes may also play a role in METH-induced toxicity. When cells were treated with indomethacin (INDO) alone, there was a time-dependent increase in NO levels from 1 to 48 h treatment. When INDO was added with METH, the increase in NO levels was further enhanced. This suggested that COX-2 mediated prostaglandin (PGs) release may have an inhibitory role in NO production.

When COX-2 protein expression was examined, striatal astrocytes showed a slight increase in COX-2 levels after treatment with AG + METH suggesting that METH-induced NO production may inhibit COX-2 expression. On the other hand, mesencephalic astrocytes showed a 4.2 fold increase in COX-2 expression after treated with INDO + METH suggesting that in this case, NO may participate in a positive feedback mechanism to upregulate COX-2 expression. From this study, it seems that there are regional selective responses in COX-2 expression after METH treatment.

When HO-1 protein levels were examined, it was shown that an induction of HO-1 expression was cortical > mesencephalic > striatal astrocytes. Striatal and mesencephalic astrocytes showed that AG can partially attenuate the increase in HO-1 levels after METH treatment, while no effect was shown for cortical astrocytes. This suggested that NO may mediate the effects of the heme-oxygenase system. When cells were treated with INDO and METH, mesencephalic astrocytes showed a

suppression in HO-1 expression to near control values while striatal and cortical astrocytes only showed a slight attenuation at 24 h post treatment. This suggested that PGs may have a role in stimulating HO-1 expression.

After 4 h METH treatment, CATH.a cells showed a 3 fold increase in the percentage of dead CATH.a cells when compared to the control group. However, when CATH.a cells were co-cultured with astrocytes, the percentage of dead CATH.a cells was further enhanced 0.5 – 1.4 fold when compared with CATH.a cells alone. When CATH.a cells were cocultured with striatal astrocytes, there was a 130 and 86 % increase in dead CATH.a cells at 4 and 48 h METH treatment respectively. However, when CATH.a cells were cocultured with mesencephalic astrocytes, METH treatment also resulted in a further increase (though not significant) in the percentage of dead CATH.a cells. There was no loss of cell viability in astrocytes, as shown by the lack of significant increases in LDH levels, suggesting that the loss of neuronal cell viability is due to astrocyte-neuronal interaction.

The present study showed that there were regional differences in astrocytic response to oxidative and metabolic stress. Striatal astrocytes showed a significant difference in the rate of change in ROS production as well as an early increase in ROS levels after METH treatment. There was also a rapid decrease in ATP content and an early decrease in $\Delta\Psi m$ in striatal astrocytes when compared to mesencephalic and then cortical astrocytes. If striatal astrocytes are more prone to oxidative and metabolic stress, this will make the neuronal environment in the striatum more susceptible to oxidative damage. The present findings showing an increase in the percentage of dead CATH.a cells when cocultured with striatal astrocytes further confirmed this hypothesis.

# 甲基苯丙胺對培養星形膠質細胞的神經毒性作用

甲基苯丙胺(METH)可引起腦紋狀體內多巴胺，5羥色胺及其運載體的耗竭和酪氨酸羥化酶活性的降低，其主要部位作用爲多巴胺神經末梢，可致神經纖維變性及星形細胞膠質化。然而，這種區域選擇性的原因尚不明瞭，而且，星形細胞膠質化究竟是多巴胺神經末梢變性引起的反應性增生，或是星形膠質細胞直接介導了METH的毒性作用也不甚清楚，本研究的目的旨在了解METH對星形膠質細胞是否有直接作用，以闡明星形膠質細胞在METH 神經毒性中所起的作用。

方法：取紋狀體，中腦和大腦皮質進行星形膠質細胞的原代培養，並用4mM METH處理0 - 48小時。應用DCFH-DA和Griess反應液分別測定活性氧化物和一氧化氮的產生以確定METH對星形膠質細胞的氧化損傷；應用染液JC-1和螢火虫熒光素分別測定線粒體膜電位和ATP的量以確定METH引起的代謝損害的程度；測定環氧合酶(COX-2)和血紅素氧合酶(HO-1)蛋白的表達了解METH處理後星形膠質細胞的高溫反應；通過神經元-星形膠質細胞的聯合培養了解兩種細胞的相互作用及星形膠質細胞對神經元損傷的影響。

結果顯示：1，METH在無神經元參與下可直接引起星形細胞膠質化；2，METH可增加星形膠質細胞內活性氧化物的產生，其中以紋狀體的星形膠質細胞內反應最早，增加最明顯；3，METH作用早期可增加星形膠質細胞內ATP水平，後期則下降，其中紋狀體的星形膠質細胞內的減少最爲明顯。METH可降低星形膠質細胞線粒體膜電位，在紋狀體和中腦的星形膠質細胞，其下降出現時間早于大腦皮質。4，METH可明顯增加星形膠質細胞的一氧化氮產生，氨基胍可顯著抑制其增加，而消炎痛可强化其產生。5，氨基胍及METH聯合使用可輕度增加紋狀體星形膠質細胞COX-2之水平；在中腦，消炎痛與METH的聯合應用導致COX-2的表達明顯增加。6，METH可增加星形膠質細胞HO-1的表達，氨基胍可部分抑制其在中腦和紋狀體星形膠質細胞中的表達；而消炎痛可完全抑制中腦星形膠質細胞中HO-1的表達。7，METH可以引起培養神經元細胞死亡，其死亡程度在聯合培養中明顯高於神經元單獨培養。

結論：本研究表明星形膠質細胞對氧化性及代謝性損傷刺激具有區域性差異，紋狀體星形膠質細胞易於受損並繼而造成局部神經元微環境改變及神經元的氧化性損害。

## List of Abbreviations

| | |
|---|---|
| $\Delta\Psi m$ | mitochondrial membrane potential |
| 5-HT | serotonin |
| 7-NI | 7-nitroindazole |
| AG | aminoguanidine |
| AIDS | acquired immunodeficiency syndrome |
| ATP | adenosine triphosphate |
| BBB | blood brain barrier |
| $Ca^{2+}$ | calcium ion |
| CNS | central nervous system |
| Co | cortex |
| $CO_2$ | carbon dioxide |
| COX-2 | cyclooxygenase-2 |
| Cu/Zn | copper/zinc |
| DA | dopamine |
| DAT | dopamine transporter |
| DCF | 2', 7'- dichlorofluorescein |
| $DCFH_2$-DA | 2', 7'-dihydrodichlorofluorescein diacetate |
| DHBA | dihydroxybenzoic acid |
| DMEM/F12 | dulbecco's modified eagle medium: nutrient mixture F-12 |
| DOPAC | dihydroxyphenylacetic acid |
| EAA | excitatory amino acid |
| EDTA | ethylenedinitrilotetraacetic acid |
| EGTA | ethylene glycol-bis(β-aminoethyl ether) |
| eNOS | endothelial nitric oxide synthase |
| FAD | flavin adenine dinucleotide |
| $FADH_2$ | reduced flavin adenine dinucleotide |
| FBS | fetal bovine serum |
| $Fe^{2+}$ | ferrous ion |
| GABA | gamma-aminobutyric acid |
| GFAP | glial fibrillary acidic protein |
| GG | glycylglycine |

| | |
|---|---|
| GLU | glutamate |
| GS | glutamine synthetase |
| GSH | glutathione |
| GSH-Px | glutathione peroxidase |
| GSH-Red | glutathione reductase |
| GSSG | glutathione disulfide |
| $H_2O_2$ | hydrogen peroxide |
| HBSS | Hanks balance salt buffer |
| HO-1 | heme-oxygenase-1 |
| HSP | heat shock protein |
| HVA | homovanillic acid |
| INDO | indomethacin |
| iNOS | inducible nitric oxide synthase |
| $K^+$ | potassium ion |
| L-NAME | $N^w$-nitro-L-arginine methyl ester |
| L-NMMA | $N^G$- monomethyl-L-arginine |
| L-NNA | $^N$G-Nitro-arginine |
| LPS | lipopolysaccharide |
| MAO-B | monoamine oxidase-B |
| Me | mesencephalon |
| METH | methamphetamine |
| MK-801 | dizocilpine |
| Mn | manganese |
| MPTP | 1-methyl-4-phenyl-1,2,3,6-tetrahydropyridine |
| LDH | Lactate dehydrogenase |
| NAD | nicotinamide adenine dinucleotide |
| NADH | reduced nicotinamide adenine dinucleotide |
| NADPH | reduced nicotinamide adenine dinucleotide |
| NaOH | sodium hydroxide |
| NMDA | N-methyl-D-aspartate |
| nNOS | neuronal nitric oxide synthase |
| NO | nitric oxide |
| $NO_2$ | nitrogen dioxide |
| NOS | nitric oxide synthase |

| | |
|---|---|
| $O_2^{\cdot-}$ | superoxide |
| $OH^{\cdot}$ | hydroxyl radicals |
| $ONOO^-$ | peroxynitrite |
| PBS | phosphate buffer saline |
| PCA | perchloric acid |
| $PGE_2$ | prostaglandin $E_2$ |
| $PGG_2$ | prostaglandin $G_2$ |
| $PGH_2$ | prostaglandin $H_2$ |
| $PGI_2$ | prostaglandin $I_2$ |
| $PGJ_2$ | prostaglandin $J_2$ |
| PGs | prostaglandins |
| PUFA | polyunsaturated fatty acid |
| REM | rapid eye movement |
| ROS | reactive oxygen species |
| SNAP | S-nitroso-N-acetylpenicillamine |
| SNP | sodium nitroprusside |
| SOD | superoxide dismutase |
| St | striatum |
| Tg | transgenic mice |
| TH | tyrosine hydroxylase |

# CHAPTER ONE: INTRODUCTION

## 1.1 Methamphetamine

Methamphetamine (METH), is a common drug of abuse. The oral form of METH is known as "speed" or "crystal", and it is usually swallowed or sniffed. The intravenous form of METH is known as "crank", the inhaled form is known as "ice" or "glass", and this is the concentrated form of METH that resembles tiny chunks of translucent glass (Sekine and Nakahara, 1987).

METH is the N-methyl homologue of amphetamine. It is a white, odourless, bitter, crystalline powder that is soluble in water and alcohol. The colour varies, it may be crystalline-white to brown depending on the process used during its manufacturing (MacKenzie and Heischober, 1997). The N-methyl group of METH allows better penetration of the blood-brain barrier. Moreover, when compared with amphetamine, METH has a significantly higher stimulant activity in the central nervous system (CNS) than in the peripheral nervous system and the cardiovascular system (MacKenzie and Heischober, 1997).

### 1.1.1 Historical Background and Epidemiology

The roots of the current epidemic of METH abuse date back centuries. Use of ephedrine was documented in China more than 5,000 years ago, and cathionone was used in East Africa in the 14th century. Both METH and cathionone belong to a class of chemicals called alkaloids, which are among nature's most potent and useful medicines. These drugs were obtained from the plants *Ephedra mahaung* and *Catha edulis*, respectively. Both were recognized for their stimulant, appetite suppressant, and bronchodilation properties.

Edeleau first synthesized amphetamine proper in 1887. In 1932, the synthetic ephedrine analog, amphetamine, was introduced and sold over-the-counter in the form of Benzedrine inhalers. Benzedrine is a type of topical decongestant and the main ingredient, amphetamine, contained in a cotton plug of inhaler, was often ingested directly or the drug was extracted from inhalers and injected. Benzedrine inhalers were abused by a wide segment of the population (e.g., athletes, professionals, and students) during the 1930s to overcome fatigue and to increase alertness (Ansis and Smith, 1979). During World War II, METH was used by soldiers as an aid to fight fatigue and to enhance performance. Millions of doses of amphetamine and METH in the guise of "awakening drugs" were supplied to service personnel during the war. After the war, surplus supplies of these drugs were dumped onto the civilian markets, most notably in Japan resulting in widespread abuse in Japan after World War II (Cho, 1990; Winger et al., 1992). Following the war, Japanese pharmaceutical companies continued to promote the drug, leading to an epidemic of amphetamine abuse in which 5% of all Japanese aged 16 to 25 became physically dependent (Snyder, 1986). The epidemic subsided following the development and passage of an amendment to the Stimulants Control Law. This amendment led to greater enforcement of the law. However, after the latent period from 1957 to 1969, METH abuse again spread rapidly throughout the nation in an epidemic. To cope with this situation, amendments were made to the Stimulants Control Law in 1973 to introduce penal provisions that were equivalent to those of the Narcotics Control Law. Unfortunately, the effectiveness of these amendments in improving the situation was limited (Fukui et al., 1994).

Over the last 50 years, epidemics of METH abuse have occurred in many other parts of the world, including Sweden (Inghe, 1969), the United Kingdom (Kiloh

and Brandon, 1962) and the United States (Kalant, 1966; Kramer et al., 1967; Miller and Hughes, 1994).

In the United States, amphetamine was available in over-the-counter form until 1945. Its popularity has continued among students and truck drivers who want to stay alert, athletes who seek increased endurance, and dieters who actually use it for reducing weight, often in conjunction with sedatives or ethanol (Brecher, 1972; Kalant, 1973; Scarpino et al., 1990; Catlin and Hatton, 1991). Amphetamine began to be used intravenously by American service men in Korea and Japan during the early 1950s. By the 1960s, intravenous abuse of amphetamine and METH were a well-publicized problem in the United States. In 1965, the Federal Drug Abuse Control Amendments further restricted the manufacture and distribution of amphetamine, and supply was shifted to the illicit clandestine "speed labs". Although seemingly overshadowed by the cocaine epidemic of the 1980s, abuse of amphetamine and METH has remained a major drug problem in the United States.

Recently, increased evidence showed that METH abuse is becoming a serious problem in Hong Kong. According to the Central Registry of Drug Abuse 40$^{th}$ report in Hong Kong in 1997, METH abuse at present constitutes only 5.4 % of the approximately 18,000 reported drug abuse cases in 1997. However, this figure is the reflection of an approximately 30 fold increase in the number of reported cases of METH abuse in the last decade with a 10 fold increase in newly reported young abusers (under 21 years old) from 1995 – 1997 alone (Government Information Centre, 1997). In fact, most of the METH is imported from Mainland China (Narcotics Bureau of the Hong Kong Police, 1997) and thus there is a continuous supply of METH and at a relatively low cost. Ephedrine, which is the raw material for METH synthesis, is mainly found in China where many illicit laboratories are

established. All these factors contribute to the increasing number of METH abusers found in Hong Kong.

### 1.1.2 The Physical Effects of METH

METH's biological half-life is about 12 hours and thus its powerful psychic effects can usually last for 1-2 days (Cook et al., 1991) but in some instances, it could last for 12 days (Kramer et al., 1967). The transit time from lung to brain is shorter than from antecubital vein to brain, therefore the rush is more rapid and powerful following inhalation of METH when compared to injection. Every drug used for recreation may be seen as having "desirable" and "undesirable" effects. For METH, these "desirable" effects include the abuser experiencing feelings of euphoria, heightened alertness and greater energy (Caldwell, 1980). At doses resulting in the desired CNS effects, METH causes very few of the undesirable peripheral signs and symptoms (Derlet and Heischober, 1990).

Since METH initially produces physical pleasure, users will therefore often continue to take METH to avoid the "down" mood they experience when the drug wears off. However, after taking METH, a "run" will develop which means the subject stays continuously awake for several hours, since the half-life of METH is about 12 hours (Cook et al., 1991). During this "run", "undesirable" effects will result including increase in heart rate, in breathing and blood pressure rates and heart palpitations may also be experienced. Pupils will become dilated, and reflexes will be faster. The mouth will become dry and swallowing will be difficult. The subject will also experience difficulty in urination (MacKenzie and Heischober, 1997). Marked weight loss will result if "runs" occurs successively. Mental status will also be altered,

including rapid mood changes, being suspicious, being preoccupied with one's thoughts and having a sense of profundity (Brust, 1993).

Acute overdose of METH causes excitement, confusion, headache, chest pain, hypertension, tachycardia, flushing, profuse sweating, and mydriasis, progressing to delirium, hallucinations, hyperpnea, cardiac arrhythmia, hyperpyrexia, seizures, shock, coma, and death (Zalis and Parmley, 1963; Espelin and Done, 1968; Ellinwood and Cohen, 1971; Edison, 1971; Kojima et al., 1984). Long-term METH abuse results in many damaging effects, including addiction. Addiction is a chronic, relapsing disease, characterized by compulsive drug-seeking and drug-use which is accompanied by functional and molecular changes in the brain. Following a "run", the subject, because of tenseness, paranoia, or exhaustion, stops taking the drug and falls asleep for usually 12 to 18 hours, this is known as a "crash". Longer "runs" are followed by more prolonged sleep, sometimes lasting several days. Psychotic symptoms are usually absent on awakening, but there is hunger, lethargy, and depression. Injections are then resumed, and a new "run" begins (Bell, 1965). Psychosis often develops after prolonged use and this type of psychosis is commonly described as closely simulating paranoid schizophrenia. Within a setting of clear consciousness, the individual experiences delusions of persecutions plus visual, tactile and auditory hallucinations and may exhibit repetitious compulsive behavior (Zakhary et al., 1967; Cox et al., 1970). Chronic METH abusers exhibit symptoms that can include violent behavior, anxiety, confusion and insomnia. They can also display a number of psychotic features, including paranoia, auditory hallucinations, mood disturbances, and delusions. The paranoia can result in homicidal as well as suicidal thoughts. Moreover, chronic METH abusers display a variety of physiologic disorders such as malnutrition, skin formications, ulcers and diseases resulting from vitamin

deficiency. Intravenous users are at risk for serious, life-threatening diseases such as AIDS, lung and cardiovascular diseases (Konuma, 1994).

METH produces physiologic dependence with evidence of withdrawal symptoms, drug dependence will often develop a few months after first exposure to METH (Kramer et al., 1967). Withdrawal from prolonged use of METH results in depression, fatigue, increased appetite and sleep, including time spent in the REM phase (Oswald and Thacore, 1963). Withdrawal symptoms are not life threatening, but depression, sometimes suicidal, can last for weeks, requiring hospitalization and treatment (Kramer et al., 1967; Angrist and Gershon, 1972). The psychosis begins to remit when drug use stops. Events that occurred during the psychotic state are usually remembered clearly thereafter (Cox et al., 1970).

### 1.1.3 Neurochemical Alternation of METH

A substantial number of animal studies showed that METH causes damage to the dopaminergic and serotonergic systems, causing long-lasting depletion of dopamine (DA) and serotonin (5-HT) and their uptake sites as well as decrease in tyrosine hydroxylase (TH) activity in the striatum (Fibiger and McGeer, 1971; Kogan et al., 1976; Seiden et al., 1976; Gibb and Kogan, 1979; Hotchkiss and Gibb, 1980a; Steranka and Sanders-Bush, 1980; Wagner et al., 1980; Bakhit and Gibb, 1981; Preston et al., 1985; Kovachich et al., 1989; Brunswick et al., 1992). METH causes an increased release of DA within the striatum (Baldwin et al., 1993; Marshall et al., 1993; O'Dell et al., 1993; Yamada et al., 1994) resulting from the disruption of the electrochemical gradient which provides energy for DA accumulation in synaptic vesicles (Sulzer and Rayport, 1990; Sulzer et al., 1992) and thus causes DA release into the synaptic cleft (Marshall et al., 1993).

Repeated low doses or a single large dose of METH to rat also results in the large decreases in 5-HT levels in several areas of the brain (Hotchkiss and Gibb, 1980a; Hotchkiss and Gibb, 1980b; Wagner et al., 1980; Bakhit and Gibb, 1981; Commins and Seiden, 1986; Seiden et al., 1988) and in a subpopulation of cell bodies in the somatosensory cortex (Commins and Seiden, 1986). Based on measurements of residual levels of 5-HT in many brain areas following METH administration, it appears that the most profound degeneration of serotonergic terminals occurs in the frontal cortex, hippocampus and amygdala (Seiden et al., 1988)

Other than the effects of DA and 5-HT release, repeated administration of high doses of METH in rats reduces neuronal concentrations of DA and 5-HT metabolites as well as the activities of their biosynthetic enzymes, TH (Fibiger and McGeer, 1971; Buening and Gibb, 1974; Kogan et al., 1976; Bakhit and Gibb, 1981) and tryptophan hydroxylase (Hotchkiss and Gibb, 1980b; Bakhit and Gibb, 1981; Peat et al., 1985; Johnson et al., 1988, 1991) respectively.

Although DA terminals in the striatum are sensitive to the toxic effects of METH, DA terminals in other brain areas including the nucleus accumbens are minimally affected by METH (Morgan and Gibb, 1980; Wagner et al., 1980; Seiden et al., 1988). Although METH-induced neurotoxicity within the nucleus accumbens has been reported to occur, a larger dose of METH is usually required to elicit these changes (Wagner et al., 1980; Seiden et al., 1988). Anatomical studies indicated that loss of the presynaptic DA and 5-HT axonal markers observed in METH treatment is related to damage of distal DA and 5-HT axon projections, and therefore in turn related to damage in the dopaminergic and serotonergic terminals (Ellison et al., 1978; Lorez, 1981; Nwanze and Jonsson, 1981; Ricaurte et al., 1982, 1984a, b; Fukui et al., 1989; Axt and Molliver, 1991).

A recent study on human postmortem brains of both drug-free neurologically normal controls and chronic METH users showed that chronic METH exposure does produce a decrease in DA, TH and dopamine transporters (DAT) (Wilson et al., 1996). Another recent study by Villemagne et al., (1998) on baboons showed that the doses of METH used in the study which are the equivalent human recreational doses (26 to 52 mg for an individual weighing 70kg), caused a decrease in striatal DAT density with larger decreases occurring after higher doses of METH. They also reported that reductions in striatal DAT were associated with decreases in DA and the DA metabolite dihydroxyphenylacetic acid (DOPAC). Therefore, these studies indicate that METH, at doses used by humans, produces long-term reductions in brain DA axonal markers in baboons. These results are consistent with those found in animal studies discussed earlier.

## 1.2 Mechanisms of METH Toxicity

### 1.2.1 Oxidative Stress

Free radicals are normal products of cellular aerobic metabolism (Freeman and Crapo, 1982; Halliwell and Gutteridge, 1985; McCord, 1985). A free radical is defined as any species that has one or more unpaired electrons. This definition includes the hydrogen atom (one unpaired electron), most transition metals and the oxygen molecule itself, which is a biradical. Molecular oxygen plays an essential role in a variety of metabolic processes invariably associated with an aerobic existence. Because of its oxidizing capacity, molecular oxygen acts primarily as an electron acceptor, which leads to the formation of a variety of oxygen-based free radicals. Superoxide ($O_2^{\cdot-}$) and hydroxyl ($OH^{\cdot}$) species are the predominant cellular oxygen-based free radicals. Although hydrogen peroxide ($H_2O_2$) itself is not a free radical, it

can yield a molecule of $OH^{\cdot}$ when one electron is being reduced. This $OH^{\cdot}$ is the strongest oxidant produced in biological systems. Together, $O_2^{\cdot-}$, $OH^{\cdot}$ and $H_2O_2$ are referred to as reactive oxygen species (ROS). The major source of ROS are the common metabolic pathways of eukaryotic cells, especially during cellular respiration and to a lesser extent phagocytosis (Chance et al., 1979; Cadenas, 1989). ROS may immediately react with cellular macromolecules and may thereby directly cause damage.

Oxidative stress refers to the cytologic consequences of a mismatch between the production of ROS and the ability of the cell to defend against them. Oxidative stress can thus occur when the production of ROS increases, scavenging of ROS or repair of oxidatively modified macromolecules decreases, or both. This imbalance results in a build-up of oxidatively modified molecules that can cause cellular dysfunction. Every life form had to develop effective defensive systems to be able to deal with the toxic ROS that are constantly produced. For that reason, various antioxidant enzymes are present. They include superoxide dismutase, catalase and glutathione peroxidase, which can detoxify ROS.

In comparison with other organs of the body, the brain may for a number of biochemical, physiological and anatomical reasons, be especially vulnerable to ROS-mediated injury. The brain is an extremely active organ that consumes more than 20% of the total oxygen intake, although it represents only 2% of the biomass. However, it is probably the least protected from ROS. The brain is rich in unsaturated lipids and therefore is more susceptible to lipid peroxidation. ROS attack cell membranes by setting off free radical chain reactions in which free radicals are passed from one macromolecule to another. This free radical chain reaction cascade results in extensive damage to cell membranes and other cellular structures (Gutteridge and

Halliwell, 1990). The brain being a high oxygen consumption organ therefore suffers an increased chance of oxidative stress. In the brain, antioxidants such as superoxide dismutase and catalase, are at a lower concentration than that of other less aerobically active tissues like the heart (Marklund et al., 1982; Bondy and Lebel, 1993). This lower antioxidant value may imply that the brain is more susceptible to oxidative stress than the other organs.

### 1.2.1.1 Superoxide ($O_2^{\cdot-}$) and Superoxide Dismutase (SOD)

$O_2^{\cdot-}$ is mainly produced in biological systems through the one-electron reduction of oxygen. Mitochondria consume about 90% of the body's oxygen and are the richest source of oxygen, in which, about 1-2% of oxygen metabolized by mitochondria is converted to $O_2^{\cdot-}$ at several sites in the mitochondrial respiratory chain (Chance et al., 1979). There are different sites at the respiratory chain in which oxygen may be partially reduced to $O_2^{\cdot-}$. For example, in the ubiquinol-cytochrome c reductase of complex III (Boveris and Chance, 1973; Boveris and Cadenas, 1975; Chance et al., 1979) and, secondarily, in the NADH dehydrogenase of complex I (Turrens and Boveris, 1980). $O_2^{\cdot-}$ that is generated can readily pass through membranes via an anion channel (Fridovich, 1986) and can oxidatively damage cellular components and can give rise to highly reactive products, such as $OH^{\cdot}$ and peroxynitrite anion ($ONOO^-$) (see sections 1.2.1.2 and 1.2.1.4) .

Mitochondria normally contain high levels of antioxidants like SOD to help remove $O_2^{\cdot-}$ (Jesberger and Richardson, 1991). To remove $O_2^{\cdot-}$, SOD metabolizes $O_2^{\cdot-}$ and forms $H_2O_2$ and molecular oxygen (McCord and Fridovich, 1969).

$$2\ O_2^{\cdot-} + 2H^+ \xrightarrow{\text{SOD}} H_2O_2 + O_2$$

There are three distinct forms of SOD in eukaryotic cells responsible for the conversion of $O_2^{\cdot-}$ to $H_2O_2$. These are cytosolic copper/zinc (Cu/Zn) SOD, mitochondrial manganese (Mn) SOD and extracellular SOD, each encoded and regulated independently (Freeman and Crapo, 1982; Fridovich, 1995).

Evidence for a role of $O_2^{\cdot-}$ in METH-induced toxicity was provided by a study in which the inhibition of SOD activity by diethyldithiocarbamate resulted in an increased neurotoxicity (DeVito and Wagner, 1989a). Recent studies also shown that over-expression of (Cu/Zn) SOD in mice can attenuate METH-induced toxicity. These transgenic mice (SOD-Tg) expressing human (Cu/Zn) SOD gene was shown to attenuate the loss of dopamine terminals and the depletion of striatal dopamine and DOPAC caused by METH in a gene dosage-dependent fashion (Cadet et al., 1994a, 1995; Hirata et al., 1996). It was also shown that increased SOD activity in the SOD-Tg mice can also protect against METH-induced neurotoxicity in striatal serontonergic terminals (Hirata et al., 1995). These studies suggested that $O_2^{\cdot-}$ may play a critical role in METH-induced oxidative stress in the striatum in mice.

### 1.2.1.2 Hydrogen Peroxide ($H_2O_2$), Catalase and Glutathione (GSH)

Apart from the dismutation of $O_2^{\cdot-}$ by SOD to form $H_2O_2$ (Freeman and Crapo, 1982), oxidative deamination of dopamine by monoamine oxidase B (MAO-B) or the auto-oxidation of dopamine can also form $H_2O_2$ (Halliwell, 1992; Chiueh et al., 1993).

$$\text{Dopamine} + H_2O + O_2 \xrightarrow{\text{MAO-B}} \text{3,4-dihydroxyphenylacetaldehyde} + NH_3 + H_2O_2$$

To a lesser extent, oxidation of NADH at complex I or $FADH_2$ at complex II can also result in mitochondrial $H_2O_2$ generation. $H_2O_2$, an oxidizing agent, is also a precursor for the highly oxidizing and tissue-damaging free radical, hydroxyl ($OH^{\cdot}$).

Most $H_2O_2$ in the brain is removed by the oxidizing of reduced glutathione (GSH) via the enzyme glutathione peroxidase (GSH-Px) (Sinet et al., 1980; Meister and Anderson, 1983; Beckman et al., 1990). GSH is the primary low-molecular-weight thiol in the cytoplasm and is a major reservoir for cysteine. GSH in conjunction with the reductant NADPH can reduce lipid peroxides, free radicals, and $H_2O_2$. GSH is converted to glutathione disulfide (GSSG) by GSH-Px, which is in turn reconverted back to GSH by glutathione reductase (GSH-Red) in order to maintain a constant amount of cellular GSH.

Catalase, which is found at very low levels in the brain, also removes $H_2O_2$. Since GSH-Px is more abundant than catalase in the brain, catalase probably plays a less important role than GSH-Px in the scavenging of $H_2O_2$ in the CNS (Marklund et al., 1982).

Recently, $H_2O_2$ was also proposed to be one of the mediators of METH-induced toxicity. PC12 rat pheochromocytoma cells over-expressing GSH-Px were shown to diminish the rise in ROS levels and lipid peroxidation resulting from METH treatment (Hom et al., 1997). This evidence further suggests that apart from $O2^{\cdot-}$, $H_2O_2$ formation also plays an important role in METH-induced neurotoxicity.

### 1.2.1.3 Hydroxyl Radicals ($OH^{\cdot}$)

$H_2O_2$ reacts with ferrous ions ($Fe^{2+}$) to form $OH^{\cdot}$ by the Fenton reaction.

$$Fe^{2+} + H_2O_2 \longrightarrow Fe^{3+} + OH^{\cdot} + OH^{-}$$

$OH^{\cdot}$ reacts at great speed with almost every molecule found in living cells. $OH^{\cdot}$ can cause DNA strand breakage and chemical alterations of the deoxyribose, purine and pyrimidine bases (Floyd and Carney, 1992). It is also capable of initiating the process of lipid peroxidation by abstracting a hydrogen atom from a polyunsaturated fatty acid (PUFA) side chain (lipid-H) in membrane lipids leading to the formation of peroxyl radicals. Lipid peroxides within a membrane can also severely disrupt the fluidity of the membrane and allow ions such as $Ca^{2+}$ to leak across the membrane and result in $Ca^{2+}$-dependent cytotoxicity (Borg, 1993). The presence of high amounts of $OH^{\cdot}$ is potentially dangerous to the CNS since the brain has a high content of PUFA.

Previous reports indicated the possibility of measuring free radical generation using salicylate (Grootveld and Halliwell, 1986). Salicylate acts as an exogenous $OH^{\cdot}$ trap in vivo, forming 2,3 and 2,5-dihydroxybenzoic acid (DHBA). Using this method, in vivo measurements of $OH^{\cdot}$ on METH-administrated rats have been reported (Kondo et al., 1994; Giovanni et al., 1995; Wrona et al., 1995; Yang et al., 1997). These studies showed that METH treatment resulted in an increase in the absolute and relative amounts of the 2,5-DHBA present in striatum after peripheral administration of salicylate (Wrona et al., 1995). All these results showed that $OH^{\cdot}$ is also formed in METH-induced neurotoxicity although a detailed mechanism is still far from clear.

#### 1.2.1.4 Nitric Oxide (NO)

NO is a byproduct during the synthesis of L-citrulline from L-arginine by nitric oxide synthase (NOS).

$$\text{L-arginine} \xrightarrow{\text{NOS}} \text{L-citrulline} + \text{NO}$$

At least three isoforms of NOS exist: the constitutively expressed, calcium-dependent form found in neurons (nNOS) (Janssens et al., 1992; Lamas et al., 1992; Sessa et al., 1992) and in endothelial cells (eNOS) (Mayer et al., 1989, 1993; Palmer and Moncada, 1989; Forstermann et al., 1991). An inducible, calcium-independent form, known as iNOS, was found in macrophages (Hevel et al., 1991; Stuehr et al., 1991; Yui et al., 1991), astrocytes (Murphy et al., 1993) and microglia (Boje and Arora, 1992; Chao et al., 1992; Murphy et al., 1993).

NO is an inorganic molecule with many physiological functions(Moncada et al., 1991). In the nervous system, it can regulate local cerebral blood flow and plays essential roles in synaptic plasticity and normal development of the brain (Moncada et al., 1991; Simonian and Coyle, 1996). However, in situations of excessive production, it may become neurotoxic (Dawson et al., 1992). NO itself is a weak oxidizing agent, but it can react with $O_2^{\cdot-}$ at physiological pH which will lead to the formation of peroxynitrite anion ($\check{O}NOO^-$) (Beckman et al., 1990).

$$O_2^{\cdot-} + NO \longrightarrow ONOO^-$$

$ONOO^-$ is an extremely reactive molecule and a powerful oxidant. It is sufficiently stable even in the presence of physiological concentrations of glutathione and other cellular antioxidants. $ONOO^-$ can oxidize some important intracellular targets e.g. thiols and zinc finger (Radi et al., 1991), as well as cause DNA breakage, cellular energy depletion and activate poly-ADP-ribose synthetase (Salgo et al., 1995; Szabo et al., 1996). $ONOO^-$ can also decompose to form cytotoxic $OH^{\cdot}$ and nitrogen dioxide ($NO_2$) spontaneously, which are potent activators of lipid peroxidation (Beckman et al., 1990; Radi et al., 1991; Crow et al., 1994).

$$ONOO^- + H+ \longleftrightarrow HOONO \longrightarrow HO^{\cdot} + NO_2$$

Furthermore, NO has been shown to inhibit the function of mitochondrial respiratory chain and disrupt normal cellular iron homeostasis (Reif and Simmons, 1990; Bolanos et al., 1994).

NO has recently been shown to be involved in METH-induced neurotoxicity. Bowyer et al., (1995) using in vivo microdialysis in rats, showed that NO generation in the caudate/putamen may augment the release of dopamine during METH exposure. In primary cultures of fetal rat mesencephalon, it was shown that the blockade of NO formation with several NOS blockers attenuated METH-mediated neurotoxicity (Sheng et al., 1996). Treatment of 7-nitroindazole (7-NI), which is a selective nNOS inhibitor, provided full protection against the depletion of dopamine and its metabolites and the loss of DAT binding sites (Itzhak and Ali, 1996). Moreover, Di Monte et al., (1996), using an in vivo mouse model, demonstrated that treatment of mice with 7-NI almost completely counteracted the loss of DA, DOPAC, and TH immunoreactivity. These results indicated that NO formation is an important step leading to METH neurotoxicity, and suggested that the cytotoxic properties of NO may be directly involved in dopaminergic terminal damage. Recently, Itzhak et al. (1998) demonstrated that by using the nNOS deficient mice, METH administration affected neither the tissue content of DA and its metabolites nor the number of DAT binding sites. Taken together, these results indicated that nNOS deficient mice are protected against METH-induced dopaminergic neurotoxicity, and further proved NO formation is a critical step in leading to METH-induced neurotoxicity.

On the other hand, Abekawa et al., (1996) showed that the co-administration of METH with $N^{w}$-nitro-L-arginine methyl ester (L-NAME), a NOS inhibitor, reduced METH-induced decreases in DA, DOPAC and homovanillic acid (HVA) content in the striatum. However, L-NAME did not reduce METH-induced decreases

in content of 5-HT in the striatum, nucleus accumbens and medial frontal cortex. This dose-related neuroprotective effect of L-NAME on dopaminergic toxicity in the striatum suggests that NO production may be related to dopaminergic damage. Although the detailed mechanisms by which NO-mediates METH neurotoxicity are not yet defined, evidence so far suggests that, apart from ROS formation, NO-mediated oxidative stress may also play an important role.

### 1.2.2 Apoptosis

There are two modes of cell death generally referred to as "necrosis" and "apoptosis". Necrotic cell death is characterized by an initial loss of plasma membrane integrity associated with cell swelling, followed by late nuclear degeneration. DNA is degraded in a random fashion, which is visualized as a continuous smear on agarose gel electrophoresis. On the other hand, apoptosis, also termed "programmed cell death" is typically associated with early chromatin condensation and nuclear disruption, followed by a later loss of plasma membrane integrity. DNA degradation is highly uniform, revealed by a laddering pattern consisting of fragments that differ in size by 180 to 200 base pair on agarose gel electrophoresis (Stern, 1995). Apoptosis is believed to play a crucial role in the differentiation and organization of the developing nervous system. Despite the identification of several regulatory mechanisms of the process, the biochemical events underlying apoptosis remain largely unknown.

Bcl2 and p53 have been shown to be involved extensively in the process of apoptotic cell death. Bcl-2 is a proto-oncogene which was first identified at the chromosomal breakpoint t (14;18) in B cell lymphomas (Tsujimoto et al., 1984). Bcl-2 was shown to promote cell survival (Nunez et al., 1990), block apoptosis

(Hockenbery et al., 1990, 1993) and prevent cellular damage caused by oxidative stress (Hockenbery et al., 1993; Kane et al., 1993). On the contrary, p53 is a tumor suppressor gene whose activation has been associated with apoptosis (Clarke et al., 1993; Lowe et al., 1993; Hermeking and Eick, 1994; Morgenbesser et al., 1994; Wagner et al., 1994). It is widely believed that p53 accumulates when DNA is damaged and arrests the cell cycle at G1 phase to allow extra time for repair. However, if the repair process fails, p53 triggers apoptosis (Lane, 1992).

Recent studies have led to the speculation that apoptosis also plays a role in METH-induced toxicity. It was reported that using immortalized neural cells obtained from rat mesencephalon, METH exposure can cause DNA strand breaks, chromatin condensation, nuclear fragmentation, and DNA laddering. This phenomenon of METH-induced apoptotic cell death can be prevented by the over-expression of bcl-2 in these cells (Cadet et al., 1997). Furthermore, Hirata and Cadet (1997) using homozygous and heterozygous p53 knockout mice showed that METH treatment caused significant decreases in DAT mRNA and the number of TH-positive cells in both the substantia nigra pars compacta and the ventral tegmental area of wild-type but not the homozygous p53-knockout mice. They also found that there was an increase in p53-like immunoreactivity in the striata of wild type mice but not in the homozygous p53 knockout mice further supporting the mechanism of neuronal cell death via apoptosis in METH-induced neurotoxicity. However, it is still unknown whether the METH-mediated neuronal apoptotic cell death observed is a consequence or otherwise of oxidative stress.

### 1.2.3 Excitotoxicity

Glutamate (GLU), is an excitatory amino acid (EAA) and neurotransmitter that is present in the brain at a high concentration and a leading endogenous toxin (Watkins and Evans, 1981; Fonnum, 1984). GLU is capable of exciting CNS neurons to such an extent as to become toxic, ultimately killing GLU-sensitive neurons through over-excitation. Olney in the early 1970s (Olney, 1969, 1978) introduced the concept and the term 'excitotoxicity' and he suggested that EAA can kill neurons in the CNS by prolonged, receptor-mediated depolarization, ultimately resulting in irreversible disturbance in ion homeostasis and other lethal sequelae (Olney, 1978, 1994; Goldberg et al., 1987; Mayer and Westbrook, 1987; Rothman and Olney, 1987, 1995; Choi and Rothman, 1990; Shaw, 1994).

Using intracerebral microdialysis, Nash and Yamamoto (1992) showed an increase in striatal GLU release after repeated administration of METH to rats. EAA and their receptors also appear to play a role in METH-induced GLU neurotoxicity, because treatment with competitive (NPC 12626 or CGS 19755) or non-competitive (MK-801, phencyclidine, or ketamine) antagonists of the N-methyl-D-aspartate (NMDA) class of EAA receptor can prevent METH-induced striatal DA depletions and reductions of TH activity in mice (Sonsalla et al., 1989, 1991). Ohmori et al. (1996) showed that METH treatment did not increase GLU release in the nucleus accumbens, a region where no dopaminergic damage was observed. These findings suggest that striatal DA neurotoxicity is mediated, in part, by an increase in extracellular concentration of GLU. It may be that enhanced release in GLU and DA worked synergistically in presynaptic DA terminals to cause the METH-induced striatal dopaminergic neurotoxicity.

### 1.2.4 Mitochondrial Dysfunction

Mitochondria are traditionally described as the "power plants" of the cell. Mitochondrial size, shape and number varies widely amongst the different cell types. Each mitochondrion has an outer membrane that is freely permeable to large molecules and an inner membrane that is relatively impermeable and contains the electron transport enzyme complexes. The inner compartment of the mitochondrion, enclosed by the inner membrane, is the matrix in which the Krebs cycle takes place. NADH and $FADH_2$ generated from the Krebs cycle act as electron donors to the series of transport enzymes of the inner mitochondrial membrane (Beal et al., 1993). Concomitantly, ejection of protons across the inner mitochondrial membrane results in an electrochemical proton gradient, which stores potential energy. Oxidative phosphorylation is the process by which the transfer of reducing equivalents (electrons) to oxygen is coupled to the synthesis of ATP by ATP synthase. The electron transport chain consists of a complex array of enzymes. They are assigned as complexes I, II, III and IV (Wallace, 1992). They catalyze the transport of electrons to molecular oxygen and thereby create an electrochemical proton motive force, whereas the complex V uses this force to form ATP from ADP and inorganic phosphate. Complex I (NADH dehydrogenase, consisting of > 30 polypeptides) oxidizes NADH. Complex II (succinate dehydrogenase, built from 4 polypeptides) receives electrons from succinate and subsequently donates them to ubiquinone to form ubiquinol. This small, lipid-soluble and mobile compound then reduces complex III (ubiquinol:cytochrome c oxidoreductase, consisting of 10 polypeptides), from where the electrons flow via cytochrome c to complex IV (cytochrome oxidase, comprising 13 polypeptides). There, most of the molecular oxygen consumed by mitochondria during respiration is reduced with four electrons to water without the liberation of partially reduced oxygen species. The protons that are expelled during electron

transport over complex I - IV from the mitochondrial matrix into the intermembrane space flow back into the matrix via complex V (ATPase, formed by 12 polypeptides). Since ATP is required for most of the cellular reactions, any means of interference with this process will greatly affect normal cellular function and may finally cause cell death.

Mitochondria are known to have a proton electrochemical gradient generated by proton pumps which is in turn driven by respiratory electron transport chains utilizing NADH and succinate (Mitchell, 1979). According to Mitchell (1966), energy stored in this gradient is primarily responsible for the conversion of ADP + $P_i$ to ATP by ATPase. This gradient has two components: the electric component (the mitochondrial membrane potential, $\Delta\Psi m$) and the chemical component (the pH gradient). In order to support a high rate of ATP synthesis, mitochondria must maintain a relatively high electrochemical gradient. Although both $\Delta\Psi m$ and pH gradient drive the synthesis of ATP, each is involved in additional biochemical events. For example, the uptake of pyruvate and GLU by mitochondria is proportional to the pH gradient, whereas the import of mitochondrial enzymes from the cytoplasm, the uptake of calcium, and the maintenance of mitochondrial protein synthesis are dependent upon $\Delta\Psi m$. Therefore, adequate ATP production is reliant on a steady $\Delta\Psi m$ and pH gradient.

The effects of METH on brain energy metabolism were first studied in the early 1960s and 1970s (Lewis and Van Petten, 1962; Nahorski and Rogers, 1973; Sylvia et al., 1977) but the results were conflicting due to the change in the levels of high-energy phosphate compounds which were only measured in either the cerebral cortex or the whole brain after METH injection. Chan et al. (1994) was the first to demonstrate that during METH-induced depletion of striatal DA, there was a

significant and rapid decrease in striatal ATP concentrations. Furthermore, the ATP-depleting effects of METH appeared to be selective because they were observed only in the striatum and not in the cerebellar cortex and hippocampus. Moreover, Chan et al. (1994) also showed that 2-deoxyglucose, an inhibitor of glucose metabolism, significantly potentiated both METH-induced striatal DA depletion and ATP loss. Together with an earlier report showing an association between the METH-induced early increase in the regional cerebral glucose consumption and long-lasting dopaminergic neurotoxicity (Pontieri et al., 1990), Chan et al. (1994) suggested a correlation between METH-induced perturbations of energy metabolism and dopaminergic neurotoxicity. It was suggested that one possible mechanism is that METH directly inhibits the mitochondrial respiratory chain, thus reducing cellular energy production. Alternatively, the ATP depletion observed could be a consequence of "metabolic stress" caused by METH on dopaminergic neurons. However, the precise sequence of events that result in dopaminergic terminal damage and its association with metabolic stress is still far from clear. Furthermore, since there was evidence of oxidative stress contributing to this injury, the relationship between metabolic stress and oxidative stress also needs further clarification.

### 1.2.5 Hyperthermia

Homeotherms generally resist cold better than heat. Heat is one of the best known stressors to mankind. A variety of disorders can elevate body temperature; those resulting from thermoregulatory failure are properly called hyperthermia. Body temperature increases when the rate of heat production exceeds the rate of heat dissipation. Hyperthermia occurs when thermoregulatory mechanisms are overwhelmed by excessive metabolic production of heat, excessive environmental

heat, or impaired heat dissipation. Hyperthermia is the most severe illness caused by high ambient temperature to the human population and is the third largest killer in the world after cardiovascular diseases and traumatic injuries to the CNS (Ellis, 1972; Sminia et al., 1994; Ellis and Wendon, 1996).

Many METH abusers have been reported to die as a result of hyperthermia with body temperature reaching over 41°C (Clark et al., 1967; Zalis et al., 1967; Kojima et al., 1984; Imanishi et al., 1997). However, the mechanism underlying hyperthermia induced by METH is still unknown.

Animals studies also showed that METH treatment produced hyperthermia in rats (Bowyer et al., 1995; Fleckenstein, 1997; Eisch and Marshall, 1998; Fukumura et al., 1998) and in mice (Funahashi et al., 1990; Ali et al., 1994a; Miller and O'Callaghan, 1994, 1995; O'Callaghan and Miller, 1994; Kuperman et al., 1997; Itzhak et al., 1998; Makisumi et al., 1998; Sonsalla et al., 1998; Yu et al., 1999).

Several studies have documented a relationship between METH-induced hyperthermia and neurotoxicity. It was demonstrated that an increase in ambient temperature increased METH-induced neurotoxicity while a decrease in the ambient temperature reduced METH neurotoxicity (Bowyer et al., 1992; Ali et al., 1994b; Miller and O'Callaghan, 1994). Furthermore, several pharmacological agents were shown to attenuate METH-induced neurotoxicity. It was shown that the administration of DA receptor antagonists fenfluramine, dizocilpine, alpha-methyl-p-tyrosine, phenytoin, aminooxyacetic acid and propranol prevented METH-induced hyperthermic effects (Albers and Sonsalla, 1995). Moreover, concurrent treatment of METH and pharmacological agents such as haloperidol (Bowyer et al., 1994), diazepam (Bowyer et al., 1994) and MK801 (Bowyer et al., 1994; Miller and O'Callaghan, 1994) reduced METH induced striatal DA depletion to a degree

predicted by their inhibition of hyperthermia. Melatonin, which is a natural hormone produced by the pineal gland and was recently suggested to act also as free radical scavenger and antioxidant (Reiter et al., 1997), was also shown to significantly diminish METH-induced hyperthermia (Itzhak et al., 1998). Moreover, pretreatment with ibogaine, which is a naturally occurring alkaloid derived from the root of the African shrub *Tabernanthe iboga*, can completely block METH-induced hyperthermia (Yu et al., 1999). These results demonstrated that hyperthermia may also be part of a complex array of mechanisms that are responsible for METH-induced neurotoxicity.

In association with this, the involvement of inducible enzymes, cyclooxygenase-2 (COX-2) (see review, Rothwell, 1992; Herschman, 1996) and heme oxygenase-1 (HO-1) (see review, Ewing and Maines, 1991; Choi and Alam, 1996) had been shown to be involved in the process of hyperthermia.

### 1.2.5.1 Cyclooxygenase-2 (COX-2)

Cyclooxygenase (COX) is a rate-limiting enzyme catalyzing the synthesis of prostaglandins (PGs) from arachidonic acid (Smith et al., 1989). PGs in humans are the predominant prostanoid detected in inflammatory conditions ranging from experimental acute edema and hyperthermia to chronic arthritis and certain neurological disorders (see review, Herschman, 1996). Since inflammation is one of the conditions in which PGs is a major product of COX activity, it is entirely conceivable that the inflammatory process itself directs the enzymatic pathway towards the generation of PGs.

COX is an integral membrane protein that sits within the inner leaflet of the lipid bilayer of the plasma membrane. It has 2 enzymatic functions: a cyclooxygenase

activity that converts arachidonic acid to prostaglandin $G_2$ ($PGG_2$) and a peroxidase activity that converts $PGG_2$ to prostaglandin $H_2$ ($PGH_2$). Moreover, COX has putative heme binding regions where the iron heme-mediated peroxidase activity take place (Smith et al., 1996). There are 2 known COX isoforms, COX-1 and COX-2. Both isoforms are similar in amino-acid sequence and enzymatic functions although they have distinct physiological and pathological roles.

COX-1 is constitutively expressed and is responsible for the physiologic production of PGs. It plays an important role in maintaining normal vascular, gastric, renal and hemostatic functions. Therefore, it is considered to play physiological roles rather than pathological ones (Goppelt-Struebe, 1995). This constitutive isoform can be found in nearly all cell types at a constant level (Vane et al., 1998).

The second isoform is COX-2, a highly inducible enzyme which is under the strict regulation of different cytokines (Nam et al., 1995), mitogen (Kujubu et al., 1991), ROS (Gunasekar et al., 1998), endotoxins (Minghetti et al., 1997) and hyperthermia (Okamoto et al., 1997). It is responsible for the increased production of PGs during inflammation (Feng et al., 1995; Porreca et al., 1996; Cao et al., 1997). In the CNS, COX-2 expression has been reported in astrocytes (O'Banion et al., 1996), microglia (Trocino et al., 1995) and neurons (Yamagata et al., 1993). Previous studies have shown that cultured astrocytes are capable of PGs synthesis and release (Seregi et al., 1987; Murphy et al., 1988; Marriott et al., 1991; Brenner et al., 1992; Boneh et al., 1993; Wilkin and Marriott, 1993; Nam et al., 1995). A comparison on the abilities of cultured astrocytes and neurons to synthesize PGs led to the suggestion that astrocytes might be the synthetically more active compartment in vivo (Keller et al., 1985; Bruner and Simmons, 1993). In distinction to peripheral tissues, COX-2 is

expressed at relatively high levels in normal brain (Yamagata et al., 1993; Breder et al., 1995; Kaufmann et al., 1996).

The best known role of PGs in the CNS is in hyperthermia, where prostaglandin $E_2$ ($PGE_2$) is an extremely potent pyretic agent in eliciting fever (Milton and Wendlandt, 1970). Pyrogens such as interleukin-1 are thought to act via hypothalamic release of PGs (Bernheim et al., 1980; Coceani et al., 1988).

It was shown that indomethacin (INDO), a COX inhibitor (Asano et al., 1989), was able to ameliorate hyperthermia-induced brain edema, extravasation of plasma protein, and neuronal and glial damage (Sharma et al., 1994). These results suggest that PGs are involved in the development of pathological changes associated with hyperthermia. Other than hyperthermia, PGs may also be key molecules in other pathological conditions of the CNS. For example, the release of PGs was sharply increased during brain ischemia / reperfusion or in traumatic injuries to the CNS (Bazan et al., 1995). Furthermore, treatment with COX-2 inhibitors were shown to attenuate hyperthermia-, glutamate- and ischemia-induced neuronal injury (Sasaki et al., 1988; Sharma et al., 1995; Beasley et al., 1998; Hara et al., 1998). Therefore, the production of PGs seems to play a key role in the development of pathological changes in CNS injuries.

#### 1.2.5.2 Heme-oxygenase-1 (HO-1)

The term "heat shock protein" (HSP) was derived from the fact that these proteins were initially discovered to be induced by hyperthermic conditions (Anathan et al., 1986; Welch, 1992; Craig and White, 1993). HSP response is a universal response of all prokaryotic and eukaryotic species when subjected to noxious stressful situations (Hightower, 1980; Anathan et al., 1986; Barbe et al., 1988; Kaufmann,

1992; Welch, 1992). Members of the HSP family have several features in common, such as, i) they are preferentially expressed following hyperthermia; ii) they are found in all living cells; iii) their amino sequences are highly conserved throughout evolution; and iv) they have a specific DNA motif (heat shock element) in the promoter region of their genes which is activated by specific heat shock transcription factor known as heat shock factor (Sarge and Morimoto, 1991; Sorger, 1991; Sarge et al., 1993; Prehn et al., 1994).

Most cells within the normal CNS express constitutive forms of HSP (Brown and Rush, 1990; Birnbaum et al., 1991). Moreover, increasing evidence suggests that HSP may play an important role during nervous system development and this was demonstrated in both the drosophila and mammalian systems (Walsh et al., 1989, 1993; Pauli et al., 1990; Chopp, 1993; Marin et al., 1993). The patterns of HSP mRNA and protein expression during the ontogeny of vertebrate and invertebrate nervous systems suggest that HSP have important functions in regulation of cell cycles, cellular differentiation, and cell maintenance at critical stages of organ development. However, HSP expression has also been used as a marker to define the extent of injury caused by particular experimental or natural disease processes. Several different families of HSP proteins are seen in areas of abnormal tissue. Expression of HSP in several experimental systems were used to define regions of hyperthermia (Brown and Rush, 1990; Marini et al., 1990; Harrison et al., 1993; Higashi et al., 1994), ischemia (Vass et al., 1988; Brown and Rush, 1990; Ferriero et al., 1990; Chopp, 1993; Higashi et al., 1994), and trauma (Brown and Rush, 1990; Xue and Grossfeld, 1993). Expression of HSP in affected cells frequently occurred in the absence of other anatomic changes, suggesting that HSP expression may be a sensitive marker of cell injury. The functions of HSP in the injured nervous system

are not clear but they have been suggested to play a protective role during injury (Lowenstein et al., 1991; Mailhos et al., 1993).

Heme-oxygenase-1 (HO-1) is a 32 kDa HSP (HSP32). The HO-1 gene has a heat shock element in its promotor region (Maines, 1988; Keyse and Tyrrell, 1989) (Donati et al., 1990; Applegate et al., 1991). It is also the rate-limiting enzyme which converts heme to bilirubin, releasing $Fe^{2+}$ and carbon monoxide (CO) (Maines, 1988, 1996). Although described as a marker of oxidative stress (Prehn et al., 1994; Westman and Sharma, 1999), HO-1 can be induced by numerous stressors including hyperthermia (Ewing and Maines, 1991) exposure to heavy metals (Applegate et al., 1991), and NO (Kim et al., 1996; Takahashi et al., 1996).

Total HO-1 activity in the brain is high and comparable to that in the spleen (Maines, 1988). Dwyer et al., (1995) suggested that the high level of HO-1 activity in the brain, an organ not actively involved in red blood cell degradation and hemoglobin disposition vis a vis the spleen, suggests that this enzyme is of physiological importance in the CNS. In pathological conditions, HO-1 had been shown to be expressed in the brains of some neurodegenerative disorders such as Alzheimer's and Parkinson's diseases (Schipper et al., 1995, 1998).

Kuperman et al., (1997) showed that a single injection of METH resulted in a biphasic induction of HSP-72 and that this induction can be blocked by ibogaine (Yu et al., 1999). This study illustrated that the induction of HSP is associated with METH-induced toxicity.

### 1.2.5.3 The Effects of Nitric Oxide (NO) on COX-2 and HO-1 Expressions

It was recently reported that excessive NO production is associated with heat stroke in patients, and the magnitude of NO production is proportional to the severity

of the illness (Alzeer et al., 1999). It was suggested that NO maybe an important mediator and integral part of the pathophysiological process resulting in heat stroke.

Previous studies on thermal injury have shown that NO is increased in a post-burn state in humans (Preiser et al., 1996) and heat-stressed rats (Hall et al., 1994; Carter et al., 1994; Canini et al., 1997). Although the exact mechanism of NO induction in heatstroke has not been entirely defined, increased NO formation from iNOS under the action of various proinflammatory cytokines has been described (Moncada and Higgs, 1991). Proinflammatory cytokines have been reported to be released in large amounts in heatstroke patients (Bouchama et al., 1991). Furthermore, thermal injury to rats also showed an increase in NO production (Carter et al., 1994).

Recently, Sharma et al., (1997) reported that heat-stress induced a marked up-regulation of nNOS in the cerebral cortex and hippocampus. An increase in nNOS immunoreactivity was found to be in distorted neurons located in the edematous regions where it was normally nNOS-negative. This suggested that hyperthermia can induce up-regulation of nNOS activity in the brain of hyperthermic rats. It had been suggested that hyperthermia-induction of NOS up-regulation may be due to the formation of free radicals (Hall et al., 1994; Goode et al., 1995). Other than nNOS upregulation, one would expect there should be also an upregulation of iNOS that can be highly induced during hyperthermic conditions. Indeed, several groups were able to demonstrate using selective nNOS inhibitors like 7-NI (Di Monte et al., 1996), and the non-selective NOS inhibitor like L-NAME (Abekawa et al., 1996), can also attenuate METH-induced hyperthermia and toxicity. Further to this, Itzhak et al., (1996, 1998) demonstrated that nNOS knockout mice were resistant to METH-induced hyperthermia and toxicity. Recently it was shown that iNOS knock out mice were also resistant to METH-induced hyperthermia (Ali and Itzhak, 1998). These

results indicated that NO formation in both neuronal and glial cells is an important step associated with METH-induced hyperthermia.

Cross talk between NO and COX is extensively documented and it was shown that COX-2 activity can be stimulated or inhibited by NO (see review, Appleton et al., 1996; Di Rosa et al., 1996; Salvemini and Masferrer, 1996). Recently, it was shown that hypoxia induced an increase in NO release and iNOS activity, this increase was accompanied by the sustained release of $PGE_2$ (Mollace et al., 1997). This effect was antagonized by COX inhibitor INDO and partially by L-NAME suggesting that NO may play a role in PGs release.

A recent study showed that the induction of HO-1 protein in astrocytes was mediated by endogenous NO production through the activation of iNOS (Takahashi et al., 1996; Kitamura et al., 1998) raising the possibility that the CO/HO system may function in concert with the NO/NOS system in the brain. Moreover, some authors also speculated that NOS upregulation is accompanied by HO-1 expression in order to counterbalance the harmful effects of NO (Vincent et al., 1994).

## 1.3 Astrocytes

### 1.3.1 Characteristics of Astrocytes

Neuroglia form about half the volume of the human brain. They are divided into two categories: macroglia and microglia. Macroglia are composed of astrocytes and oligodendrocytes. Astrocytes are the most abundant cell type in the CNS (Kuffler et al., 1984). The ratio of astrocytes to neurons in the CNS is about 10:1 (Pope, 1978). They are derived from the neuroectoderm of the neural tube. They are star-shaped cells and their processes radiate from the perikaryon and can often be traced as far as the walls of blood vessels or to the subpial surface of the CNS (Pannese, 1994).

Morphologically, astrocytes can be classified into 2 types: protoplasmic and fibrous. Fibrous astrocytes occur mainly in the white matter, and have 10-30 long, thin, smooth-surfaced, poorly branched processes. In contrast, the protoplasmic astrocytes occur mainly in the gray matter. They exhibit many processes, with respect to fibrous astrocytes, their processes are more numerous, thicker, shorter, and more extensively branched and have an irregular surface. It should be noted that protoplasmic astrocytes can transform into fibrous form following injury (Pannese, 1994). Various biochemical markers can be used to identify astrocytes. For example, glial fibrillary acidic protein (GFAP), are subunits of glial-specific intermediate filaments (Eng et al., 1971; Dahl and Bignami, 1973; Bignami and Dahl, 1974) and is an astrocyte marker commonly used for both in vivo and in vitro studies. Other than GFAP, the enriched S-100 (Hyden and McEwen, 1966; Hansson et al., 1980) and glutamine synthetase (GS) (Martinez-Hernandez et al., 1977; Hallermayer et al., 1981) are also markers for astrocytes.

### 1.3.2 Astrocyte Functions

Astrocytes have previously been assigned the passive role of protecting and supporting neurons (Barres, 1991). However, with the increase in biochemical and physiological knowledge of astrocytes, and given their close relation with neurons, astrocytes have been shown to participate more actively in the process of neuroprotection and neurodegeneration than previously thought.

Biochemically, astrocytes regulate the concentration of extracellular potassium ($K^+$) (Hounsgaard and Nicholson, 1983; Walz, 1989), GLU (Schousboe, 1981; Schousboe et al., 1993), GABA (Larsson et al., 1986) and other biogenic amines (Pelton et al., 1981; Kimelberg and Pelton, 1983; Semenoff and Kimelberg, 1985).

Furthermore, astrocytes contain GS (Martinez-Hernandez et al., 1977), an enzyme which converts GLU to glutamine using ammonia and ATP, via a high-affinity uptake system (Hertz, 1979). This represents an important mechanism for ammonia and GLU detoxification in the brain (Sugiyama et al., 1989).

Physically, the end feet of astrocytes are a major component that contributes to the formation of the blood-brain barrier (BBB), by inducing the formation of tight junctions between endothelial cells (Janzer and Raff, 1987). The BBB serves to maintain a stable microenvironment in the CNS by restricting and regulating the passage of different substances between the blood vessels and the cerebral interstitial space (Cancilla et al., 1993).

Astrocytes are the major sites of energy metabolism in the CNS (Hamprecht and Dringen, 1995). Glycogen, a storage form of glucose, is mainly found in astrocytes (Cataldo and Broadwell, 1986a; Cataldo and Broadwell, 1986b). The breakdown of glycogen can be induced by hormones such as noradrenaline. Astrocytes have also been shown to metabolize the medium chain fatty acids like octanoic acids to ketone bodies, which are the dominant energy resources of the brain when undergoing starvation (Geiger, 1958). Moreover, the cytosolic form of malic enzyme appears to be prominent in astrocytes. Malic enzymes can convert the Kreb's cycle intermediate malate to pyruvate, which can then be used locally or transported to other cells for energy production. It appears that astrocytes can function as a processing plant, forming energy rich compounds such as fatty acids and amino acids for the utilization of neighbouring cells (Magistretti, 1988; Dringen and Hamprecht, 1992).

Astrocytes have been demonstrated to possess receptors for neurotransmitters such as GLU (Backus et al., 1989; Cull-Candy and Wyllie, 1991; Matute et al., 1994)

GABA (Hosli and Hosli, 1990; Fraser et al., 1994; Bureau et al., 1995) and serotonin (Hosli and Hosli, 1987; Whitaker-Azmitia et al., 1990). They are also believed to participate in immunological responses in the CNS (Fontana and Fierz, 1985; Fontana et al., 1986; Prochiantz and Mallat, 1988). Certain experiments have shown that astrocytes may perform immunological functions in vitro; more precisely, they are able to present antigens to T-lymphocytes. Moreover, astrocytes are believed to participate in the establishment of neuronal circuits (Denis-Donini et al., 1984).

Astrocytes are known to contain MAO-B (Levitt et al., 1982) which is the major enzyme responsible for the degradation of DA in the CNS (Gaal and Hermecz, 1993). Furthermore, astrocytes contain a large amount of antioxidants such as GSH, Cu/Zn-SOD, Mn-SOD and catalase (Hirsch, 1992). Therefore, astrocytes have an important role to play in the defense mechanism against oxidative stress in the CNS.

Astrocytes are not structurally independent cells but rather are organized into a syncytium that is mediated by gap junctions (Kettenmann et al., 1983). These junctions are vital for intercellular communication and cellular homeostasis. Thus, one can conceptualize the potential for an enormous recruitment of astrocytes in response to physiologic or pathological stimuli.

pH regulation in the nervous system is an essential homeostatic function. Significant effects of pH on astrocytes are the closure of the intercellular gap junctions (Bennett et al., 1991), which are the likely molecular basis of the astrocyte syncytium. Other more general effects will be the change of pH on enzyme activities and ion channels. It has been shown that the control of pH in the mammalian CNS is independent of that of the systemic pH (Katzman and Pappius, 1973). Among their other homeostatic functions, astrocytes may also play a key role in such pH regulation. In agreement with this, significant pH changes have been shown recently

in mammalian astroglial cells during intense neuronal activity that paralleled opposite changes in extracellular pH (Chesler and Kraig, 1987, 1989; Chesler, 1990).

Furthermore, astrocytes are not morphologically static as their shape can be transformed during neuronal injury (Hatten, 1985), change in neurotransmitter levels (Cornell-Bell et al., 1990) or various physiologic states (Hatton, 1990). During CNS injury, one of the most characteristic astrocytic responses is termed 'reactive astrogliosis' (gliosis, reactive gliosis or astrocytosis). Reactive astrogliosis can occur either adjacent to the site of injury or it can extend far beyond it. It is characterized by astrocyte proliferation and extensive hypertrophy of the cell body and cytoplasmic processes (Eng and Ghirnikar, 1994). Activated, reactive astrocytes exhibit cytological, biochemical and histological transformations which include increases in nuclear diameter, elevated DNA levels, heightened oxidoreductive enzymes activity, and increased synthesis of GFAP, vimentin, GS and glycogen (Eng and Shiurba, 1988). Moreover, ultrastructural studies have shown that there is an increase in the numbers of mitochondria, Golgi complexes, endoplasmic reticulum, lysosomes, vesicles, microtubules, dense bodies and lipofuscin pigment in reactive astrocytes. The most striking finding is the presence of bundles of intermediate filaments like GFAP and vimentin, which at times appear to fill the entire cytoplasmic compartment (Nathaniel and Nathaniel, 1981). However, the biochemical events that precede and trigger astrocyte activation are unknown.

Reactive astrogliosis is thought to play a role in the healing phase following CNS injury by actively monitoring and controlling the molecular and ionic contents of the extracellular space of the CNS. These important extracellular constituents that may be regulated by reactive astrocytes include potassium ions, neurotransmitters, trophic factors, nutrients and metabolic waste products (Kimelberg and Ransom,

1986; Reier, 1986; Walicke et al., 1986). In contrast to a role in healing CNS injury, astrogliosis may produce pathological effects by interfering with the function of residual neuronal circuits, by preventing remyelination, or by inhibiting axonal regeneration (Reier et al., 1983; Reier, 1986).

### 1.3.3 The Role of Astrocytes in METH-induced Neurotoxicity

Previous studies have shown the presence of reactive astrogliosis in the striatum of METH-treated mice and rats in vivo (Hess et al., 1990; Pu and Vorhees, 1993, 1995; Pu et al., 1994; Broening et al., 1997) and in vitro (Sheng et al., 1994; Stadlin et al., 1998). Since reactive astrogliosis is often associated with neuronal damage (Eng, 1988; O'Callaghan, 1991), a close relationship between METH-induced degeneration of dopaminergic terminals in the striatum and reactive astrogliosis may also exist.

Astrocytes are situated in a key position between the microvessels and the other cell types like neurons and oligodendrocytes. Glucose and oxygen, which are the most important substrates for the generation of energy, must pass through the astrocytes to reach their metabolic destination in the neurons and oligodendrocytes. Therefore, this strategic location of astrocytes in the CNS may play a balancing role in controlling energy metabolism of the brain. In fact, one may speculate that astrocytes are probably more resistant to METH than neurons since astrocytes have an alternative pathway of energy production. 1-methyl-4-phenyl-1,2,3,6-tetrahydropyridine (MPTP) is a compound which is used as a Parkinson's disease model and was shown to damage both the dopaminergic terminals and cell bodies. In MPTP-induced toxicity in astrocytes, Di Monte et al. (1992) showed that an increase in consumption of glucose and lactate production, with a glucose/lactate ratio of

1.85:1 was an early event suggesting that glycogenolysis had taken place, leading to the anaerobic formation of ATP. Astrocytes can utilize the accumulated energy reservoir, glycogen (Guth and Watson, 1968; Cataldo and Broadwell, 1986a), in conditions of energy crisis. Alternative mechanisms explaining the increased resistance of astrocytes may lie in the adaptive mechanisms available to astrocytes in response to adverse conditions. Activated glycogenolysis in astrocytes after MPTP treatment suggested that there was an energy demand during cytotoxicity (Magistretti et al., 1986). It is unclear whether glycogenolysis occurs during METH-induced neurotoxicity, investigation into the energy status of astrocytes during METH treatment will further clarify this phenomenon.

The repeated continuous administration of a higher dose of METH to mice has been shown to produce a degenerative change in nigral dopaminergic neurons and their axon terminals (Sonsalla et al., 1989), which is related to an increase in extracellular concentration of GLU (Abekawa et al., 1994). Since METH-mediated toxicity has been implicated to be related to an increased release of GLU and/or an increased sensitivity of NMDA receptors to GLU, the effects of METH-induced neurotoxicity may depend on the ability of astrocytes to remove the extracellular GLU. Astrocytes contain GS (Martinez-Hernandez et al., 1977) which converts GLU to glutamine via a high-affinity uptake system (Hertz, 1979), therefore they may have a protective role against METH-induced excitotoxic injury. Low GS levels in astrocytes can result in the insufficient removal of extracellular GLU and therefore will lead to the activation of NMDA receptors on neurons, or increase in neuronal intracellular $Ca^{2+}$ thus resulting in neuronal cell death. Stadlin et al (Stadlin et al., 1998) reported that, after METH administration, a rapid decline in GS was observed in striatal as well as mesencephalic astrocytes. Astrocytes in the dopaminergic areas

may be more susceptible to METH-induced toxicity due to their inability to remove excess GLU. This reduced detoxification capability of striatal astrocytes will further increase the vulnerability of surrounding neuronal terminals to METH-induced injuries. Increased extracellular amount of GLU as well as depleted astrocytic GS content in the striatum may account for the regional selectivity in METH injuries. However, the precise sequence of events is still far from clear.

Astrocytes also contain relatively high concentrations of GSH and GSH-Px when compared to neurons (Slivka et al., 1987; Raps et al., 1989). The presence of high GSH levels in these cells suggested that astrocytes are the major site for $H_2O_2$ detoxification in the CNS and thus protecting them as well as neighbouring neurons from oxidative-induced injury. Neurons that lack GSH must therefore rely on nearby astrocytes to offer protection against $H_2O_2$-induced toxicity. Studies showed that the generation of ROS is one of the mechanisms of METH neurotoxicity (Seiden and Vosmer, 1984; Wagner et al., 1985; DeVito and Wagner, 1989b; Cadet et al., 1994b; Cubells et al., 1994; Giovanni et al., 1995). Astrocytes therefore may play an important role in protecting the neurons against oxidative stress. However, the role of astrocytes in METH-induced oxidative stress has yet to be elucidated.

It has been shown that when astrocytes become reactive, the number of mitochondria (see review, Norenberg, 1994) and the glycogen content (see review, Haymaker et al., 1970) are increased. This modification may imply that the astrocytes are well prepared to generate more energy for the combating of injury. Since it was shown that METH causes astrogliosis in vivo (Hess et al., 1990;Pu and Vorhees, 1993, 1995; Pu et al., 1994; Broening et al., 1997) and in vitro (Sheng et al., 1994; Stadlin et al., 1998), this may reflect an increase in energy demands by the astrocytes to compensate for the ATP loss (Chan et al., 1994) caused by METH. However, how

astrocytes react to METH-induced ROS production and subsequent neuronal injury awaits further elucidation.

Cervós-Navarro et al., (1998) demonstrated that the GFAP immunoreactivity was remarkably increased in animals subjected to a 4 h heat stress at 38°C. This staining was more intense in brain stem (pons, medulla), cerebellum, thalamus and hypothalamus, striatum and parts of the hippocampus. Moreover, selective upregulation of vimentin expression was also observed. This study clearly demonstrated that astrocytes are also involved in the pathological mechanisms of hyperthermic brain injury. Since altered expressions of GFAP and vimentin were both observed in cultured astrocytes after METH treatment (Stadlin et al., 1998), it could therefore be speculated that astrocytes may also participate in mediating the METH-induced hyperthermic response.

## 1.4 Aim of Project

Although evidence so far has shown that oxidative stress, GLU excitotoxicity and metabolic stress participate in METH-induced neurotoxicity, the mechanism and the sequence of events whereby such neurotoxicity occurs is still far from clear. It was demonstrated that METH has deleterious effects on the dopaminergic (Fibiger and McGeer, 1971; Buening and Gibb, 1974; Wagner et al., 1980; Ricaurte et al., 1982; Seiden et al., 1988) and serotonergic system (Hotchkiss and Gibb, 1980a, b; Wagner et al., 1980; Bakhit et al., 1981; Commins and Seiden, 1986; Seiden et al., 1988) in the mammalian brain. Evidence so far showed that the dopaminergic terminals at the striatum are most severely affected with pronounced DA depletion in the striatum (Seiden et al., 1975, 1988; Ellison et al., 1978; Wagner et al., 1980; Finnegan et al., 1982; Preston et al., 1985). It remains unclear why dopaminergic terminals are more

vulnerable to METH-induced metabolic and oxidative stress. Apart from dopaminergic terminal damage, prominent astrogliosis was also observed in the striatum (Hess et al., 1990; Pu and Vorhees, 1993, 1995; Pu et al., 1994; Broening et al., 1997) suggesting that astrocytes may also play a role in this toxicity. Astrocytes are the main sites of energy metabolism and GLU removal in the CNS and therefore play an important role in maintaining a balanced microenvironment. Furthermore, astrocytes also contain a large amount of antioxidants in the CNS, thus protecting the neurons from oxidative stress. Given the important functional role of astrocytes in the CNS, their role in mediating METH-induced oxidative and metabolic stress therefore cannot be overlooked.

At present, it is unclear whether astrogliosis is a result of the degenerating dopaminergic terminals or a mediator of this event. Although O'Callaghan and Miller (1994) speculated that this astrocytic response is a consequence of the degenerating dopaminergic terminals, there is no direct evidence to date to suggest that this is the case. The aim of the project is therefore to clarify the role of astrocytes in contributing to METH-induced neurotoxicity.

To achieve this goal, astrocytes were cultured from the cortex (with the removal of frontal cortex), striatum and ventral mesencephalon of neonatal C57/BL6 mice and then treated with 4 mM METH and examined at different time points during 48 h of treatment. Striatum was selected because this is the region where the dopaminergic axon terminals are situated. Ventral mesencephalon is the location of the dopaminergic cell bodies and the cortex was selected to serve as a non-dopaminergic control. The rationale for examining astrocytes from three different brain regions is to clarify whether astrocytes may be an important element governing the selective vulnerability of the striatum to METH treatment.

In order to establish the sublethal dosage of METH, a dose dependent study was conducted. Different doses of METH was dissolved in the culture medium and added to the cultured astrocytes for 48 h. The effects of METH on cell viability was then assessed using the lactate dehydrogenase (LDH) assay. A dose response curve was constructed to establish the LD50 and the appropriate concentration that was below the LD50 was chosen.

METH-induced astrogliosis was observed using phase contrast photomicroscopy. Since it was reported that METH caused ATP depletion in the rat striatum in vivo (Chan et al., 1994), it was pertinent to examine whether astrocytes contribute to the energy depletion observed in vivo. ATP content of astrocytes from striatum, mesencephalon and cortex was therefore measured in order to ascertain the effects of METH on astrocytic energy status. To further assess metabolic changes resulting from METH treatment, mitochondrial function measured as change of $\Delta\Psi m$ levels in living astrocytes was examined using a J-aggregate-forming dye, 5,5',6,6'—tetrachloro-1,1',3,3'-tetraethylbenzimidazolylcarbocyanine iodide (JC-1, Molecular Probes, Inc. USA).

It has been shown that oxidative stress plays an important role in mediating METH-induced toxicity. Since astrocytes contain a large amount of antioxidants, it is pertinent also to study whether astrocytes participate, and to what extent, in the generation of ROS after METH treatment. To achieve this goal, the level of ROS production in the cultured astrocytes was measured using the non-fluorescent probe 2',7'-dihydrodichlorofluorescein diacetate ($DCFH_2$-DA). $DCFH_2$-DA readily crosses cell membrane and is hydrolyzed by intracellular esterase to form 2',7'-dichlorofluorescin (DCFH), which is another non-fluorescent species. In the presence of ROS, DCFH will be oxidized to highly fluorescent 2',7'-dichlorofluorescein (DCF)

and can be detected spectrofluorometrically. $DCFH_2$-DA was shown to mainly detect $H_2O_2$ production (LeBel et al., 1992; Hockberger et al., 1996). NO has also been shown to be involved in METH-induced oxidative stress due to its reaction with $O_2^{\cdot-}$ to form the powerful oxidant $ONOO^-$ (see Section 1.2.1.4). The astrocytic production of NO after METH-treatment was examined. Extracellular nitrite and nitrate levels, an index of NO generated, were measured by the Griess reaction. The selective iNOS inhibitor, aminoguanidine (AG), was added to confirm whether astrocytic NO production was due to iNOS activation.

METH treatment induces hyperthermia (see Section 1.2.5). At present, it is unclear that whether astrocytes are also involved in the mediation of METH-induced hyperthermia. To investigate whether the presence of PGs would alter METH-mediated NO production, COX-2 inhibitor indomethacin (INDO) (Asano et al., 1989) was used. Moreover, the METH-induced COX-2 and HO-1 protein expression were also examined using Western blot analysis. Astrocytes were further treated with AG and INDO to examine whether inhibiting iNOS and COX-2 respectively can block the alternation of COX-2 and HO-1 protein expression.

After establishing the effects of METH on astrocytic energy metabolism and ROS production, a co-culture system was employed to further establish whether this change in astrocytic function is responsible for mediating neuronal cell death. In METH-induced neurotoxicity, it is still unclear whether the astrocytes or the neurons take an initiative role in causing oxidative stress. To clarify this astrocytic-neuronal interaction, neurons was first cultured alone and treated with METH in order to establish a baseline for comparison. Due to the difficulties in obtaining a pure DA neuronal culture, a catecholaminergic cell line was used. The use of a homogeneous

population of neuronal cells would enable a clear elucidation of how astrocytes may contribute to METH-induced neuronal toxicity.

CATH.a is a catecholaminergic cell line (kindly provided by Dr D.M. Chikaraishi, Duke University Medical Center, USA) that synthesizes abundant DA and norephinephrine and expresses TH, dopamine β-hydroxylase and DAT. It exhibits neuronal properties such as neurofilaments and synaptophysin but lack glial intermediate filaments. This cell line was derived from TH-positive tumors in transgenic mice carrying the SV40 T antigen oncogene under the transcriptional control of 773 base pairs of 5' flanking sequences from the rat TH gene (Suri et al., 1993; Lazaroff et al., 1996). Mesencephalic, striatal and cortical astrocytes were cocultured with CATH.a cells for 1 day and then harvested at 4, 24, 48 h after METH treatment in order to examine the percentage of dead CATH.a cells. Neuronal cell death was then examined using a Live/Dead cell kit (Molecular Probe, USA). Pure CATH.a cells were also treated with the same dose and time point of METH to act as a comparison with the results obtained from CATH.a-astrocyte cocultures. These results not only enable us to ascertain the role of astrocytes in mediating METH-induced toxicity, but also to further clarify the astrocytic-neuronal interaction associated with this injury process.

# CHAPTER TWO: MATERIALS AND METHODS

## 2.1 Cell Cultures

### 2.1.1 Astrocyte Cultures

Astrocytes were cultured from newborn C57 BL/6 mice provided by the animal house of the Chinese University of Hong Kong. All the procedures were done in strict sterile conditions. Animals were killed by decapitation and their heads were rinsed immediately with 70% alcohol. Cerebral cortices (without frontal cortices), striatum and ventral mesencephalon were isolated and minced in cold sterile $Ca^{2+}$ and $Mg^{2+}$ free Hanks balanced salt solution (HBSS, supplemented with 15mM HEPES and 0.35g sodium bicarbonate in 1L, pH 7.4, Gibco). The tissues were dissociated in 0.125% trypsin solution (1:1 vol./vol. of 0.25% trypsin solution: HBSS) for 10 min at 37°C. The trypsinization process was terminated by the addition of an equal volume of serum-containing medium. The mixture was centrifuged at 1800rpm for 5 min, resuspended and mechanically dissociated with an 18.5 gauge needle. The mixture was further dissociated through 70 μm pore size sterile nylon Nitex mesh (Spectrum Medical Industries Inc.). Cell viability was estimated using trypan blue (Sigma) and the total number of cells were calculated on a haemocytometer. The mixture was diluted to give a seeding density of 1 x $10^7$ cells per 75$cm^2$ poly-L-lysine-coated culture flask (Falcon, Becton Dickinson and Company). After seeding, the cells were kept in a humidified incubator at 5% CO2 / 95% air, 37°C. The culture medium was changed after 3 days of seeding and thereafter, it was changed twice a week. The culture medium was composed of Dulbecco's modified Eagle's medium containing Ham's nutrient mixture F-12 (DMEM/F12, Gibco), supplemented with 10% heat inactivated fetal bovine serum (FBS, Gibco), 1.2g sodium bicarbonate, 1% penicillin

(1000unit/ml, Gibco) and 1% streptomycin (1000ug/ml, Gibco). When the cells became confluent after 10-14 days of incubation, non-astrocytic cells were removed by shaking at 260rpm for 18-20 h at 37°C (Lab-Line Orbit Environ-shaker). After shaking, the non-adherent cells were removed and the intact cells were rinsed twice with HBSS. The cultures contained over 95% astrocytes on the basis of staining for glial fibrillary acidic protein (GFAP) (results not shown).

Prior to the biochemical assays, subcultures were obtained first by trypsinizing the astrocytes with 6ml of 0.05% trypsin and EDTA for 10 min. Serum-containing medium was then added to stop the reaction. Astrocytes were then centrifuged, resuspended in serum-containing medium and viability obtained. The cells were then diluted to give a seeding density of 4 x $10^5$ cells per 35mm poly-L-lysine-coated culture dish (Corning, USA) and further cultured for another 3 days.

### 2.1.2 CATH.a Cell line and Astrocytes Co-cultures

CATH.a cells were grown in medium containing RPMI 1640 supplemented with 8 % horse serum (Gibco), 4 % FBS (Gibco), 1% penicillin (1000unit/ml, Gibco) and 1% streptomycin (1000µg/ml, Gibco). The cells were passaged twice a week using 0.25% trypsin without EDTA (Gibco). CATH.a cells of 20-40 passages were used in this experiment.

To establish the CATH.a–astrocyte cocultures, astrocytes were first subcultured onto poly-L-lysine-coated 13mm-diameter round glass coverslips placed onto a 24-well plate (1 x $10^5$ cells per well; Nunclon™, Nunc) and grown for 5 days in DM/F12 medium with 10% FBS. Then the CATH.a cells were seeded on top with a seeding density of 3.2 x $10^4$ per well and were grown in 1 ml of RPMI 1640 medium supplemented with 8 % horse serum and 4 % FBS for another 1 day. CATH.a cell

lines and CATH.a-astrocyte cocultures were all cultured in this condition for 1 day prior to 4 mM METH treatment. Cells were harvested at 4, 24 and 48 h after METH treatment. Cells cultured in medium only was used as controls.

## 2.1 Treatment

### 2.2.1 METH Treatment

Astrocytes obtained from cortex, mesencephalon and striatum were initially treated with 0, 0.5, 1, 2, 3, 4, 6mM METH for 48 h to establish the LD50 for METH on astrocytes. Results showed that the LD50 for METH on astrocytes was 6mM (results not shown), therefore in the present study, a sub-lethal dose of 4mM METH was used.

At time intervals of 0, 4, 8, 12, 24, 48 h of METH treatment, cells were collected for biochemical assays. The culture media was collected for either lactate dehydrogenase (LDH) assay to assess cell viability or for nitrite and nitrate measurements.

For the CATH.a-astrocyte cocultures, 4 mM METH was dissolved in 4% FBS and 2% horse serum in RPMI 1640 medium.

### 2.2.2 Inhibition of Cyclooxygenase-2 (COX-2) and Inducible Nitric Oxide Synthase (iNOS)

300 μM of aminoguanidine (AG), the iNOS inhibitor, was added together with 4 mM METH in serum free DM/F12 medium to determine whether the blocking of iNOS was able to attenuate METH-induced NO formation (Section 2.7). At the same time, COX-2 and HO-1 protein expression was also examined by Western blot analysis and the addition of AG was to determine whether the blocking of iNOS-

stimulated NO release could suppress or enhance the activation of these 2 inducible enzymes after METH treatment (Section 2.8.1).

Similarly, 10 μM indomethacin (INDO) was added together with 4 mM METH in serum free DM/F12 medium to examine whether the blocking of COX-2 activity can attenuate or enhance METH-induced NO production. Similarly, in examining COX-2 and HO-1 protein expression using Western blot analysis, the addition of INDO was used to determine whether the blocking of COX-2 activity will suppress or enhance the activity of COX-2 and HO-1 expression after METH treatment. (Section 2.8.1).

## 2.3 Lactate Dehydrogenase (LDH) Assay

The cytotoxicity of METH on astrocytes was determined from the release of LDH into the culture medium. LDH is released when the cells undergo increased activities of glycolysis due to the failure of mitochondrial ATP formation. The measurement of the LDH activity was carried out according to the method of Amador et al. (Amador E et al., 1963). The principle of the assay is based on LDH catalyzing the oxidation of lactate to pyruvate with simultaneous reduction of nicotinamide adenine dinucleotide (NAD) and is shown as follows:

$$\text{Lactate} + \text{NAD} \xrightarrow{\text{LDH}} \text{Pyruvate} + \text{NADH} + \text{H}^+$$

The formation of the reduced nicotinamide adenine dinucleotide (NADH) results in an increase in absorbance at 340nm which is directly proportional to LDH activity in the sample. At 0, 4, 8, 12, 24, 48 h after METH treatment, the culture media were collected, and 50 μl of medium from each sample were mixed with 1 ml pre-warmed (30°C) LD-L reagent (Sigma Diagnostics, LDH-L 50 kit; Sigma, USA)

The reaction was left to stand for 30 seconds and the initial reading was recorded spectrophotometrically (Beckman DU-7500) at 340 nm at 30°C. The reaction mixture was further incubated for 60 seconds and the final reading was recorded. The change of absorbance (ΔA) per minute (Δ/min) was obtained by subtracting the initial reading from the final reading. The determination of the LDH activity (U/L) is according to the following equation:

$$\text{LDH Activity (U/L)} = \frac{\Delta A \text{ per min} \times \text{total reaction volume} \times 1000}{6.22 \times \text{sample volume} \times \text{light path}}$$

where "ΔA per min" represent the change in absorbance per minute at 340 nm; total reaction volume is equal to 1.05 ml; sample volume is 0.05ml; coefficient of extinction of NADH is 6.22; light path is 1cm; and 1000 is the factor to convert units per ml to units per liter.

$$\text{LDH Activity (U/L)} = \frac{\Delta A \text{ per min} \times 1.05 \times 1000}{6.22 \times 0.05}$$

One unit of LDH activity is defined as the amount of enzyme that will catalyze the formation of 1 μmol of NADH per minute under the conditions of the assay procedure.

LDH released into the culture medium was assayed as an index for astrocytic viability during the 48 h METH treatment. For each time point studied, media from 3 dishes were obtained. Three independent experiments were performed for the entire study.

## 2.4 Assay for Reactive Oxygen Species (ROS) Formation

ROS was measured according to LeBel and Bondy (LeBel and Bondy, 1990) using the non-fluorescent probe '2,7'-dichlorofluorescin diacetate (DCFH-DA, Molecular Probes Inc. USA). DCFH-DA readily crosses cell membranes and is hydrolyzed by intracellular esterase to form non-fluorescent 2',7'-dichlorofluorescin (DCFH). In the presence of ROS, DCFH will be oxidized to the highly fluorescent 2',7'-dichlorofluorescein (DCF).

To perform this assay, astrocytes were subcultured onto poly-L-lysine-coated 24-well plates (Nunclon™, Nunc) at a seeding density of 1 x $10^5$ cells per well. At 0, 4, 8, 12, 24, 48 h of METH treatment, the culture media were removed and cells gently washed once with phosphate buffer saline (PBS, pH 7.4). The cells were then incubated in 480 µl 40 mM Tris buffer (Sigma, pH 7.4) with the addition of 20 µl of DCFH-DA (2.5 mg/ml; final concentration = 10 µg/ml) in methanol and incubated for 15 min at 37°C. The same volume of methanol (without DCFH-DA) was added to another cell sample to correct for autofluorescence generated by the cells. The correction for autofluorescence was less than 10% of the total. Fluorescence was then measured with a fluorescent spectrophotometer (excitation at 488 nm, emission at 525 nm, 37°C; Cytofluor 2350, Millipore). The reading was expressed as DCF fluorescence per dish. Six independent experiments were performed for each time point, and for each treatment and control group.

To determine the rate of change of ROS production in astrocytes during METH treatment, a similar experiment was performed but with some minor modifications. Cultured medium was removed and the cells were gently washed twice with PBS. The cells were then incubated in 480 µl 40 mM Tris buffer with the addition of 20 µl of DCFH-DA (2.5 mg/ml; final concentration = 10µg/ml) in methanol and incubated for 15 min at 37°C. The same volume of methanol without

DCFH-DA was added to correct for autofluorescence generated by the cells. Cell sample measurement of DCF commenced after 15 min of DCFH-DA pre-incubation (t=0). At this time point, 50 µl of 44 mM METH (4 mM final concentration) was added in 40 mM Tris buffer. The same volume of 40 mM Tris buffer was added for the control. Fluorescence was monitored every 15 min for both the METH-treated and control samples for 120 min. Trypan blue (0.2%) was added at t=120 to ascertain cell viability. Since the astrocytes were incubated only in Tris buffer during the course of this experiment, it was not possible to measure the ROS formation beyond 120 min without affecting the viability of the cells, therefore DCF fluorescence was not measured beyond 120 min treatment. Four independent experiments were performed for each treatment and control group.

## 2.5 Assay for Adenosine Triphosphate (ATP) Content

The firefly luciferase assay (Lemasters and Hackenbrock, 1979) was used to measure the ATP content in astrocytes. Crude extract of firefly luciferase (E) contains luciferin ($LH_2$) which in presence of ATP can undergo a luminescence reaction based on the following luciferase-catalyzed reactions:

$$E + LH_2 + ATP \xleftrightarrow{Mg^{2+}} E\cdot\ LH_2AMP + PPi \qquad (1)$$

$$E\cdot\ LH_2AMP + O_2 \longrightarrow E + CO_2 + AMP + \text{oxyluciferin} + \text{light} \qquad (2)$$

The initial activation step, Reaction (1), is the formation of enzyme-bound luciferyl adenylate ($E\cdot\ LH_2AMP$) and pyrophosphate ($PP_i$) from $LH_2$ and ATP. Reaction (1) is reversible and requires a divalent cation such as $Mg^{2+}$. The luciferyl adenylate-enzyme complex then reacts irreversibly with molecular oxygen [Reaction

(2)] to produce AMP, $CO_2$ and oxyluciferin, and a concomitant emission of light which can be captured by a luminometer.

At 4, 8, 12, 24 and 48 h incubation with 4mM METH, culture media were removed and cells were washed twice with PBS (pH 7.4). The astrocytes were then scraped off in 1 ml 5% perchloric acid (PCA) with a rubber policeman and transferred to individual eppendorf tubes. The tubes were centrifuged and 20 µl of the supernatant was mixed with 505 µl 5% PCA. 188 µl 2N NaOH was added to neutralise PCA. 20µl of the mixture was again taken from the final solution to mix with 180 µl glycylglycine (GG) buffer (75 mM glycylglycine + 15 mM $MgCl_2$, pH 7.8). 10ml of GG buffer was added to each vial to dissolve the crude extract of firefly luciferase (Sigma). 200 µl of the enzyme solution was then added to each control and METH-treated tubes and the luminescence was recorded by the luminometer (AutoLumat LB953, Berthold). The ATP content for each sample was calculated from the standard curves, which was constructed by reading the luminescence of different concentrations of ATP (0, 50, 100, 150, 250 and 500 pmol). Since ATP is hydrolyzed during the course of measurement, a correction factor for the standard was obtained by measuring the absorbance of 0.05 mM ATP with the spectrophotometer at 254 nm. This absorbance of the standard was then divided by 15.4 (extinction coefficient for ATP) and multiply by 200 (to give final concentration of 10 mM). The ATP content of each sample was read from the standard curve constructed. The control group consists of astrocytes without METH treatment and was designated as 0 h. The experiment was repeated 5 times for each time point studied.

## 2.6 Determination of Mitochondrial Membrane Potential ($\Delta\Psi m$)

JC-1 is a ratiometric, dual emission fluorescent dye that reflects changes in $\Delta\Psi m$ in living cells. JC-1 forms J-aggregates that is a de-localized lipophilic cation with positive charges and is taken up by mitochondria in accordance to the Nernst equation, without the complication of pH and ionic strength. JC-1 has 2 emission wavelengths, 527 nm (green) for the monomer form and 590 nm (red) for the J-aggregate form. The red fluorescence is only predominant when $\Delta\Psi m$ is high and during cell injury when there is a decrease in $\Delta\Psi m$, there will be an increase in green fluorescence. The examination of red and green fluorescent signals will reflect how the $\Delta\Psi m$ was being affected under METH-induced metabolic stress.

Astrocytes were subcultured onto poly-L-lysine-coated 25mm-diameter round glass coverslips (VWR Scientific) and grown for 5 days in DMEM/F12 medium (with 10% FBS) prior to the determination of $\Delta\Psi m$. After the cells were treated with 1ml of 4 mM METH in serum free DMEM/F12 medium for 0, 4, 8, 12, 24 and 48 h, they were washed briefly with pre-warmed HBSS and incubated with JC-1 at 10 µg/ml in HBSS at room temperature for 20 min. The cells were subsequently washed twice with dye-free HBSS and then mounted onto a living cell chamber (Autofluor® Cell Chamber, Molecular Probes) containing HBSS. The results were captured with a BIO-RAD MRC 1024 laser confocal scanner (BIO-RAD Corp., Hercules, CA) on a Zeiss Axiophot inverted microscope (Zeiss, Germany). A Nikon 63x oil immersion objective was used and the optimal optical signals were obtained by averaging 8 – 10 successive scans using Kalman filtering. The 488 nm argon ion laser and fluorescence emissions at 522 ± 30 nm and 585 nm for peak fluorescence for the monomer (527 nm) and J-aggregate (590 nm) of JC-1 respectively was used. The results were analyzed using the Confocal Assistant 4.2 (BIO-RAD).

## 2.7 Determination of Nitrite Levels in Cultured Astrocytes

Nitric oxide (NO) will degrade rapidly (half-life ~ 5 seconds) (Dawson and Snyder, 1994) to form nitrite ($NO_2^-$) and nitrate ($NO_3^-$) when reacting with oxygen (Schmidt and Kelm, 1996). NO activity was therefore indirectly measured by the accumulation of $NO_2^-$ in the culture medium from 1 - 48 h after METH treatment. The supernatant of the astrocyte cultures were collected and the total level of $NO_2^-$ was determined spectrophotometrically using the Griess reaction according to Schmidt et al (Schmidt and Kelm, 1996). Prior to this, $NO_3^-$ was first reduced to $NO_2^-$ by nitrate reductase (0.1 unit/ml; Boehringer Mannheim). Firstly, the supernatant was centrifuged at 1000 x g for 15 min at room temperature to remove residual cells and debris. All subsequent steps were done in red polypropylene tubes to protect against light-sensitive nitrate reductase. $NO_3^-$ was reduced stoichiometrically to $NO_2^-$ by incubating 150 µl of sample aliquots for 15 min at 37°C in the presence of 0.1 U/ml nitrate reductase, 50 µM NADPH, and 5 µM FAD in a final volume of 160 µl. When nitrate reduction is completed, NADPH was then oxidized with 10 U/ml lactate reductase dehydrogenase (raised from rabbit muscle; Boehringer Mannheim) and 10 mM sodium pyruvate to avoid interference with $NO_2^-$ determination. Samples were incubated for 5 min at 37°C in a final volume of 170 µl.

When nitrate reduction was complete, samples were cooled down to 4°C. 1 mM sulfanilamide and then 0.1 M HCl was added to a final volume of 200 µl (diazotization). This was followed by centrifuging samples at 1000 x g for 15 min at 4°C. An aliquot of 150 µl of each supernatant fraction was transferred to 96-well microtiter plates, and were read at 540 nm using a microplate reader (Nunc 269620). From the absorbance of each well containing the sample, the average absorbance of a row of wells containing 150 µl water was subtracted to give absorbance value $A_1$

(blank). 10 µl of 1 mM naphthylethylene-diamine was added to all the sample wells including the blank, and incubated at room temperature for 10 min before the plates were read again (to let the product of diazotization react with naphthylethylene-diamine to form an azo derivative), subtracting the blanks ($A_1$) to give the absorbance value ($A_2$). The level of $NO_2^-$ formation was signified as the change in absorbance of $A_2$-$A_1$ and results were plotted against a nitrate/nitrite standard curve. The detection limit was 30 pmol/50 µl sample and results were expressed as µM $NO_2^-$. The data from 4 – 6 independent experiments were expressed as the mean ± standard error of mean.

## 2.8 Western Blot Analysis

After removal of culture medium, intact cells were first washed twice with cold PBS and then scraped with a rubber policeman using 80 µl lysis buffer (20 mM Pipes, 0.25 M Sucrose, 1 mM EDTA, 1 mM EGTA, 10 mM monothioglycerol, 5 µM leupeptin, 1 mM phenylmethanesulonyl fluoride, 0.1% SDS, (all from Sigma, pH 7.4). Cells were then sonicated for 5 min and 10 µl of cell extracts were used for the measurement of protein content (Lowry et al., 1951). The determined amount of protein was then electrophoresed in SDS-polyacrylamide gel (acrylamide, Sigma) in a Mini Protean II Electrophoresis Cell (BIO-RAD). After electrophoresis, the proteins were transferred to a 0.45 µM nitrocellulose membrane (Hybond, Amersham) by the Trans-Blot SD Semi-Dry Transfer Cell. The membrane was then blocked with 1 % Tween-20 (USB, Amersham) in PBS at room temperature for 1 h. After blocking, the membrane was then incubated overnight with the primary antibody, then washed with 0.05% Tween-20 and incubated with horseradish peroxidase-conjugated secondary antibody (Amersham) for 1 h. The membrane was again rinsed with 0.05% Tween-20

for 30 min and incubated with reagents from the Enhanced Chemiluminescent Kit Plus (Amersham) for 1 min for the development of fluorescence. The membrane was then placed on the X-ray film (Boehringer Mannheim) and the film was developed by a film processor (X-OMAT, Kodak). The relative density of the bands was measured by a densitometer (GS-750, BIO-RAD) and analyzed by Molecular Analysts (version 1.4, BIO-RAD).

### 2.8.1 COX-2

COX-2 protein content was determined in astrocytes that are classified into i) control, ii) METH-treated, iii) AG, iv) AG + METH, v) COX-2 and vi) COX-2 + METH groups. 20 μg of protein from each group was electrophoresed in 10% SDS-polyacrylamide gel. Goat anti-COX-2 (1:500, Santa Cruz) primary antibody and horseradish peroxidase-conjugated rabbit anti-goat IgG (1:1,500, Santa Cruz) secondary antibody was used.

### 2.8.2 HO-1

HO-1 protein content was determined in astrocytes that are classified into i) control, ii) METH-treated, iii) AG, iv) AG + METH, v) COX-2 and vi) COX-2 + METH groups. 20 μg of protein from each group was electrophoresed in 12% SDS-polyacrylamide gel. Rabbit anti-HO-1 (1:2,000, StressGen) primary antibody and horseradish peroxidase-conjugated hamster anti-rabbit IgG (1:2,000, Amersham) secondary antibody was used.

## 2.9 Viability Assay for CATH.a Cell Line

To determine the viability of CATH.a cells as well as CATH.a-astrocyte cocultures after METH treatment, a Live/Dead® Viability/Cytotoxicity Kit (Molecular Probes, USA) was employed. This kit provides a two-color fluorescence cell viability assay based on the simultaneous determination of live and dead cells with two probes that measure two recognized parameters of cell viability – intracellular esterase activity and plasma membrane integrity. Live cells are distinguished by the presence of ubiquitous intracellular esterase activity, determined by the enzymatic conversion of the non-fluorescent cell permeable calcein AM to the intensely fluorescent calcein. The polyanionic calcein is well retained within live cells, which produces an intense uniform green fluorescence in live cells with excitation at 495 nm and emission at 515 nm. Ethidium homodimer (EthD-1) enters cells with damaged membranes and undergoes a 40-fold enhancement of fluorescence upon binding to nucleic acids, thereby producing a bright red fluorescence in dead cells when undergoing excitation at 495 nm and emission at 635 nm. EthD-1 is excluded by the intact plasma membrane in live cells thus is specific to only damaged plasma membranes.

CATH.a cells and CATH.a-astrocyte cocultures were harvested at 4, 24 and 48 h after METH treatment. Cells were gently washed once with sterile, tissue-culture grade PBS. Cells were then incubated with 200 µl of combined LIVE/DEAD assay reagents (4 µM EthD-1 and 2 µM calcein AM in sterile, tissue-culture grade PBS) per well for 30 min at room temperature. 10 µl of fresh combined LIVE/DEAD assay reagents was added to a microscope slide and the coverslip containing the cultured cells was then inverted and mounted onto the slide. The number of live and dead CATH.a cells were counted under a fluorescence microscope (Zeiss, Germany) with

filters having wavelength of 485 nm for calcein (which labels the live cells) and wavelength of 530 nm for EthD-1 (which labels the dead cells).

## 2.10 Statistics

All the data are expressed as the mean ± standard error (SEM). One-way ANOVA was used for ROS (time course), ATP, $NO_2^-$ measurements as well as CATH.a-astrocyte cocultures. This was followed by post-hoc Bonferroni test for ROS, ATP and $NO_2^-$ and independent t-test between control and METH treatment in the coculture system. P values $< 0.05$ are considered as significant.

For the rate of change in ROS assay, linear regression lines were fitted to the time points studied and the equality of slopes (rate of change) was then compared. Significant trend differences among the groups were tested with a F-test, p values $<$ 0.001 was considered as significant.

For LDH assay, an independent t-test was used to compare the difference between control and METH-treated groups.

# CHAPTER THREE: RESULTS

## 3.1 The Effects of METH Treatment on Cultured Astrocytes

### 3.1.1 Lactate Dehydrogenase (LDH) Activities

Table 1 showed the results of LDH activity at 0 and 48 h after 4 mM METH treatment. 4mM METH treatment on cultured astrocytes resulted in no significant differences in LDH activities during the 48 h incubation period. In striatal astrocytes, LDH activities were 3.44 ± 1.50 to 6.22 ± 0.06 U/L from 0 – 48 h treatment. In mesencephalic astrocytes, LDH activities were 2.10 ± 0.56 to 1.77± 0.21 U/L from 0 – 48 h METH treatment. LDH activity in cortical astrocytes was shown to be 2.39 ± 0.80 U/L at 0 h, reaching a maximum of 4.23 ± 0.8 U/L at 48 h. Since there was no significant increase in LDH activity from 0 to 48 h signifying minimal loss of cell viability. Results from other time points were not shown.

### 3.1.2 Morphological Changes

Figures 1 to 3 showed the morphology changes in astrocytes after 48 h of METH treatment. Prior to METH treatment, astrocytes showed a protoplasmic appearance (Fig.1a-c). After 48 h 4 mM METH exposure, striatal astrocytes and mesencephalic astrocytes showed considerable astrogliosis when compared with their control groups (Fig. 3a,b). Fibrous astrocytes with slender processes were more prominent in these 2 regions when compared to cortical astrocytes (Fig. 3c). A large amount of vacuoles were also shown to be present in the cytoplasm of astrocytes cultured from all 3 regions (Fig. 2a-c). These vacuoles were visible in all METH-treated astrocytes as earlier as 8 h post-treatment.

Table 1 Data are expressed as means (U/L) ± S.E. from four separate experiments. Values in the treated groups at 48 h were not significantly different from control (0 h) after comparisons using independent *t* test.

LDH activity

| | U/L | |
|---|---|---|
| | 0 h | 48 h |
| Striatum | 3.44 ± 1.50 | 6.22 ± 0.06 |
| Mesencephalon | 2.10 ± 0.56 | 1.77 ± 0.21 |
| Cortex | 2.39 ± 0.80 | 4.23 ± 0.80 |

Fig. 1 Phase contrast micrographs of control astrocytes cultured from (a) striatum (St), (b) mesencephalon (Me) and (c) cortex (Co). Cells were without METH treatment and incubated in culture medium for 48 h. (x100 magnification)

Control

St

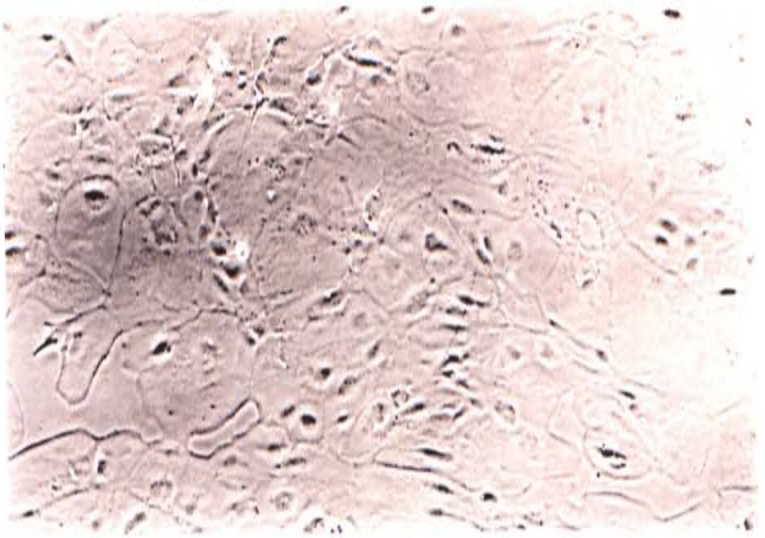

(a)

Me

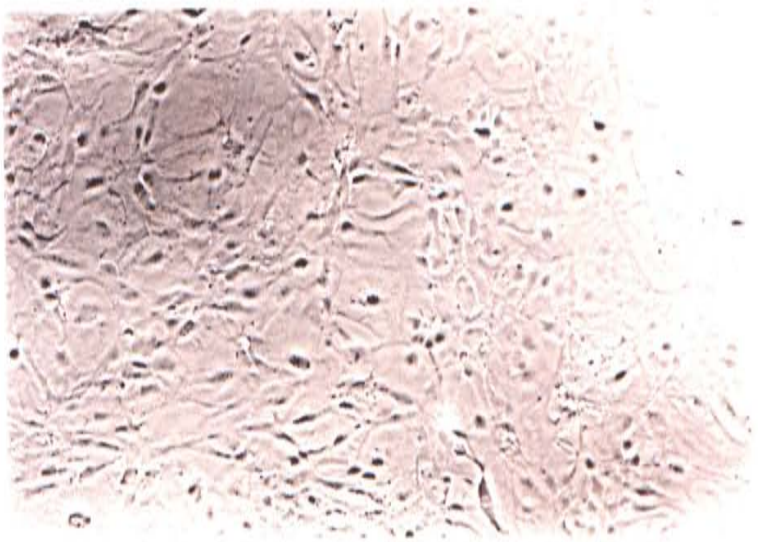

(b)

Co

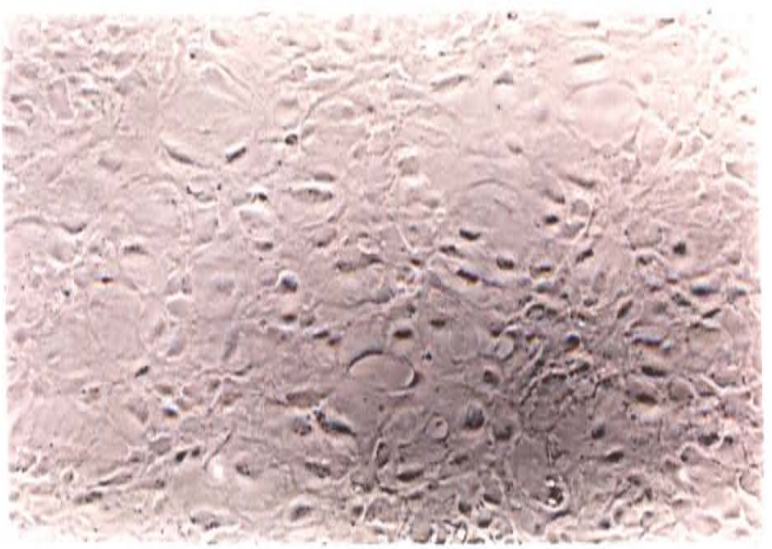

(c)

Fig. 2 Phase contrast micrographs of cultured astrocytes from (a) striatum (St), (b) mesencephalon (Me) and (c) cortex (Co) after 8 h METH treatment. Arrows indicate the presence of vacuoles. (x100 magnification)

Meth - 8h

St

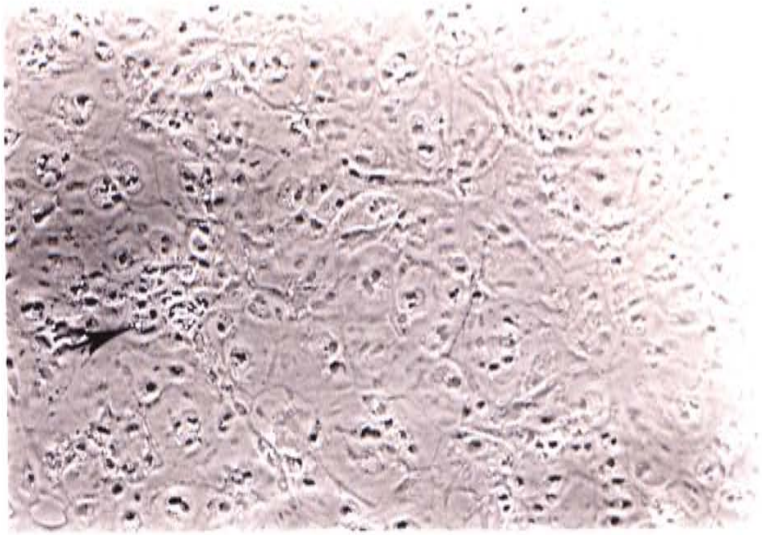

(a)

Me

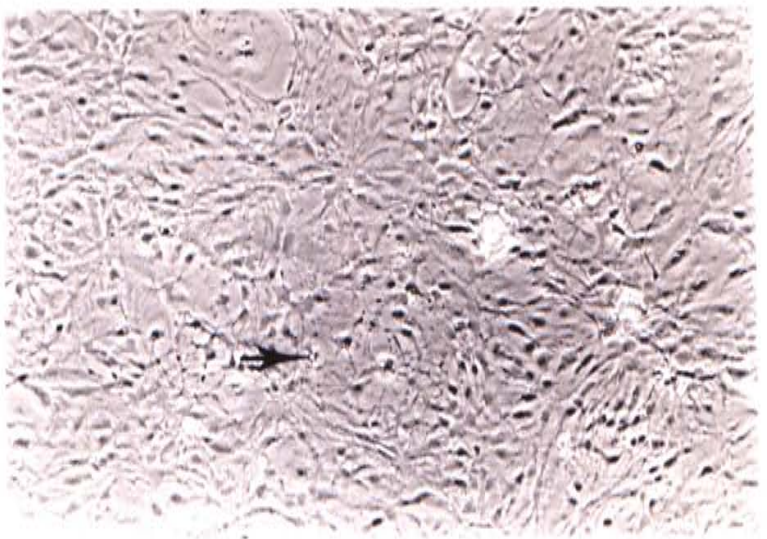

(b)

Co

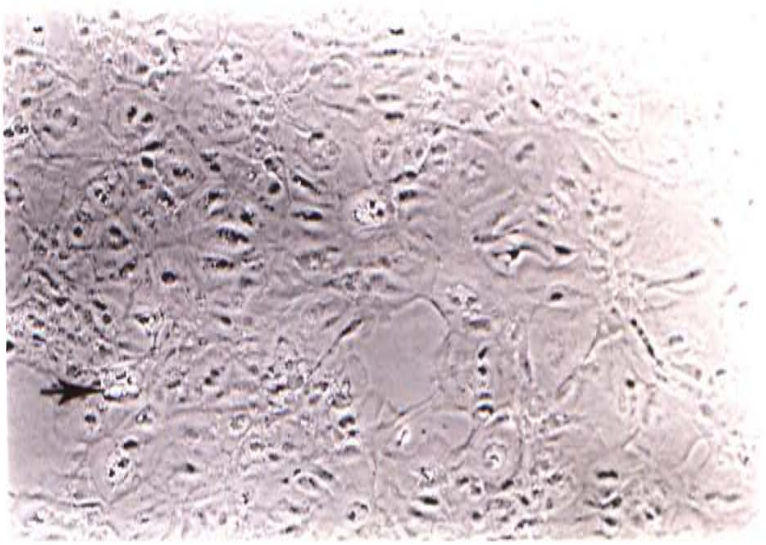

(c)

Fig. 3 Phase contrast micrographs of cultured astrocytes from (a) striatum (St), (b) mesencephalon (Me), and (c) cortex (Co) after 48 h METH treatment. Intense astrogliosis was observed with St > Me > Co. (x100 magnification)

Meth - 48h

St

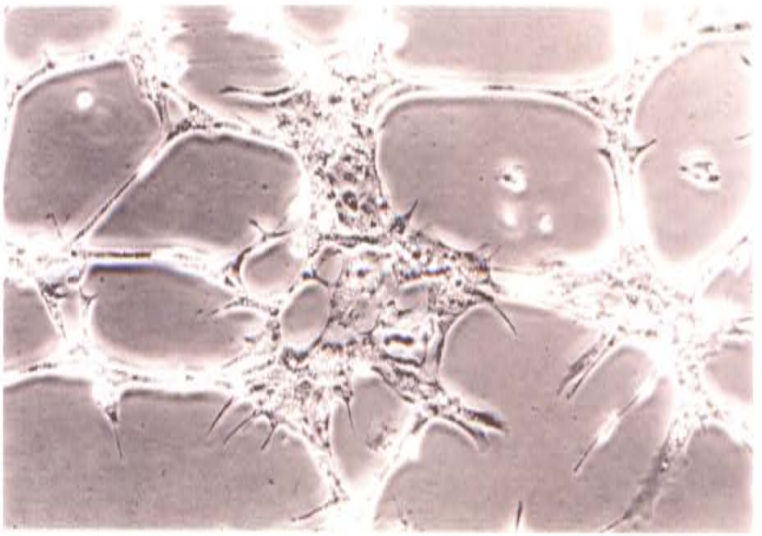

(a)

Me

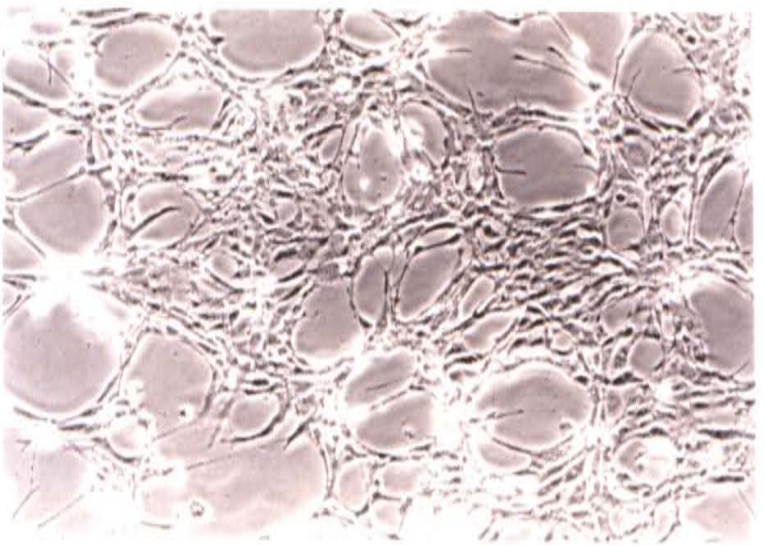

(b)

Co

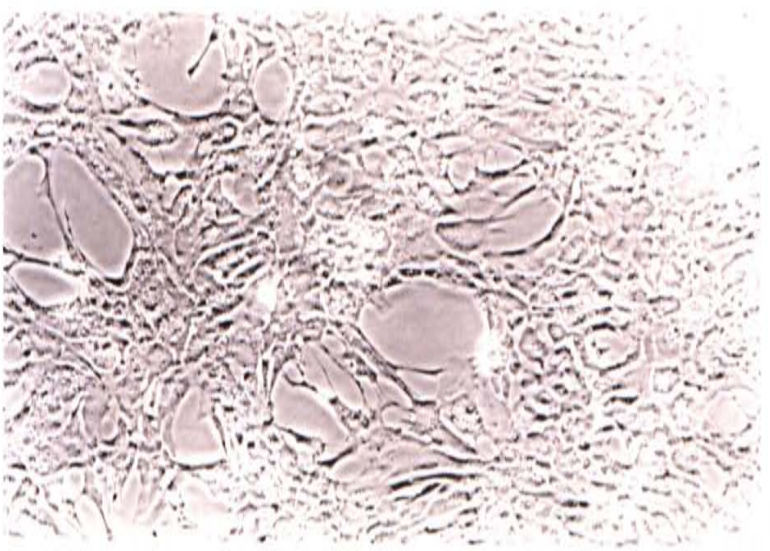

(c)

### 3.1.3 The Production of Reactive Oxygen Species (ROS)

#### 3.1.3.1 Rate of change (0 – 120min)

The rates of ROS production in striatal, mesencephalic and cortical astrocytes were shown to be different during the 120 min of METH treatment. In control striatal astrocytes, the rate of change (slope coefficient = 25.43; 2144.54 ± 34.03 to 5099.65 ± 263.48 U from 0 to 120 min) is significantly ($p<0.001$) higher than that of control cortical (slope coefficient = 20.73; 2118.63 ± 127.72 to 4520.96 ± 445.61 U from 0 to 120 min) and mesencephalic (slope coefficient = 19.61; 2127.17 ± 46.86 to 4404.48 ± 182.65 U from 0 to 120 min) astrocytes (Fig. 4).

In METH-treated striatal astrocytes, the rate of change (slope coefficient = 31.96; 2019.42 ± 89.84 to 5768.83 ± 724.64 U from 0 to 120 min) was significantly ($p<0.001$) greater than that of its control group (slope coefficient = 25.43) (Fig. 5a).
In METH-treated mesencephalic astrocytes, there was no significant difference in the rate of change (slope coefficient = 23.81; 2128.17 ± 60.82 to 4970.67 ± 414.38 U from 0 to 120 min) when compared with the controls (slope coefficient = 19.61)(Fig. 5b). There was also no significant difference between the rate of change in METH-treated cortical astrocytes (slope coefficient = 23.85; 2216.81 ± 83.18 to 5026.54 ± 182.62 U from 0 to 120 min) and controls (slope coefficient = 20.73)(Fig. 5c).

#### 3.1.3.2 Time course (0 – 48 h)

After 4 mM METH treatment, striatal astrocytes (Fig 6a) showed a significant increase ($p < 0.05$) in ROS formation from 8 h onwards when compared to mesencephalic and cortical astrocytes (Fig. 6b, c). In striatal astrocytes (Fig. 6a), a 20 and 55 % increase in ROS formation was reached at 8 h ($p < 0.05$; 1318 ± 45.26 U to

Fig. 4 The amount of DCF formed in control striatal (St), mesencephalic (Me), and cortical (Co) astrocytes during 120 min of METH treatment. Data were obtained from 4 independent experiments and are expressed as mean DCF fluorescence units. Regression analysis showed that the rate of change of striatal astrocytes was significantly (F-test, p value $< 0.001$) greater than that of mesencephalic and cortical astrocytes.

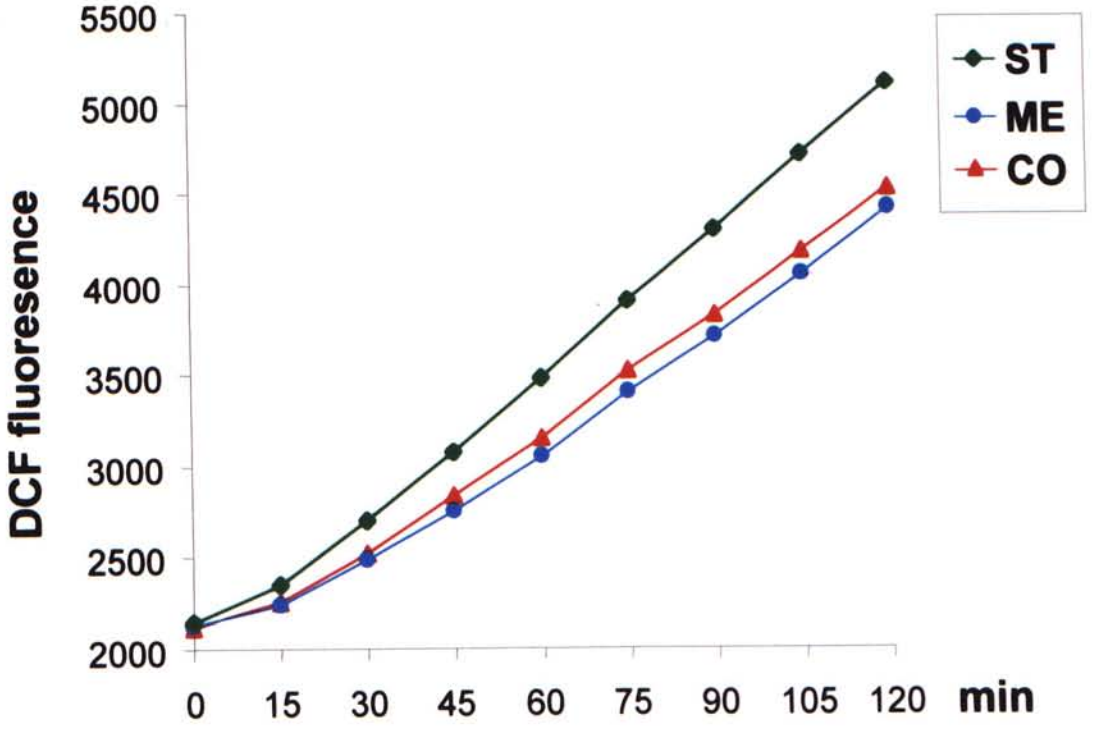
DCF fluoresence
5500
5000
4500
4000
3500
3000
2500
2000
0
15
30
45
60
75
90
105
120
min
ST
ME
CO

Fig. 5 The amount of DCF formed in striatal (a), mesencephalic (b) and cortical (c) astrocytes during 120 min of METH treatment. Data were obtained from four independent experiments and are expressed as mean DCF fluorescence units ± S.E. Regression analyses showed that there is a significant (F-test, p value < 0.001) increase in the rate of change in METH-treated striatal astrocytes when compared to control cells. No significant rate of change was observed in METH-treated mesencephalic nor cortical astrocytes.

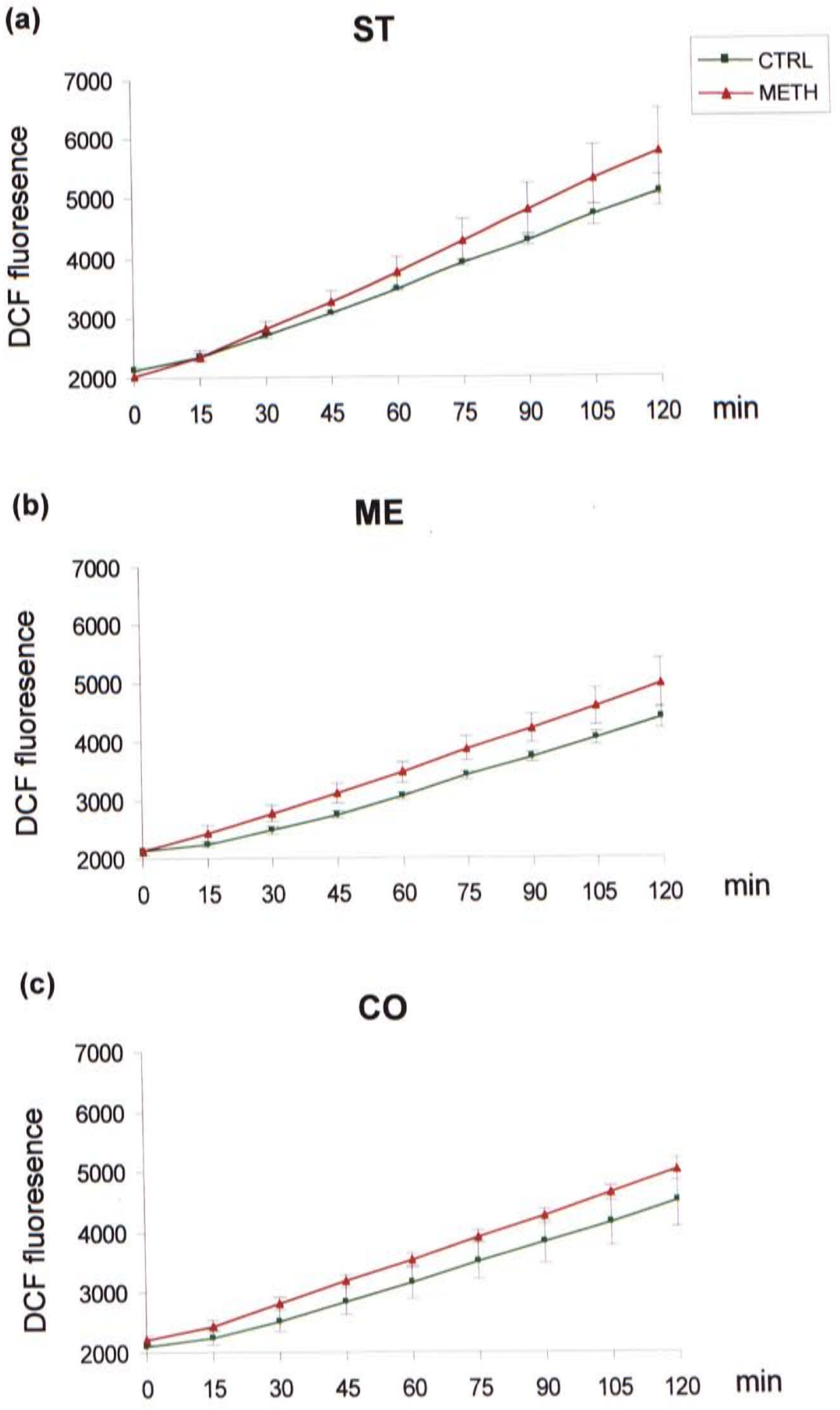
(a)
ST
CTRL
METH
DCF fluoresence
7000
6000
5000
4000
3000
2000
0
15
30
45
60
75
90
105
120
min
(b)
ME
DCF fluoresence
7000
6000
5000
4000
3000
2000
0
15
30
45
60
75
90
105
120
min
(c)
CO
DCF fluoresence
7000
6000
5000
4000
3000
2000
0
15
30
45
60
75
90
105
120
min

Fig. 6 The amount of DCF formed in striatal (a), mesencephalic (b) and cortical (c) astrocytes after 0 – 48 h of 4 mM METH treatment. Data were obtained from six independent experiments and are expressed as mean DCF fluorescence units ± S.E.

* Statistically different ($p < 0.05$) from the values obtained from astrocytes with no METH treatment (0 h).

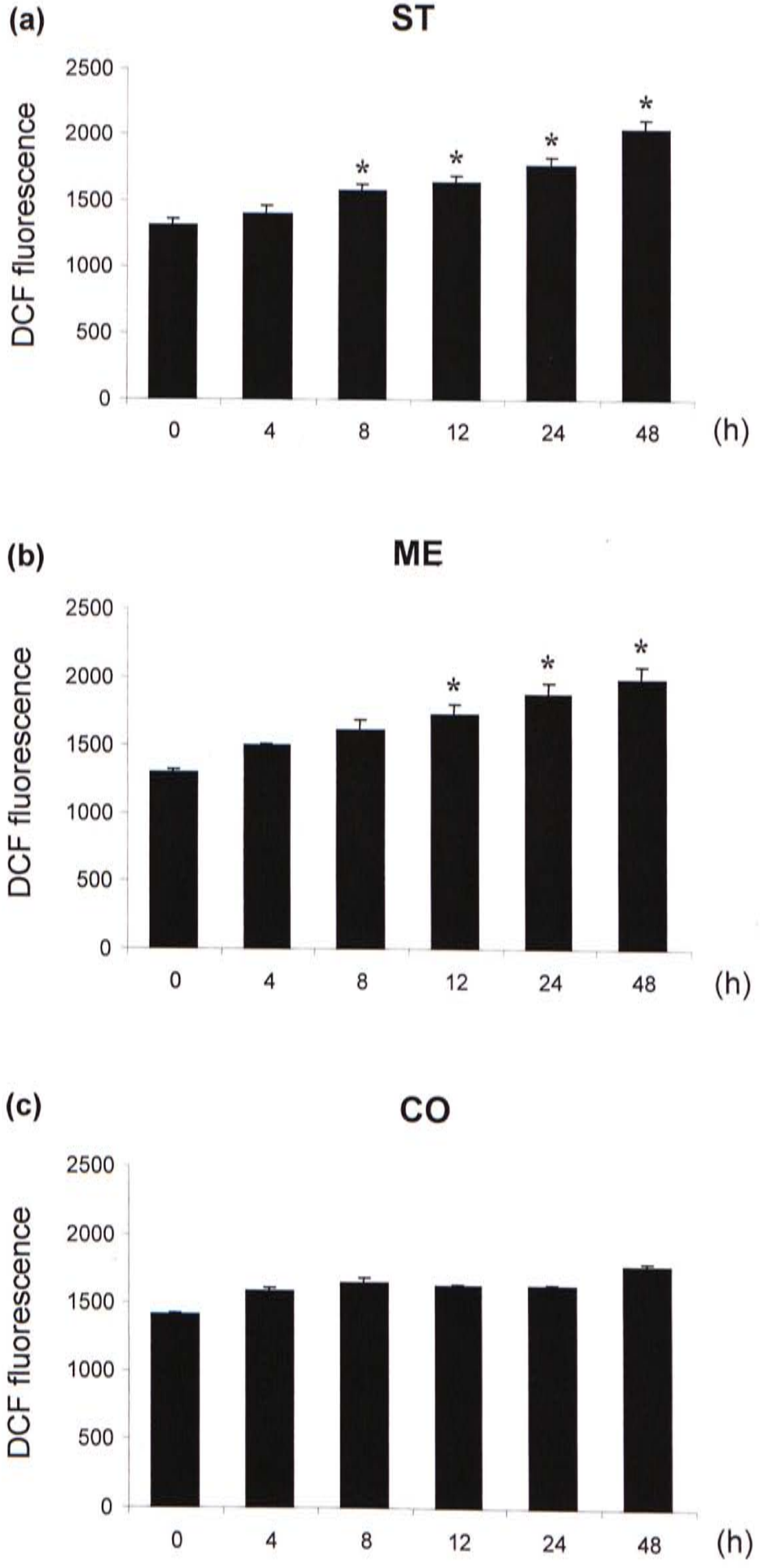
(a)
ST
DCF fluorescence
2500
2000
1500
1000
500
0
0
4
8
12
24
48
(h)
*
(b)
ME
DCF fluorescence
2500
2000
1500
1000
500
0
0
4
8
12
24
48
(h)
*
(c)
CO
DCF fluorescence
2500
2000
1500
1000
500
0
0
4
8
12
24
48
(h)

1580 ± 49.95 U at 0 to 8 h) and 48 h ($p < 0.05$; 1318 ± 54.26 U to 2042 ± 73.80 U at 0 to 48 h) respectively.

Mesencephalic astrocytes showed a significant increase in ROS formation from 12 h METH treatment (Fig. 6b). At 12 h METH treatment, a 33 % increase ($p < 0.05$; 1299 ± 20.34 to 1727 ± 72.10 U at 0 to 12 h) was reached, by 48 h, a 53% increase ($p < 0.05$; 1299 ± 20.34 to 1990 ± 102.16 U at 0 to 48 h) was shown. For cortical astrocytes (Fig. 6c), there was no significant increase in ROS formation during 0 to 48 h METH treatment (Fig. 6c). The ROS levels reached a maximum of 25% increase from 0 (1415 ± 9.77 U) to 48 (1772 ± 30.11 U) h treatment.

### 3.1.4 Change in ATP Content

During the course of the 48 h METH treatment, astrocytes from all three regions showed a similar pattern of an initial increase followed by a decrease in ATP levels. Striatal astrocytes showed a significant ($p < 0.05$) increase in ATP levels at 4 h (49.41 ± 3.69 nmol/mg) METH treatment when compared with controls at 0 h (31.21 ± 2.44 nmol/mg protein) (Fig. 7a). This was followed by a slight decline in ATP levels at 8 and 12 h followed by a significant increase at 24 h (50.56 ± 3.32 nmol/mg protein) METH treatment. These increases at 4 and 24 h were 58 and 62% respectively to that of controls. However, by 48 h METH treatment, ATP levels reached a significant decrease (19.15 ± 4.98 nmol/mg protein) of 39% to that of control values.

Mesencephalic astrocytes showed a significant ($p < 0.05$) increase in ATP levels at 12 h (54.03 ± 3.70 nmol/mg protein) with a 50% increase when compared to controls at 0 h (36.06 ± 1.88 nmol/mg protein) (Fig. 7b). From 12 h onward, ATP levels declined gradually reaching near the control values (33.11 ± 1.86 nmol/mg

Fig. 7 The effects of 4 mM METH treatment on ATP content in striatal (a), mesencephalic (b) and cortical (c) astrocytes. Values are expressed as means (nmol ATP/mg protein) ± S.E. (n = 6)

* Statistically different ($p < 0.05$) from the values obtained from astrocytes with no METH treatment (0 h).

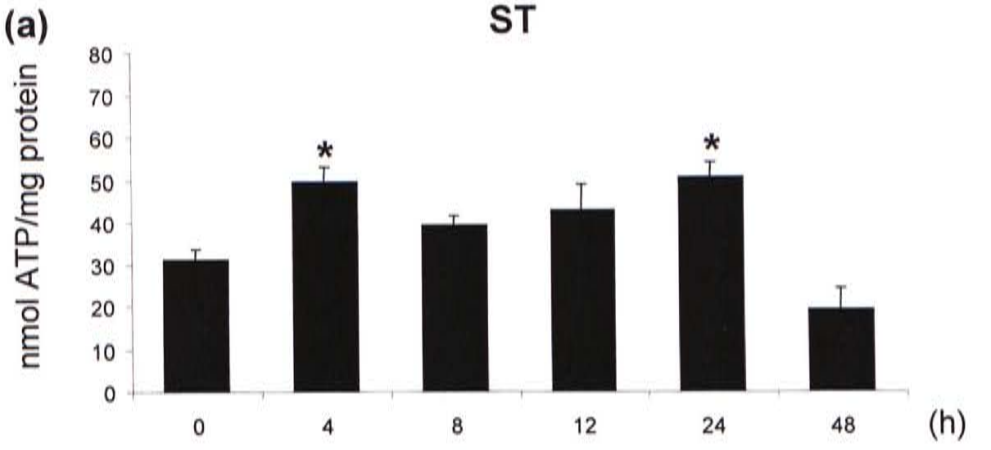
(a)
ST
nmol ATP/mg protein
80
70
60
50
40
30
20
10
0
*
*
0
4
8
12
24
48
(h)

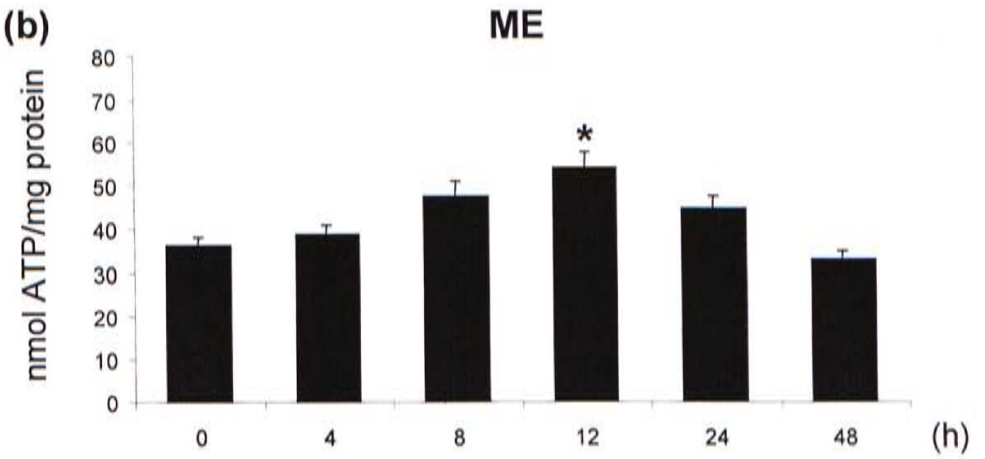
(b)
ME
nmol ATP/mg protein
80
70
60
50
40
30
20
10
0
*
0
4
8
12
24
48
(h)

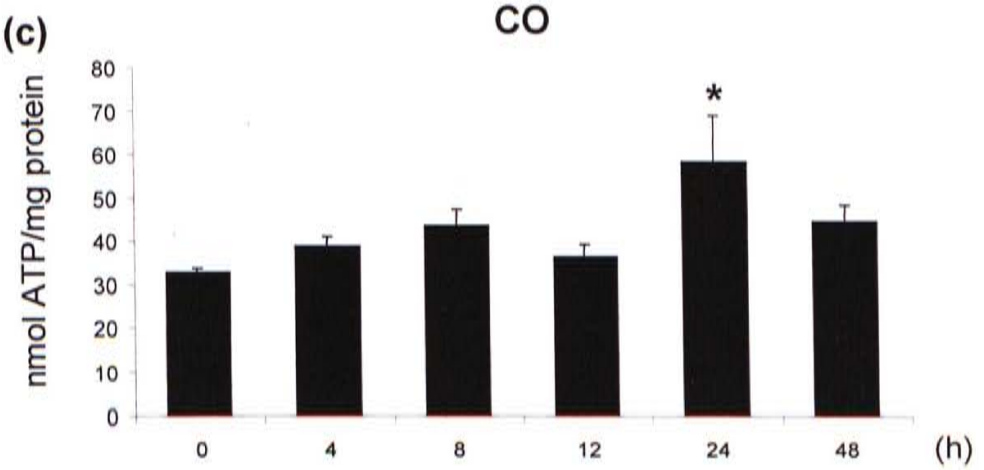
(c)
CO
nmol ATP/mg protein
80
70
60
50
40
30
20
10
0
*
0
4
8
12
24
48
(h)

protein) at 48 h treatment. For cortical astrocytes, at 24 h METH treatment, a 78% increase ($p < 0.05$; $32.56 \pm 1.11$ to $58.10 \pm 10.43$ nmol/mg protein at 0 to 24 h) in ATP levels was observed (Fig. 7c). By 48 h METH treatment, ATP levels were 36% ($44.30 \pm 4.03$ nmol/mg protein) higher than that of controls.

### 3.1.5 Change in Mitochondrial Membrane Potential ($\Delta\Psi m$)

JC-1, a $\Delta\Psi m$-sensitive dye was used to assess the change in $\Delta\Psi m$ after METH treatment. Hyperpolarized mitochondria (JC-1-red fluorescence) were exclusively and prominently present in the cytoplasm of all untreated astrocytes (Fig. 8a, 9a, 10a). On the other hand, depolarized mitochondria (JC-1-green fluorescence) were found in astrocytes treated with METH (Fig.8b,c, 9b,c, 10b,c).

In both striatal and mesencephalic astrocytes, the drop in $\Delta\Psi m$ occurred as early as 8 h after METH treatment (Fig. 8b, 9b). However, this drop in $\Delta\Psi m$ was only observed in cortical astrocytes after 12 h of METH treatment (Fig. 10b).

By 48 h of METH treatment, astrocytic $\Delta\Psi m$ for all three regions were mostly depolarized, they were characterized by the abundant green fluorescence observed in the cytoplasm. (Fig. 8c, 9c, 10c). Vacuoles were also observed in the cytoplasm of these cells. This phenomenon was also described (Section 3.1.2) when observed under phase contrast microscopy.

### 3.1.6 Nitrite levels after METH treatment

(a) Striatal astrocytes (Fig. 11a)

Striatal astrocytes showed that there was an increase in nitrite level in the control group during 48 h of incubation. The nitrite level reached a significant increase at 24 h ($2.71 \pm 0.21$ μM at 1 h to $4.21 \pm 0.14$ μM at 24 h; $p < 0.05$). By 48 h

Fig. 8 Confocal microscopy images of striatal astrocytes showing the control (a), 8 h METH-treated (b), and 48 h METH-treated (c) groups. Red fluorescence indicates mitochondria with a high $\Delta\Psi m$ while green fluorescence indicates mitochondria with a low $\Delta\Psi m$.
Arrows indicate the presence of vacuoles. (x 630 magnification)

# Striatum

control

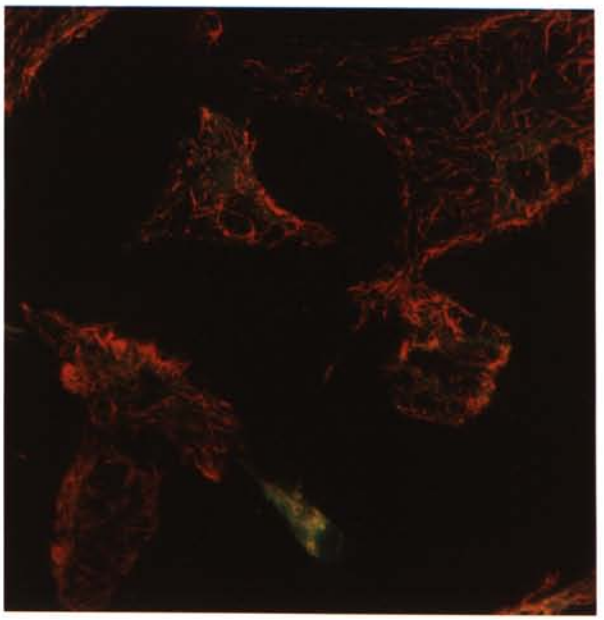

(a)

Meth - 8h

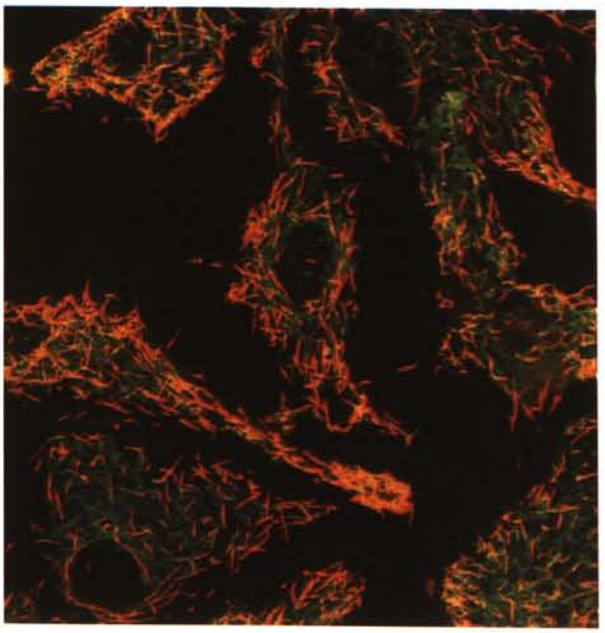

(b)

Meth - 48h

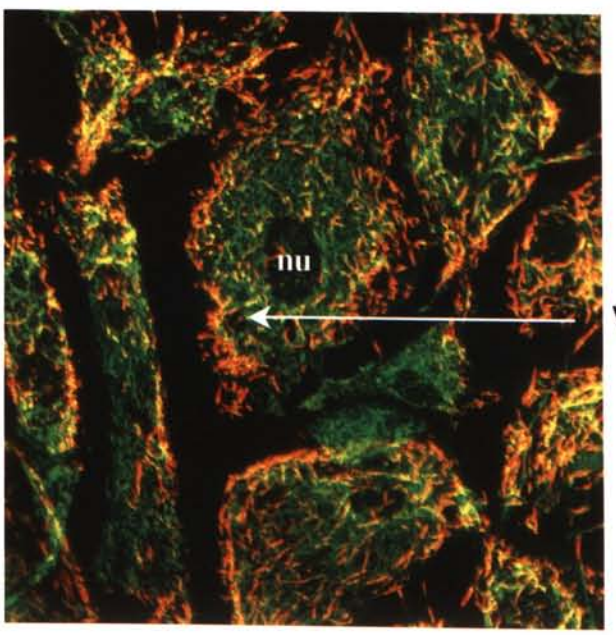


(c)

Fig. 9 Confocal microscopy images of mesencephalic astrocytes showing the control (a), 8 h METH-treated (b), and 48 h METH-treated (c) groups. Red fluorescence indicates mitochondria with a high $\Delta\Psi m$ while green fluorescence indicates mitochondria with a low $\Delta\Psi m$.
Arrows indicate the presence of vacuoles. (x 630 magnification)

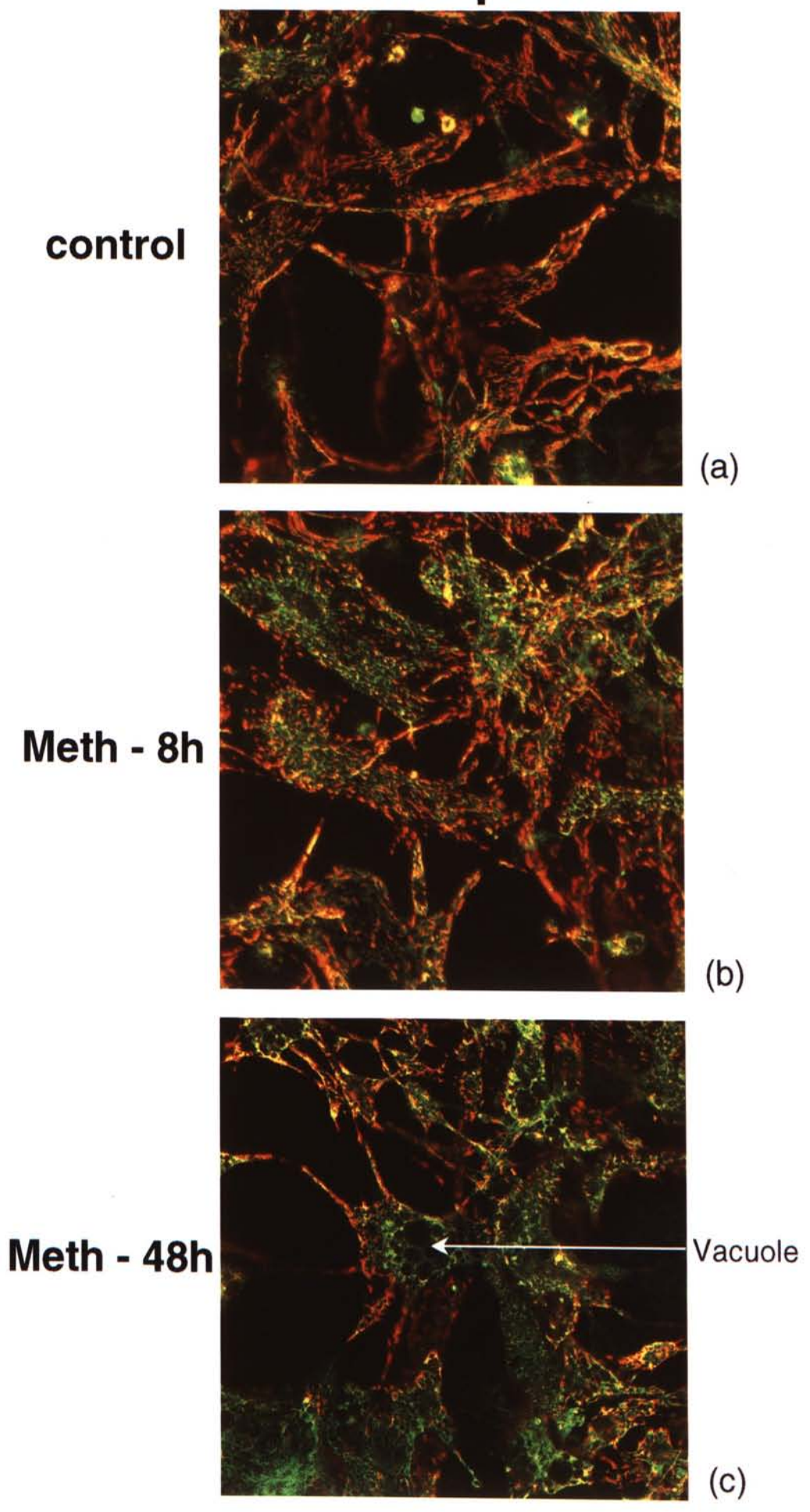
Mesencephalon
control
(a)
Meth - 8h
(b)
Meth - 48h
Vacuole
(c)

Fig. 10 Confocal microscopy images of cortical astrocytes showing the control (a), 12 h METH-treated (b), and 48 h METH-treated (c) groups. Red fluorescence indicates mitochondria with a high $\Delta\Psi m$ while green fluorescence indicates mitochondria with a low $\Delta\Psi m$.
Arrows indicate the presence of vacuoles. (x 630 magnification)

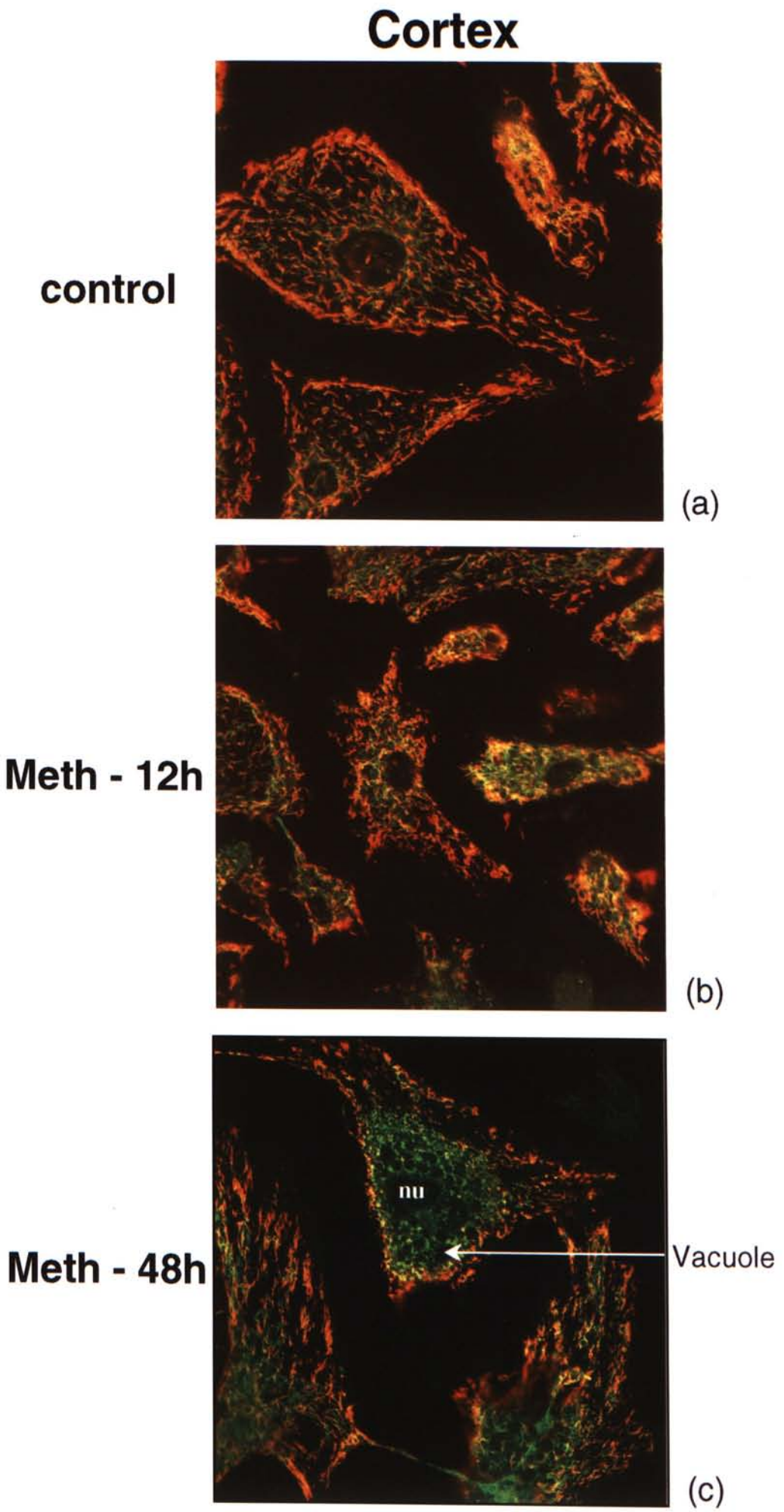
Cortex
control
(a)
Meth - 12h
(b)
nu
Meth - 48h
Vacuole
(c)

Fig. 11 Amount of nitrite released into the medium from striatal (a), mesencephalic (b) and cortical (c) astrocytes cultured in control (Ctrl), 4 mM METH (METH), 300 μM aminoguanidine (AG) or 300 μM AG with 4 mM METH (AG + METH) media. Values are expressed as means (μM) ± S.E. (n=4).

# Statistically different ($p<0.05$) between the METH or AG with the control.

* Statistically different ($p<0.05$) between AG + METH and METH.

§ Statistically different ($p<0.05$) between the time points.

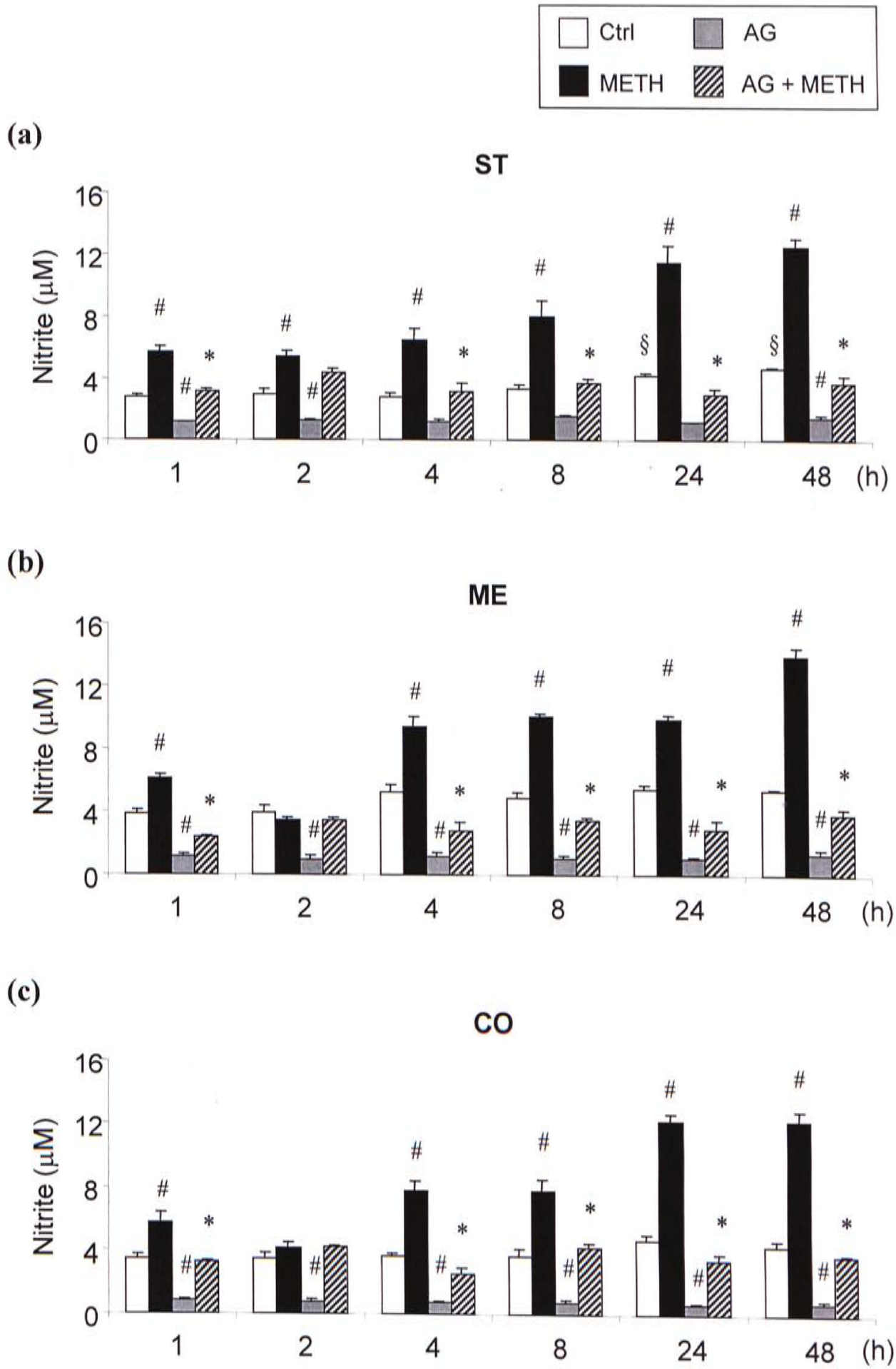
Ctrl
AG
METH
AG + METH
(a)
ST
Nitrite (μM)
16
12
8
4
0
1
2
4
8
24
48
(h)
(b)
ME
(c)
CO

incubation, it reached a 71% increase (4.64 ± 0.09 μM; $p < 0.05$). After 4mM METH treatment, striatal astrocytes showed a rapid increase in nitrite levels from 1 h (5.63 ± 0.41 μM) onwards. This represents a one fold significant ($p < 0.05$) increase when compared to the control. By 48 h treatment, a maximum of 1.7 fold (12.52 ± 0.52 μM; $p < 0.05$) increase in nitrite level was reached when compared with the control.

(b) Mesencephalic astrocytes (Fig. 11b)

Unlike striatal astrocytes, control mesencephalic astrocytes only showed a slight increase (not significant) in nitrite levels during 48 h of incubation. However, the overall basal nitrite levels of mesencephalic astrocytes (3.85 ± 0.24 μM at 1 h and 5.32 ± 0.15 μM at 48 h) were higher than that of striatal astrocytes.

At 1 h after METH treatment, mesencephalic astrocytes showed a 60% increase (6.14 ± 0.20 μM; $p < 0.05$) in nitrite level when compared with the control. Significant increases in nitrite levels were observed from 4 h onwards, reaching a maximum of 1.6 fold at 48 h (13.94 ± 0.51 μM; $p < 0.05$).

(c) Cortical astrocytes (Fig. 11c)

Control cortical astrocytes showed a slight increase (not significant) in nitrite levels that were similar to those of control mesencephalic astrocytes. A 27% increase in nitrite level was observed at 48 h (4.27 ± 0.39 μM) when compared with 1 h (3.38 ± 0.28 μM) of incubation. After METH treatment, there was a gradual increase in nitrite level and this increase was also significant at 1 h post-treatment. Significant increases were observed from 4 h onwards reaching a 1.86 fold increase (12.21 ± 0.71 μM) at 48 h treatment.

### 3.1.7 The Effects of Aminoguanidine (AG) on Nitrite levels

In this experiment, astrocytes were treated with either AG + METH or AG only. When astrocytes were treated with AG alone, there were significant reductions in nitrite levels in astrocytes from all three regions when compared with their respective controls (Fig. 11). When AG was added with METH, there were also significant reductions in nitrite levels when compared with their respective METH-treated groups.

(a) Striatal astrocytes (Fig. 11a)

When striatal astrocytes were treated with AG alone, there were marked reductions in nitrite levels reaching lower than control levels for all the time points studied. At 1 h to 48 h after AG treatment, a 59 to 69 % decrease ($1.10 \pm 0.06$ and $1.45 \pm 0.15$ μM respectively; $p < 0.05$) in nitrite levels was observed when compared with their corresponding controls. When the striatal astrocytes were treated with AG + METH, the nitrite levels were also decreased along all the time points studied. These decreases were significant ($p < 0.05$) along all the time points studied, with the exception at 2 h, when compared with METH treatment alone. A 45 ($3.09 \pm 0.18$ μM) and 70 % ($3.71 \pm 0.44$ μM) decrease at 1 and 48 h respectively were observed when compared with the corresponding METH treatment groups. When compared to the control groups at 1 h treatment, the nitrite level was reduced to near control value ($3.09 \pm 0.18$ μM in AG + METH vs $2.71 \pm 0.21$ μM in control). Similarly, at 48 h of AG + METH treatment, the nitrite level was $3.71 \pm 0.44$ μM, which is near the control value ($4.64 \pm 0.09$ μM).

(b) Mesencephalic astrocytes (Fig. 11b)

Similar to that observed for striatal astrocytes, AG treatment alone in mesencephalic astrocytes, also showed a marked reduction in nitrite levels. There was a 71 (1.13 ± 0.81 μM) and a 74% (1.38 ± 0.22 μM) decrease in nitrite levels at 1 and 48 h respectively when compared to their corresponding controls. There were significant differences ($p < 0.05$) between the AG treatment group and the control group at all time points studied.

When the mesencephalic astrocytes were treated with AG + METH, the nitrite levels were also reduced along all the time points studied. These decreases were significant ($p < 0.05$) along all the time points studied, with the exception at 2 h, when compared to METH treatment alone. A 61 (2.41 ± 0.08 μM) and 73% (3.79 ± 0.36 μM) decrease at 1 and 48 h respectively were observed when compared with the corresponding METH treatment groups. When compared to the control groups, at 1 h AG + METH treatment, nitrite levels was reduced to near control values (2.41 ± 0.08 μM in AG + METH vs 3.85 ± 0.24 in control). At 48 h treatment, the nitrite level (3.79 ± 0.36 μM) was also near the control value (5.32 ± 0.15 μM).

(c) Cortical astrocytes (Fig. 11c)

Similar to that shown in striatal and mesencephalic astrocytes, cortical astrocytes also showed a decrease in nitrite levels when treated with AG alone. A 76 (0.81 ± 0.14 μM) and 82% (0.76 ± 0.17 μM) decrease in nitrite levels were observed at 1 and 48 h respectively when compared to their corresponding controls. There were significant differences ($p < 0.05$) between the AG treatment group and the control group at all time points studied.

When the cortical astrocytes were treated with AG + METH, the nitrite levels were also reduced along all the time points studied. This decrease was significant ($p <$

0.05) along all the time points with the exception of 2 h post-treatment when compared to the METH treated group. A 43 % (3.24 ± 0.12 μM) and 70 % (3.68 ± 0.07 μM) decrease at 1 and 48 h respectively were observed when compared with their corresponding METH treatment groups. When compared to the control groups, nitrite levels of the AG + METH groups were reduced to near control values (3.24 ± 0.12 μM in AG + METH vs 3.38 ± 0.28 μM in control) at 1 h and (3.68 ± 0.07 μM in AG + METH vs 4.27 ± 0.39 μM in control) at 48 h.

### 3.1.8 The Effects of Indomethacin (INDO) on Nitrite levels

Results from this study showed that when cells were treated with INDO alone, there was a time-dependent increase in nitrite levels from 1 to 48 h treatment. When INDO was added with METH, the increase in nitrite levels was further enhanced (Fig. 12).

(a) Striatal astrocytes (Fig. 12a)

When these cells were treated with INDO alone, there was a gradual increase in nitrite levels from 1 (4.05 ± 0.26 μM) to 48 h (9.82 ± 0.54 μM) treatment. This increase was significant ($p < 0.05$) at 48 h INDO treatment in which a 110 % increase was observed when compared with the control.

When cells were treated with INDO + METH, a further increase in nitrite levels was observed. Nitrite levels ranged from 8.07 ± 0.12 to 17.22 ± 1.34 μM from 1 – 48 h respectively. This increase in nitrite levels was significantly ($p < 0.05$) higher than that of METH treatment only for all the time points studied. A 43 and 38% increase at 1 and 48 h respectively were observed when compared to METH-treated groups.

Fig. 12 Amount of nitrite released into the medium from striatal (a), mesencephalic (b) and cortical (c) astrocytes cultured in control (Ctrl), 4 mM METH (METH), 10 μM indomethacin (INDO) and 10 μM INDO with 4 mM METH (INDO + METH) media. Values are expressed as means (μM) ± S.E. (n=4).

# Statistically different ($p<0.05$) between the METH or INDO with the control.

* Statistically different ($p<0.05$) between INDO + METH and METH.

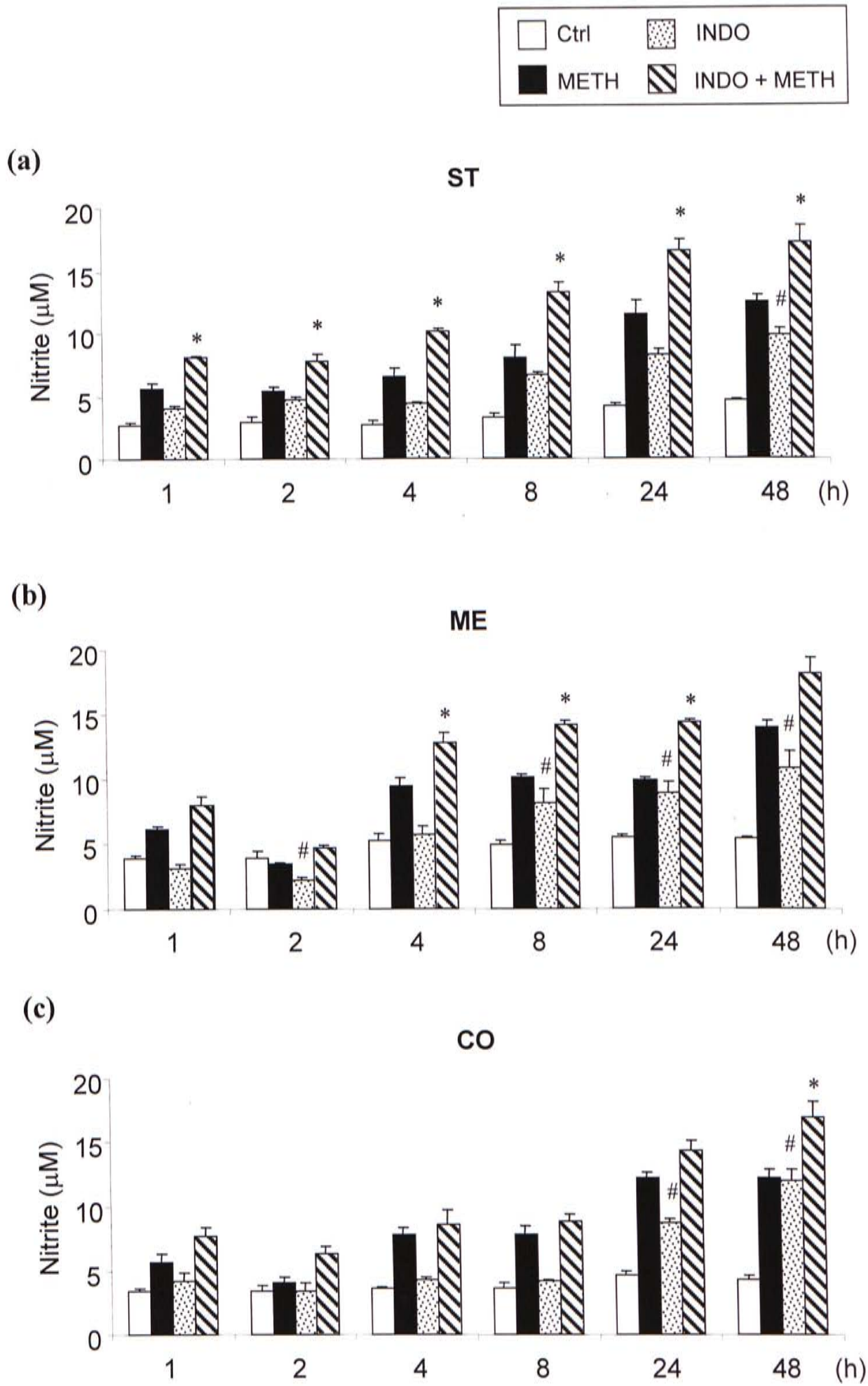
Ctrl
INDO
METH
INDO + METH
(a)
ST
Nitrite (μM)
20
15
10
5
0
1
2
4
8
24
48
(h)
(b)
ME
Nitrite (μM)
20
15
10
5
0
1
2
4
8
24
48
(h)
(c)
CO
Nitrite (μM)
20
15
10
5
0
1
2
4
8
24
48
(h)

(b) Mesencephalic astrocytes (Fig. 12b)

Cells treated with INDO alone also showed a gradual increase in nitrite levels when compared with the control group. The levels of nitrite ranged from 3.06 ± 0.37 to 10.79 ± 1.29 μM at 1 – 48 h treatment. This increase was significant ($p < 0.05$) at 2, 8, 24 and 48 h treatment when compared with the corresponding control groups. At 48 h INDO treatment, the nitrite level was 1 fold greater than that of the control.

When mesencephalic astrocytes were treated with INDO + METH, there was a further increase in nitrite levels when compared with the METH-treated group. The level of nitrite ranged from 7.98 ± 0.70 to 18.12 ± 1.17 μM at 1 – 48 h treatment. This increase was significant ($p < 0.05$) at 4, 8, 24 h treatment when compared with their corresponding METH-treated groups. This represented an approximate 35 – 45 % increase in nitrite levels at these significant time points studied.

(c) Cortical astrocytes (Fig. 12c)

INDO treatment alone also caused an increase in nitrite levels in cortical astrocytes from 24 h treatment. The level of nitrite ranged from 4.15 ± 0.71 to 11.94 ± 0.93 μM at 1 – 48 h treatment. At 24 and 48 h treatment, the increase in nitrite level reached a 87 % and 180 % significant ($p < 0.05$) increase respectively.

When treated with INDO + METH, the level of nitrite was also further enhanced. The level of nitrite ranged from 7.68 ± 0.63 to 16.93 ± 1.24 μM at 1 – 48 h incubation. At 48 h treatment, the level of nitrite was 39% ($p < 0.05$) greater than that of METH treatment only.

### 3.1.9 Change in Cyclooxygenase-2 (COX-2) Protein Levels

The present study examined the change in COX-2 levels after the METH treatment. Changes in COX-2 expression were further examined using the iNOS inhibitor AG (Fig. 13a) as well as the COX-2 inhibitor INDO (Fig. 13b).

(a) Striatal astrocytes (Fig. 13a(i) & Fig. 13b (i))

Striatal astrocytes treated with METH resulted in a 40% (Fig. 13a(i)) to 60% (Fig. 13b(i)) decrease in COX-2 protein expression at 48 h when compared to the control. At 24 and 48 h METH treatment, a breakdown product of approximately 47 kDa was observed. The co-administration of 300 μM AG and METH did block the slight decrease in COX-2 expression, however, it did not block the appearance of the ~47kDa breakdown product (Fig. 13a(i)).

However, the treatment of cells with METH and 10 μM INDO did not alter the pattern of COX-2 expression (Fig. 13b(i)). Similar to that observed for AG + METH, INDO + METH also did not ameliorate the protein breakdown product observed at 24 and 48 h treatment.

(b) Mesencephalic astrocytes (Fig. 13 a(ii) & Fig. 13b(ii))

There was minimal change in COX-2 protein levels in cells treated with METH when compared to their controls (Fig. 13a(ii) and Fig. 13b(ii)). Similar to that observed in striatal astrocytes, a ~ 47 kDa breakdown product was observed at 24 and 48 h METH treatment. When cells were treated with AG and METH, there was no change in COX-2 protein levels (Fig. 13a(ii)). However, when cells were treated with INDO and METH, there was a 4 - 5 fold increase in COX-2 protein levels that was observed from 1 to 48 h treatment (Fig. 13b(ii)). The ~ 47kDa breakdown product that was commonly observed after METH treatment could be observed as early at 4 post treatment.

Fig. 13a A representative Western blot of cyclooxygenase-2 (COX-2) protein expression in striatal (i), mesencephalic (ii) and cortical (iii) astrocytes cultured in control, 4 mM METH, 300 μM AG or 300 μM AG + 4 mM METH media. Change in the relative levels of COX-2 expression from 1 to 48 h was expressed as a percentage of the control.

(a)

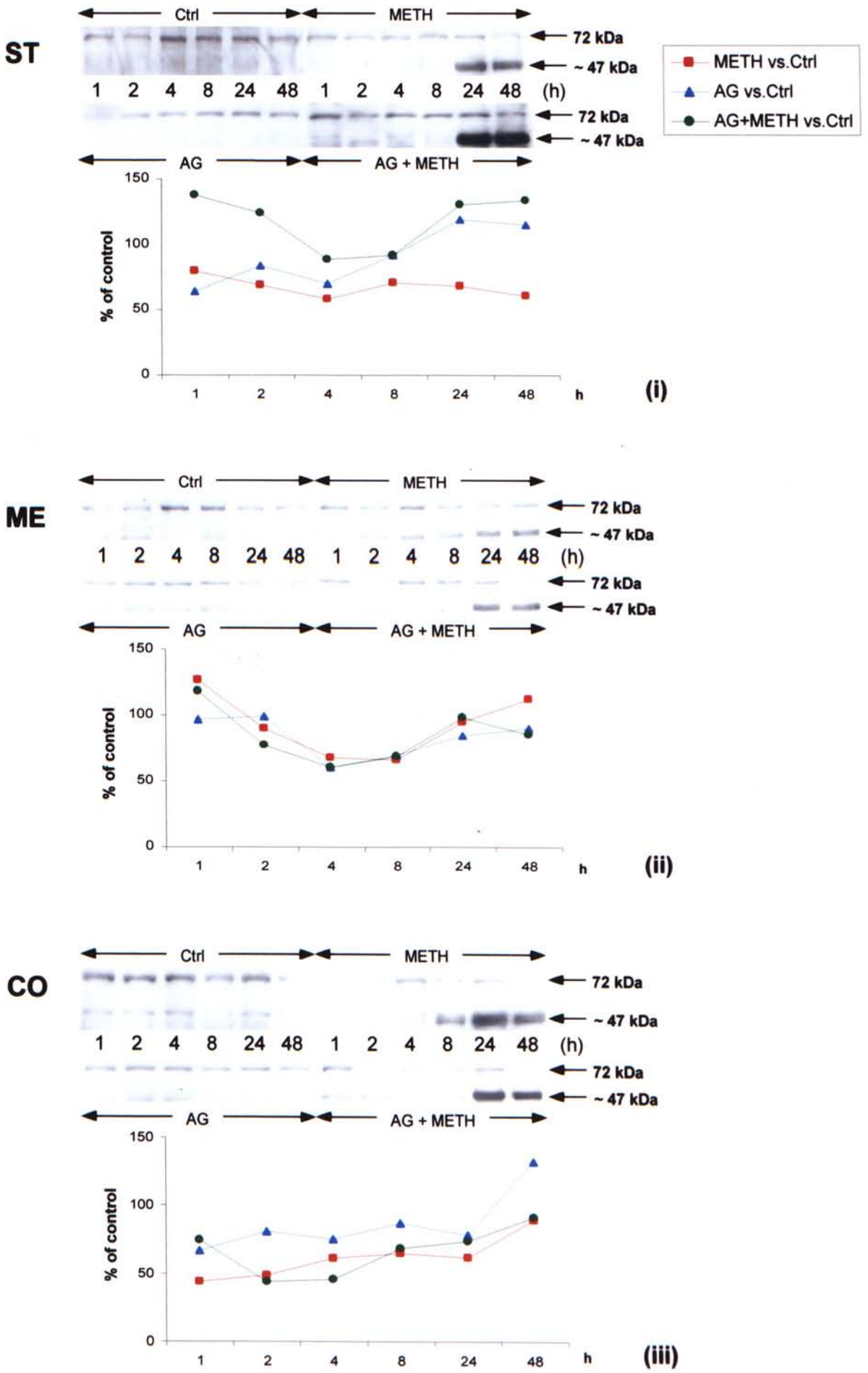
ST
Ctrl
METH
72 kDa
~ 47 kDa
1 2 4 8 24 48 1 2 4 8 24 48 (h)
AG
AG + METH
% of control
150
100
50
0
1 2 4 8 24 48 h
(i)
METH vs.Ctrl
AG vs.Ctrl
AG+METH vs.Ctrl
ME
(ii)
CO
(iii)

Fig. 13b A representative Western blot of cyclooxygenase-2 (COX-2) protein expression in striatal (i), mesencephalic (ii) and cortical (iii) astrocytes cultured in control, 4 mM METH, 10 μM INDO or 10 μM INDO + 4 mM METH media. Change in the relative levels of COX-2 expression from 1 to 48 h was expressed as a percentage of the control.

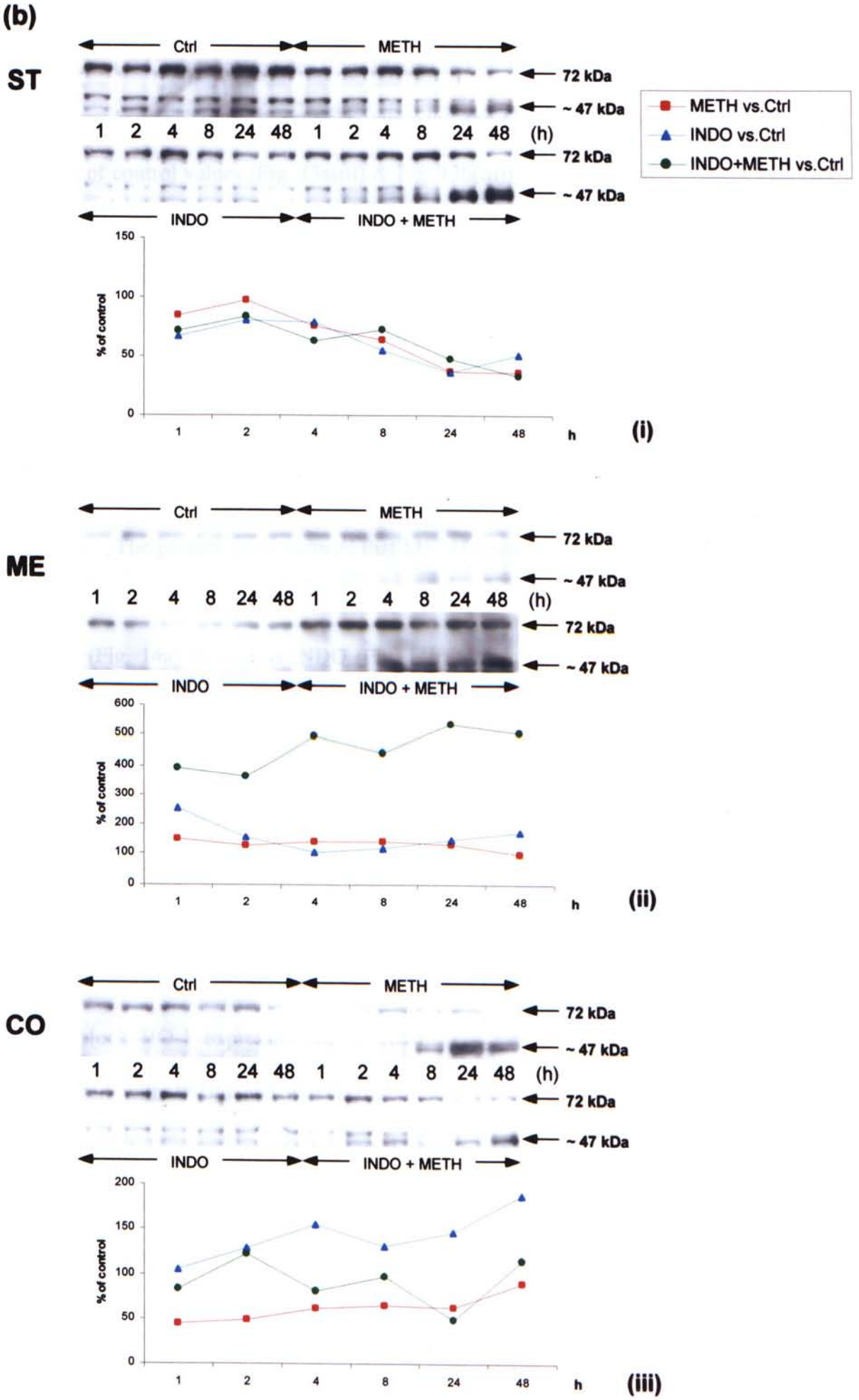
(b)
ST
Ctrl
METH
72 kDa
~ 47 kDa
1 2 4 8 24 48 1 2 4 8 24 48 (h)
INDO
INDO + METH
METH vs.Ctrl
INDO vs.Ctrl
INDO+METH vs.Ctrl
% of control
h
(i)
ME
(ii)
CO
(iii)

(c) Cortical astrocytes (Fig. 13a(iii) & Fig. 13b(iii))

In METH-treated cortical astrocytes, the COX-2 level was 10 – 50% below that of control values (Fig. 13a(iii) & Fig. 13b(iii)). When cells were treated with AG and METH, there were minimal changes in COX-2 levels although the breakdown product could be readily observed (Fig. 13a(iii)). Similarly, after INDO and METH treatment, there were also minimal changes in the COX-2 levels and that the treatment of INDO did not ameliorate the presence of the breakdown product (Fig. 13b(iii)).

### 3.1.10 Change in Heme-oxygenase-1 (HO-1) Protein Levels

The present study showed that METH treatment result in the elevation of HO-1 levels in astrocytes cultured from all three regions. Cells were further treated with AG (Fig. 14a) as well as INDO (Fig. 14b) to examine whether inhibiting iNOS and COX-2 respectively can block the elevation of HO-1 protein expression.

(a) Striatal astrocytes (Fig. 14a(i) & Fig. 14b(i))

In METH-treated striatal astrocytes, there was an increase in HO-1 level from 8 – 48 h post treatment, reaching a maximum of 1.85 (Fig. 14b(i)) – 3 (Fig. 14a(i)) fold increase by 48 h treatment. The addition of 300 μM AG with METH partially blocked the METH-induced HO-1 expression. At 48 h post-treatment, AG was shown to block HO-1 expression by approximately 50% (Fig. 14a(i)). When cells were treated with INDO and METH, there was no change in the HO-1 level at 24 h treatment. However, at 48 h treatment, there was a partial effect (Fig. 14b(i)).

(b) Mesencephalic astrocytes (Fig. 14a(ii) & Fig. 14b(ii))

When mesencephalic astrocytes were treated with METH, there were sharp and rapid elevations in HO-1 levels from 2 h onwards (Fig. 14a(ii) and Fig. 14b(ii)). A 5 fold increase at 2 h was observed. Cells treated with AG alone also showed an

Fig. 14a A representative Western blot of heme-oxygenase-1 (HO-1) protein expression in striatal (i), mesencephalic (ii) and cortical (iii) astrocytes cultured in control, 4 mM METH, 300 μM AG or 300 μM AG + 4 mM METH media. Change in the relative levels of HO-1 expression from 1 to 48 h was expressed as a percentage of the control.

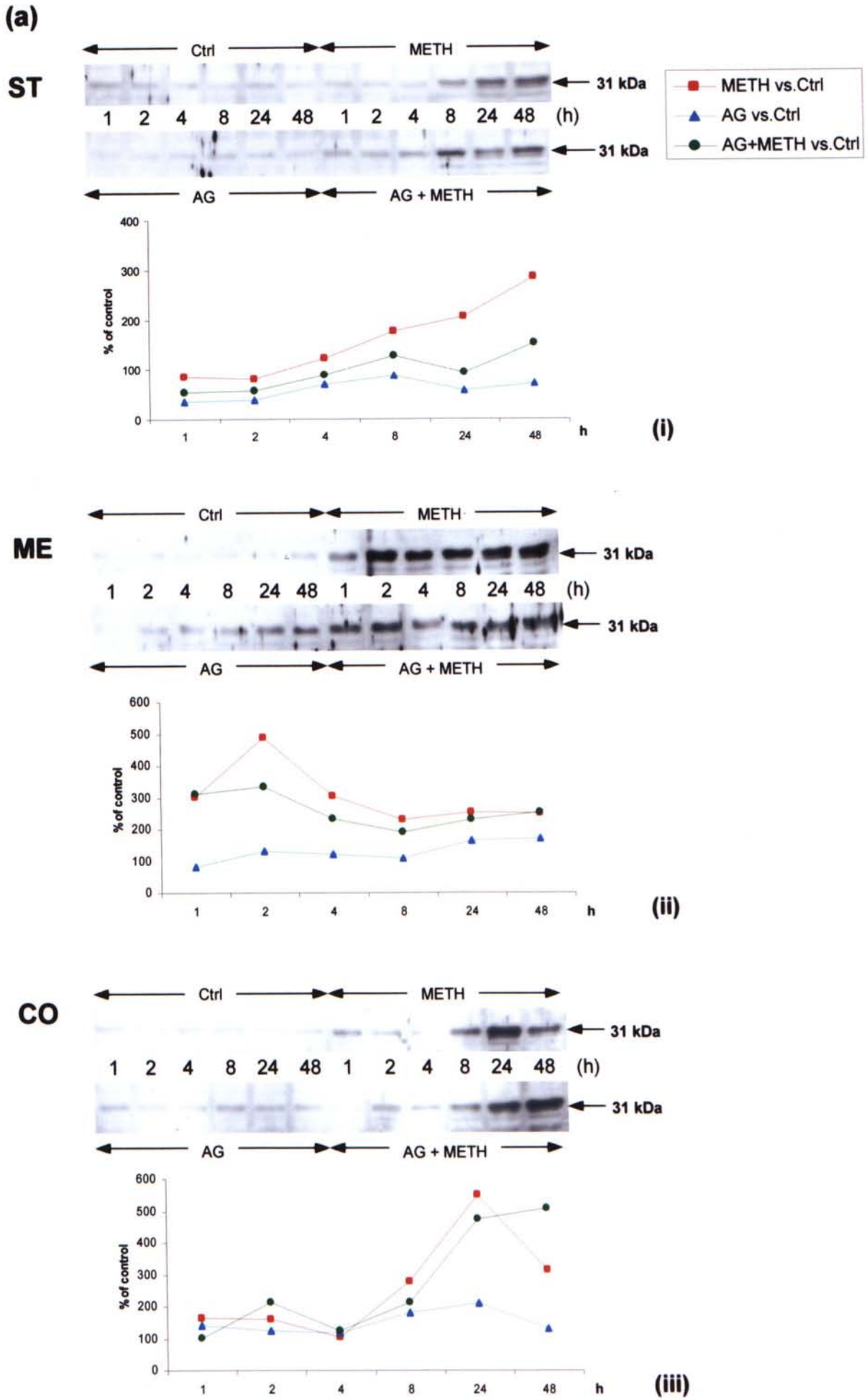
(a)
ST
Ctrl
METH
31 kDa
1 2 4 8 24 48 1 2 4 8 24 48 (h)
31 kDa
AG
AG + METH
METH vs.Ctrl
AG vs.Ctrl
AG+METH vs.Ctrl
% of control
h
(i)
ME
Ctrl
METH
31 kDa
1 2 4 8 24 48 1 2 4 8 24 48 (h)
31 kDa
AG
AG + METH
% of control
h
(ii)
CO
Ctrl
METH
31 kDa
1 2 4 8 24 48 1 2 4 8 24 48 (h)
31 kDa
AG
AG + METH
% of control
h
(iii)

Fig 14b A representative Western blot of HO-1 protein expression in striatal (i), mesencephalic (ii) and cortical (iii) astrocytes cultured in control, 4 mM METH, 10 μM INDO or 10 μM INDO + 4 mM METH media. Change in the relative levels of HO-1 expression from 1 to 48 h was expressed as a percentage of the control.

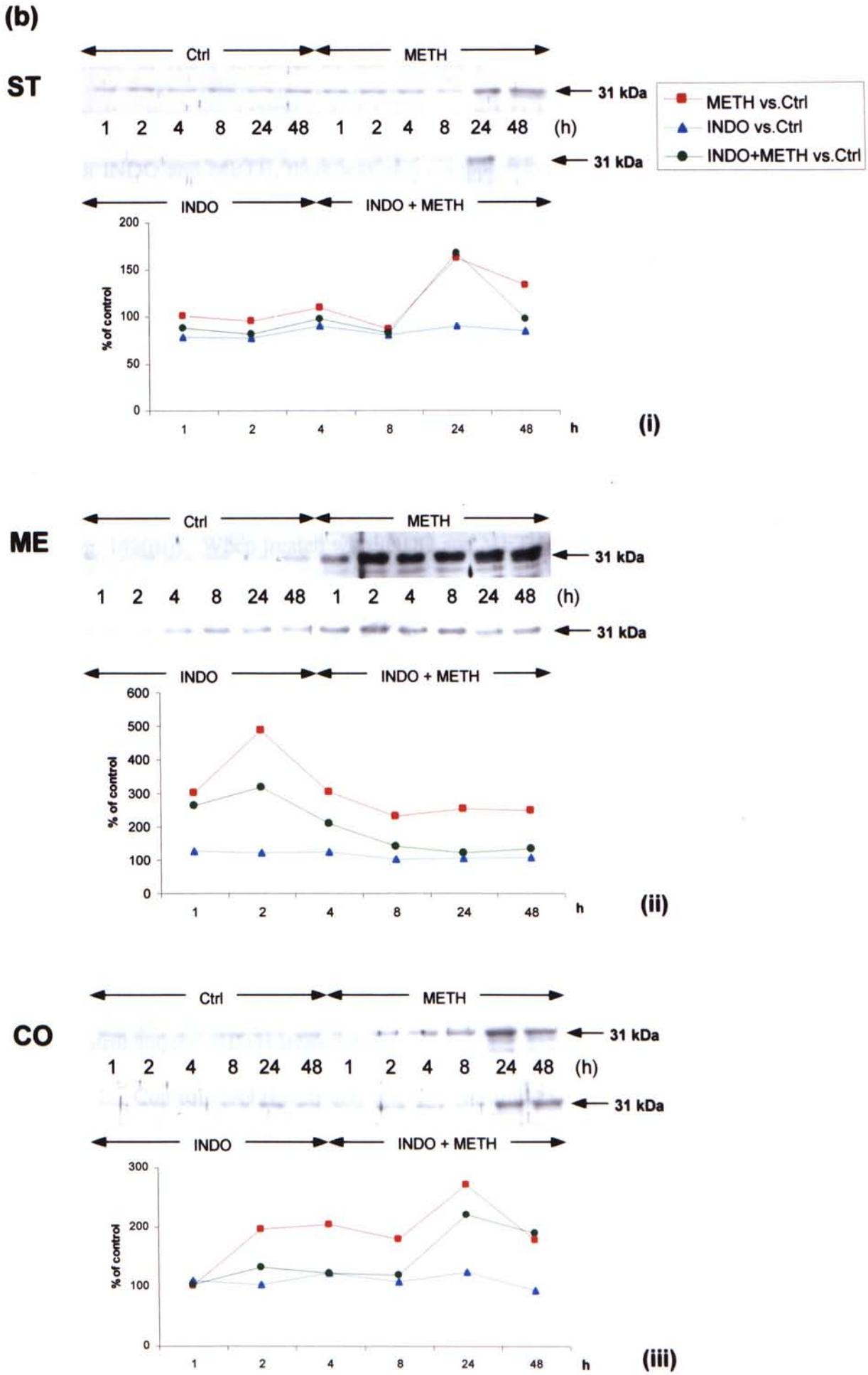
(b)
ST
Ctrl
METH
31 kDa
1 2 4 8 24 48 1 2 4 8 24 48 (h)
31 kDa
METH vs.Ctrl
INDO vs.Ctrl
INDO+METH vs.Ctrl
INDO
INDO + METH
% of control
h
(i)
ME
Ctrl
METH
31 kDa
1 2 4 8 24 48 1 2 4 8 24 48 (h)
31 kDa
INDO
INDO + METH
% of control
h
(ii)
CO
Ctrl
METH
31 kDa
1 2 4 8 24 48 1 2 4 8 24 48 (h)
31 kDa
INDO
INDO + METH
% of control
h
(iii)

increase in HO-1 levels at 24 and 48 h (Fig. 14a(ii)). Addition of AG to METH partially attenuates METH-induced increase in HO-1 levels. When cells were treated with INDO and METH, there was also a suppression of HO-1 levels to near control levels (Fig. 14b(ii)).

(c) Cortical astrocytes (Fig. 14a(iii) & Fig. 14b(iii))

Cortical astrocytes showed an approximately 3 (Fig. 14b(iii)) to 5 fold (Fig. 14a(iii)) increase in HO-1 protein content at 24 h after METH treatment. Although to a lesser extent, this increase was sustained till 48 h post-treatment. When cells were treated with AG and METH, AG cannot block the METH-induced HO-1 increase (Fig. 14a(iii)). When treated with INDO and METH, there was a slight attenuation in METH-induced HO-1 expression at 24 h treatment (Fig. 14b(iii)).

## 3.2 Cell Viability on CATH.a-Astrocyte Cocultures After METH Treatment

Figure 15 showed the percentage of dead cells in CATH.a cell line as well as CATH.a-astrocyte cocultures with or without METH treatment. The percentage of dead CATH.a cells without METH treatment increased from 3.1 ± 0.8 to 13.4 ± 2.3% at 4 to 48 h. METH treatment resulted in an increase of 12.4 ± 1.5 to 17.4 ± 1.7% dead cells at 4 to 48 h. There was a significant increase ($p < 0.05$) at 4 h between the control and the METH-treated group.

Control CATH.a-striatal astrocyte cocultures showed the percentage of dead CATH.a cells ranging from 11.1 ± 2.3 to 18.6 ± 0.9% at 4 to 48 h. There was a significant difference ($p < 0.05$) at 4 h between the CATH.a-astrocyte cocultures and that of CATH.a cell line.

METH treatment enhanced the percentage of CATH.a dead cells from 29.2 ± 0.8 to 32.5 ± 4.2% at 4 to 48 h. This increase was significant ($p < 0.05$) at 4 and 48 h

Fig. 15 The percentage of dead CATH.a cells observed in CATH.a cells alone (CL), CATH.a cells cocultured with astrocytes from the striatum (ST + CL), mesencephalon (ME + CL) and cortex (CO + CL) before and after METH treatment. Values are expressed as means (% of dead CATH.a cells) ± S.E. (n=8).

* Statistically different ($p<0.05$) between the METH and control groups at each time point studied

\# Statistically different ($p<0.05$) between the cell line and the cocultures.

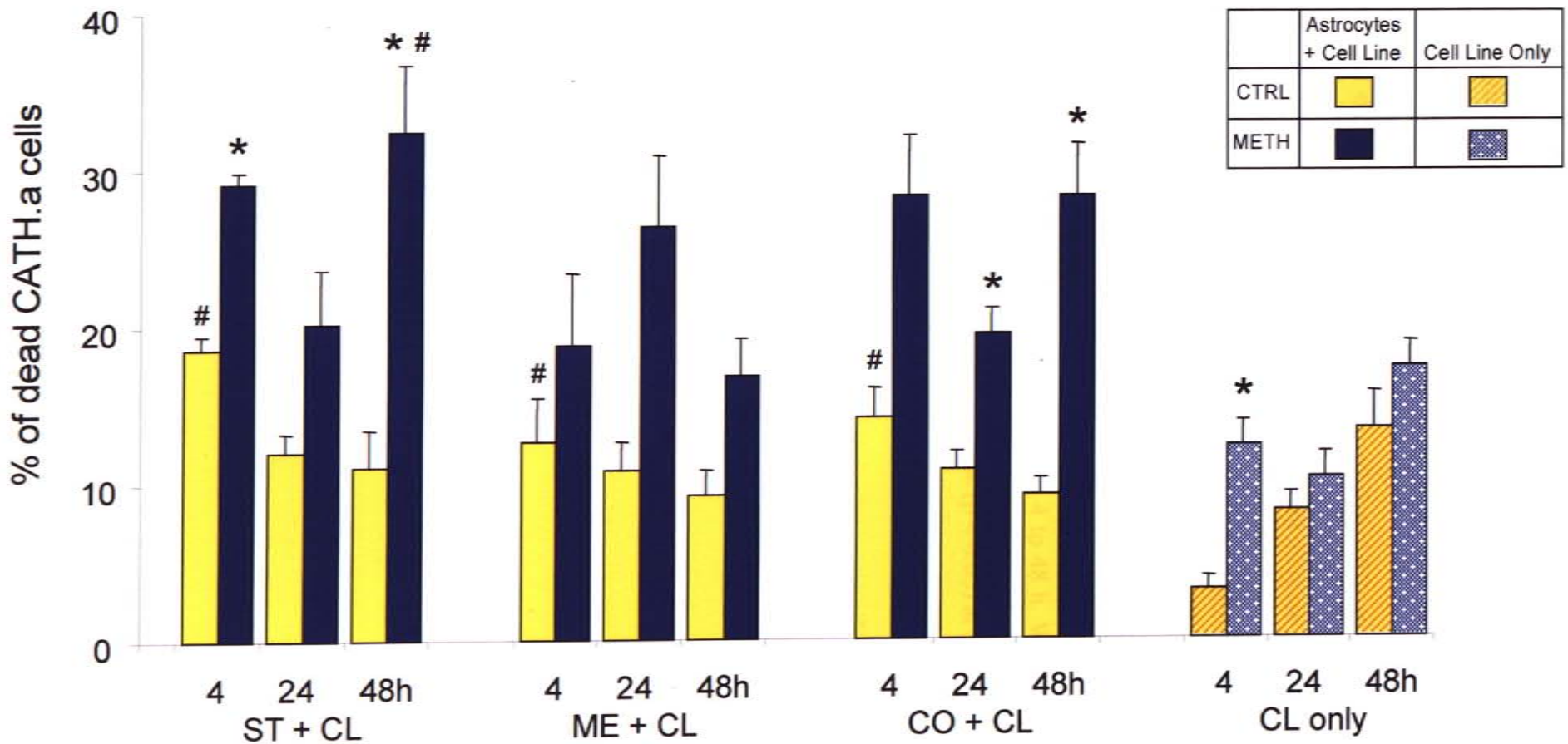
% of dead CATH.a cells
40
30
20
10
0
Astrocytes + Cell Line
Cell Line Only
CTRL
METH
4 24 48h
ST + CL
4 24 48h
ME + CL
4 24 48h
CO + CL
4 24 48h
CL only

when compared with their corresponding controls. When compared to CATH.a cell line only, a significant difference ($p < 0.05$) at 48 h was observed.

In CATH.a-mesencephalic astrocyte cocultures, the percentage of dead CATH.a control cells ranged from 9.3 ± 1.5 to 12.7 ± 2.8% at 4 to 48 h. When compared to CATH.a cell line only, there was a significant increase ($p < 0.05$) at 4 h.

METH treatment also resulted in a further increase (not significant) in the percentage of dead cells (16.9 ± 2.3 to 18.8 ± 4.7% at 4 to 48 h).

In CATH.a–cortical astrocytes cocultures, the percentage of dead CATH.a control cells ranged from 9.3 ± 1.0 to 14.1 ± 0.0% at 4 to 48 h. When compared to CATH.a cell line only, there was a significant increase ($p < 0.05$) at 4 h incubation.

METH treatment caused an increase to approximately 28.4 ± 3.8% percentage of dead CATH.a cells at 4 – 48 h. This increase was significant ($p < 0.05$) at 24 and 48 h post-treatment when compared to their corresponding controls.

## CHAPTER FOUR: DISCUSSION AND CONCLUSION

The present study showed that METH can induce astrogliosis without any neuronal influence. Astrocytes from striatum, mesencephalon and cortex were shown to change from a protoplasmic (inactive) to a fibrous (reactive) form during 48 h of METH treatment. Striatal and mesencephalic astrocytes showed a greater extent in astrogliosis when compared to cortical astrocytes.

Astrogliosis had been suggested to be a useful marker of neurotoxicity given that astrocytes become reactive in response to diverse neurotoxic insults in the CNS (Eng, 1988; O'Callaghan, 1991; Norenberg, 1994) and this is governed by the rate of astrocytic proliferation and hypertrophy (Eng and Ghirnikar, 1994). Other than morphological changes, activated, reactive astrocytes also exhibit numerous cytological and biochemical changes, including increase in cytoskeletal intermediate filament proteins GFAP, vimentin, glutamine synthetase (GS) and oxidoreductive enzyme activities(Eng and Shiurba, 1988).

Earlier results from our laboratory reported that METH-induced astrogliosis in vitro resulted in the change in GFAP, vimentin levels and GS levels (Stadlin et al., 1998). This study demonstrated that when astrocytes were treated with METH, there was a biphasic response in GFAP levels. Striatal astrocytes demonstrated an initial decrease in GFAP levels at 8 h prior to a marked increase at 48 h. There was also a concomitant increase and decrease in vimentin levels at these time points respectively. On the contrary, mesencephalic and cortical astrocytes responded with an initial increase in GFAP content at 8 h post-treatment, followed by a decrease at 48 h METH treatment. Similarly, vimentin levels were contrasting to that of GFAP levels. It was suggested that this may be reflective of vimentin levels pertaining to the

active proliferating pool, whereas the declined GFAP levels observed from 8 h onwards were reflective of the morphologically differentiated pool (Stadlin et al., 1998). It had also been suggested that the inhibition of GFAP synthesis immediately following injury is a protective mechanism whereby astrogliosis is a delayed response (Eng and Shiurba, 1988).

In previous in vivo studies of METH-induced neurotoxicity, reactive astrogliosis were shown to be present in the striatum after 3 days of METH treatment (Hess et al., 1990; Pu et al., 1994; Pu and Vorhees, 1995; Broening et al., 1997). An in vitro study on rat fetal mesencephalic cells showed that astrogliosis occurred 24 h after METH treatment (Sheng et al., 1994). The present study showed that astrogliosis occurred as early as 8 h post-treatment. Although O'Callaghan and Miller (1994) suggested that astrogliosis is the result of METH-induced neuronal injury, the present study however showed that METH can induce astrogliosis in the absence of neurons. Therefore, astrogliosis after METH treatment is not just a marker for neuronal toxicity, but that reactive astrocytes may have an important role in mediating METH-induced neurotoxicity as well.

Vacuolation was observed in astrocytes from all three regions by 8 h METH treatment. Vacuole formation was also observed in cultured ventral midbrain neurons after METH treatment (Cubells et al., 1994). This suggested that vacuole formation is not a cell-type specific phenomenon. METH is a weak base that alkalized acidic intracellular organelles like lysosomes, endosomes and synaptic vesicles (Sulzer and Rayport, 1990). Astrocytic swelling represents one of the earliest pathological features of most CNS injuries, in which adaptive responses to ionic, pH and osmolarity changes were made in order to maintain homeostasis for the neuronal environment (Kimelberg and Ransom, 1986). Since METH will result in the change

in intracellular pH, vacuolation may be an early response to such a change. The further examination of pH changes using an pH indicator fluorescent probe, 2',7'-(bis-carboxyethyl)-5,6-carboxylfluorescein (BCECF) may elicit this association.

In a previous study of our laboratory, another astrogliosis marker, GS, was also examined. GS catalyzes the conversion of glutamine from GLU and ammonia in astrocytes (Martinez-Hernandez et al., 1977) and therefore, is a pivotal enzyme in disposing the neurotoxic effects of GLU and ammonia and also in providing glutamine for oxidative stress. It was shown that the amount of GS were depleted more rapidly in striatal astrocytes followed by mesencephalic astrocytes reaching 10% of control by 48 h, whereas cortical astrocytes showed only a 50% depletion by 48 h treatment (Stadlin et al., 1998). GS is an enzyme known to be inactivated by metal-catalyzed oxidation reactions, and it had been shown that the decrease in GS activity observed in Alzheimer's disease is a result of cumulative oxidative damage (Carney and Floyd, 1991; Floyd, 1991; Smith et al., 1991). It had been reported that there was a rapid depletion of GS obtained in striatal and mesencephalic astrocytes, suggesting that astrocytes of the dopaminergic system are more sensitive to METH-induced oxidative injury. Therefore METH can act directly on astrocytes in vitro to induce oxidative injury to these cells, this may in turn contribute to METH-induced neuronal injury. In the present study, it was demonstrated that METH induced ROS production in astrocytes during the 48 h of METH treatment. The order of response time and the amount of ROS production after METH treatment is striatal > mesencephalic > cortical astrocytes. When the rate of change in ROS production was examined in astrocytes with or without METH treatment, it was shown that, control striatal astrocytes showed a significant increase in rate of change when compared to astrocytes from the other 2 regions. When striatal astrocytes were treated with METH

for 120 min, the rate of change of ROS production was significantly higher than its control group. From the present study, it seemed that striatal astrocytes are more prone to ROS production and that they are the most sensitive to METH toxicity.

Although the cellular and molecular events involved in METH-induced neurotoxicity remains to be elucidated, oxidative stress has been suggested to be one of the prime candidates (Wagner et al., 1980; Seiden and Vosmer, 1984; DeVito and Wagner, 1989a; Cubells et al., 1994; Giovanni et al., 1995; Cadet and Brannock, 1998; Moszczynska et al., 1998; Yamamoto and Zhu, 1998; LaVoie and Hastings, 1999).

In the present study, it was shown that astrocytes were also subjected to oxidative stress after METH administration. Astrocytes from the dopaminergic areas seemed to be most vulnerable since the highest amount of ROS was generated from these cells. Given that DA neurons are the most vulnerable to METH-induced toxicity, the release of ROS from astrocytes may further enhance neuronal toxicity. Indeed this was the case, in the astrocyte-neuronal cocultures, it was demonstrated the percentage of neuronal cell death was increased approximately 2 fold when cocultured with astrocytes and in particular, striatal astrocytes. Recently, it was shown that striatal astrocytes participated in the deamination of DA via monoamine oxidase B, a process that can be inhibited by METH resulting in increased intracellular DA formation (Kita et al., 1998). This increase in DA content may lead to further autoxidation of DA resulting in increase free radicals production. Given that there is an increase in ROS production in striatal astrocytes as demonstrated in the present study, as well as METH's ability to inhibit its role in DA deamination, striatal astrocytes may play an important role in the enhancement of dopaminergic nerve terminals to oxidative damage after METH treatment

It seemed therefore astrocytes may mediate METH-induced neurotoxicity via oxidative stress with regional selectivity.

Furthermore, Moszczynska et al., (1998) showed that levels of glutathione (GSH) are selectively decreased in striatum of rodents exposed to high neurotoxic doses of METH. It is well known that astrocytes contain relatively high concentrations of GSH and glutathione peroxidase (GSH-Px) when compared with neurons (Slivka et al., 1987; Raps et al., 1989). The presence of high GSH levels in these cells suggested that astrocytes are the major site for $H_2O_2$ detoxification in the CNS and thus protecting them as well as neighboring neurons from oxidative-induced injury. Therefore, depleted striatal GSH content may indicate that striatal astrocytes are less capable to removing ROS thus making the striatal region more prone to METH-induced oxidative stress.

Mitochondrial electron transport has long been recognized as a major intracellular source of ATP production. In addition, mitochondria is one of the key targets for the toxic actions of ROS. ROS themselves may have deleterious effect on respiratory chain function. Studies on isolated mitochondria suggest that oxidative damage to the respiratory chain results in deficiencies of complexes I and II followed by complex III and then, in some systems, complex IV (Narabayashi et al., 1982; Hillered and Ernster, 1983; Zhang et al., 1990), and therefore, interfering with ATP production.

In the present study, METH caused the most rapid ATP depletion in striatal astrocytes when compared to mesencephalic and cortical astrocytes. Striatal astrocytes seemed to be less capable in maintaining a high ATP content during METH treatment. This present result clearly demonstrated that astrocytes from non-dopaminergic areas, for example, the cerebral cortex, are less affected after METH treatment Cortical

astrocytes maintain almost the same ATP level after 48 h METH treatment as untreated control.

Chan et al., (1994) showed that doses of METH that depleted striatal DA also caused a significant and rapid decrease in striatal ATP concentrations. The ATP-depleting effects of METH appear to be selective because they were observed only in the striatum and not in the cerebellar cortex and hippocampus. The results here are in line with this in vivo study where ATP depletion was also shown to be selectively in the striatal region but not in cortex. Pontieri et al. (1990) also showed that there was an association between the METH-induced early increase in the regional cerebral glucose consumption and long-lasting dopaminergic neurotoxicity (Pontieri et al., 1990). More recently, it was reported that exposure to METH or prolonged hyperpyrexia decreased mitochondrial immunoreactivity (Burrows and Meshul, 1999). All these findings plus the present results suggested a correlation between METH-induced perturbations of energy metabolism and dopaminergic neurotoxicity.

The present study also showed that there was a reduction in mitochondrial membrane potential ($\Delta\Psi m$) after METH treatment in all astrocytes. $\Delta\Psi m$ were shown to decrease at 8 – 12 h post treatment in which striatal astrocytes showed a decrease in $\Delta\Psi m$ at 8 h treatment whereas cortical and mesencephalic showed a decrease at 12 h post-treatment. It is known that marked increases in mitochondrial $Ca^{2+}$, increased in ROS levels, or partial failure of the respiratory complexes, acting either individually or together, can induce a decrease in $\Delta\Psi m$ (Richter and Schlegel, 1993). Therefore, disruption of this electric potential may be another marker for the indication of astrocytes' energy status. The earlier reduction in $\Delta\Psi m$ that was observed in striatal astrocytes (8 h post-treatment) may be related to the its rapid loss in ATP suggesting that METH alters the energy status of astrocytes. This earlier disruption of $\Delta\Psi m$ and

rapid depletion of ATP production may render these cells having an additive effect in METH-induced neuronal injury.

The present study clearly demonstrated that METH alone can stimulate the production of NO from astrocytes cultured from all three regions from 1 h post treatment. nNOS had been suggested to play an important role in METH-induced dopaminergic neurotoxicity as demonstrated in nNOS knockout mice (Itzhak et al., 1998) and other in vivo (Abekawa et al., 1996; Di Monte et al., 1996; Itzhak and Ali, 1996) and in vitro (Sheng et al., 1996) studies where neuroprotection can be observed if nNOS was suppressed. It was proposed from these studies that one of the mechanisms of METH-induced toxicity may be due to the release of GLU (Nash and Yamamoto, 1992), resulting in a sustained activation of NMDA receptors. This will result in increased NO formation, $Ca^{2+}$ influx and stimulation of nNOS (Di Monte et al., 1996;Itzhak et al., 1998). This tenet was also supported by either the NMDA receptor antagonist dizocilpine (MK-801) (Sonsalla et al., 1989, 1991) in the protection against METH-induced DA depletion or the use of NOS inhibitor $^{N}$G-nitro-arginine (NNA) and L-NAME in the protection against METH-induced DA release in the striatum (Bowyer et al., 1995).

The role of astrocytes and iNOS stimulation and NO production were recently reported to be also involved in METH-induced toxicity. iNOS knockout mice can attenuate METH-induced neurotoxicity (Ali and Itzhak, 1998) and therefore it was believed that iNOS, which located mainly in astrocytes (Park et al., 1994), are involved in METH-induced injury as well.

From the present study, it is clear that in the absence of neurons or high GLU content, METH can also stimulate NO production in astrocytes. This release was suggested to be due to the induction of iNOS since the addition of selective iNOS

inhibitor, aminoguanidine (AG), attenuated NO production. It had been shown that astrocytes in culture do not express NMDA receptors (Backus et al., 1989; Cornell-Bell et al., 1990) although astrocytes in situ can express NMDA receptors in some brain regions like cortex, thalamus, hippocampus, olfactory bulb, amygdala, but not in the striatum and mesencephalon (Porter and McCarthy, 1997). Given that the astrocytes cultured from all three regions had a similar increase in NO formation, in this case, it is unlikely that the stimulation of NMDA receptors participated in the release of NO. This implied that the mechanisms of neuronal and astrocytic NO release might be different.

Another role of NO in association with METH-induced toxicity may be related to the effects of METH-induced hyperthermia as it was observed in nNOS knockout mice where METH had no significant effect on body temperature in these mice (Itzhak et al., 1998) or where L-NAME was able to antagonize the hyperthermic effects of METH (Taraska and Finnegan, 1997). On the other hand, $PGE_2$ is a major putative pyrogenic substance in the CNS that regulated by its rate-limiting enzyme COX-2 (Kluger, 1991). Increasing evidence suggests that there is considerable "cross-talk" between COX and NOS (Appleton et al., 1996; Di Rosa et al., 1996; Salvemini and Masferrer, 1996). Therefore, a COX-2 inhibitor indomethacin (INDO) was also added to examine the interaction of $PGE_2$ with METH-induced NO release. The current results showed that INDO not only unable to inhibit the METH-induced NO release, but rather increased NO release instead. When INDO was added with METH, the level of NO was further enhanced. Based on these findings, one could speculate that in the pathway of METH-induced NO release, $PGE_2$ may take an inhibitory role since the blocking of COX-2 activity resulted in an increase in NO production in the control group. METH treatment further enhanced this release of NO levels. An

inhibitory action of PGs on NO production had been illustrated in J774.2 macrophages in which exogenously added $PGI_2$ (iloprost) and $PGE_2$, both at nanomolar concentrations, inhibited the LPS-stimulated induction of iNOS (Marotta et al., 1992). A similar role for PGs on the NO pathway has also been demonstrated in murine peritoneal macrophages primed in vivo and activated in vitro with LPS (Raddassi et al., 1993). $PGE_2$ added during the transition from primed to activated state, i.e. at the same time as LPS, decreased, while INDO increased, both NO production and cytostatic activity suggesting an inhibitory action of PGs on iNOS induction in these cells.

To further examine METH-induced hyperthermic effects on astrocytes, COX-2 protein expression was also investigated using Western blot analysis. There was minimal change in COX-2 expression after METH treatment suggesting that $PGE_2$ mediated hyperthermic effects in astrocytes may not be the main pathway in METH-induced neurotoxicity.

However, striatal astrocytes showed a slight increase in COX-2 levels after co-administration of AG + METH suggesting that METH-induced NO production may inhibit COX-2 expression. This relationship was also reported in fetal ovine astrocytes in which application of sodium nitroprusside (SNP), which is an exogenous NO-donor, reduced basal production of PGs (Busija and Thore, 1997). In other cell models, the SNP has been found to inhibit both the expression of COX-2 and the activity of this enzyme in J774.2 macrophages challenged with LPS (Swierkosz et al., 1995). Moreover, L-NMMA caused a significant increase in $PGI_2$ release and increased COX-2 protein expression suggesting that endogenous NO had a similar inhibitory role. Therefore, METH-induced NO release may exert an inhibitory effect

on COX-2 expression in striatal astrocytes, although cells from other 2 regions showed minimal response.

On the other hand, mesencephalic astrocytes showed a 4.2 fold increase of COX-2 protein expression after co-administration of INDO and METH. As mentioned earlier, INDO alone or together with METH was shown to enhance NO release in control or METH-treated astrocytes. It seems quite likely that METH-stimulated massive NO release after removal of $PGE_2$ may be the crucial factor in eliciting the COX-2 protein expression. It can be speculated that NO may participate in a positive feedback mechanism to upregulate COX-2 expression once after the blocking of $PGE_2$ synthesis was initiated. This may explain the increase in COX-2 protein observed in mesencephalic astrocytes. Thus, in this case, NO may possibly take a stimulatory role in mesencephalic astrocytes to produce more COX protein, restoring $PG_2$ synthesis. Previous studies have shown that NO was found to activate PGs production in murine astroglia (Molina-Holgado et al., 1995). One possible interaction has been suggested to be at the level of the enzyme, since the COX-2 enzyme is a potential target for NO because it contains an iron-heme center at its active site (Yonetani et al., 1972). However, at present it is unclear whether the COX-2 activities are also being upregulated. Further study in measuring $PGE_2$ levels would further clarify this point. Moreover, it is of interest that there is an opposite role in modulating COX-2 by NO between striatal and mesencephalic astrocytes. This may be one of the reasons for regional selectivity of METH-induced neurotoxicity.

Cortical astrocytes showed a lesser extent in pyrogenic effects suggested that astrocytes in this region may provide better protection against METH toxicity.

COX-2 breakdown products were observed in astrocytes of all 3 regions after METH treatment. It seemed that METH destroys COX-2 protein integrity, however, how this may affect $PGE_2$ activity in the cascade of events awaits further studies.

The degree in which hyperthermia contributes to METH-induced neurotoxicity is not fully understood, numerous reports showed that both lowering of the ambient temperature (Bowyer et al., 1992; Ali et al., 1994a) or the administration of various pharmacological agents like MK-801, dopamine receptor antagonists, fenfluramine, propranolol, etc (Miller and O'Callaghan, 1994; Albers and Sonsalla, 1995; Farfel and Seiden, 1995) protected against METH-induced toxicity. Albers and Sonsalla (1995) however argued that hyperthermia may not be required for METH-induced neurotoxicity based on the evidence that reserpine, a compound that lowers core temperature, did not provide protection against METH-induced toxicity. In contrast, Cappon et al. (1997) showed that the administration of METH together with elevated ambient temperature induced hyperthermia, reduced striatal DA level and increased GFAP expression. These effects were not evident if ambient temperature was not increased. This study not only suggested that hyperthermia was necessary to produce METH-induced neurotoxicity, but that reactive astrocytes also played a role in this hyperthermic response.

The present study showed that there was an induction of HO-1 protein expression with the level of expression being cortical > mesencephalic > striatal astrocytes. HO-1 is a HSP (Shibahara et al., 1987) and was shown to be induced in the brain by hyperthermia (Ewing and Maines, 1991). HSP production as a consequence of METH treatment has also been demonstrated. It was shown that there was an increased expression in 72-kDa HSP (HSP72) in the hippocampus and striatum after an acute dose of METH (Goto et al., 1993; Kuperman et al., 1997). Since HO-1 is

rarely induced in neuronal cells (Ewing and Maines, 1991; Dwyer et al., 1995), it thus seemed possible that astrocytes may also participate in the heat shock response to METH treatment.

The present study showed that there was METH-induced HO-1 expression in astrocytes cultured from all 3 regions. This effect was partially inhibited by the addition of iNOS inhibitor, AG, in striatal and mesencephalic astrocytes suggesting that NO may mediate the effects of the heme-oxygenase system. The effects of NO on the heme-oxygenase system was also demonstrated in human glioblastoma cell line T98G where the addition of NO donors induced HO-1 expression (Takahashi et al., 1996). Furthermore, it was also known in astrocytes that LPS- or SNAP- induced enhancement of $NO_2^-$ and HO-1 levels could be inhibited by NOS inhibitor such as NNA suggesting NO and iNOS production by astrocytes may cause the autocrine and paracrine induction of HO-1 (Kitamura et al., 1998). These authors suggested that NO induced HO-1 expression may be mediated by the activation of activator protein-1 (AP-1) and/or the metal-responsive transcription factor-1 (MTF-1) site on the promoter region of HO-1 gene.

However, the lack of effect by AG in suppressing HO-1 expression in cortical astrocytes suggested that there may be other factors apart from NO that is involved in HO-1 induction. HO-1 gene has a heat-shock element in its promoter that can be upregulated not only by hyperthermia but by other factors including oxidative stress (Dalton et al., 1996). Oxidative stress associated HO-1 induction had been demonstrated in glutathione depletion or exposure to hydrogen peroxide ($H_2O_2$) in the brain (Dwyer et al., 1992; Ewing and Maines, 1993) and other mammalian cells (Applegate et al., 1991; Bauer et al., 1998). There was an increase in ROS level in cortical astrocytes although it was relatively lower than that of striatal and

mesencephalic astrocytes, however, it may be sufficient to induce HO-1 expression. Therefore, cortical astrocytes may offer better protection to nearby neurons and thus indicating that this non-dopaminergic area is the least affected under METH toxicity.

The present study demonstrated that $PGE_2$ would also be involved in METH-induced neurotoxicity. It was shown that HO-1 level in mesencephalic astrocytes was fully attenuated whereas in striatal and cortical astrocytes, HO-1 level was only partially attenuated. Previous studies showed that in porcine aortic endothelial cells, $^{12}\Delta$-$PGJ_2$, metabolite of PGs, stimulated HO-1 activity. Therefore, in this case, it is not surprising that suppression of PGs synthesis can attenuate the METH-induced HO-1 expression. However, the detailed mechanism behind is still far from clear.

The present result demonstrated that NO, COX-2 and HO-1 are involved in METH-mediated hyperthermic effects.

In METH-induced neurotoxicity, it is still unclear whether the astrocytes or the neurons take an initiative role in mediating this toxic cascade. In the present study, CATH.a-astrocyte cocultures were established to examine this interaction. Results indicated that when CATH.a cells were cocultured with astrocytes, there was a decrease in CATH.a cell viability. When treated with METH, this loss of cell viability was further decreased. This decrease in CATH.a cell viability was evident as early as 4 h incubation. Since there was no significant increase in LDH activity in astrocytes during the 48 h of METH treatment, it can be assumed that the decrease in CATH.a cell viability is a result of astrocytic oxidative and metabolic stress and not loss in astrocytic cell viability. Results from METH-treated CATH.a-astrocytes cocultures suggested that astrocytes may exert adverse influences to neurons. When CATH.a cells were cocultured with striatal astrocytes, the percentage of dead cells observed at 4 h METH treatment increased 5 and 1.5 fold in cocultures and CATH.a cells

respectively. In this case, it seems that striatal astrocytes further enhanced METH-induced neuronal toxicity. In vivo studies showed that METH causes a massive dopaminergic terminal damages in the striatum (Fibiger and McGeer, 1971; Kogan et al., 1976; Seiden et al., 1976; Gibb and Kogan, 1979; Hotchkiss and Gibb, 1980b; Steranka and Sanders-Bush, 1980; Wagner et al., 1980; Kovachich et al., 1989; Brunswick et al., 1992). If striatal astrocytes in this region produced the highest amount of ROS and suffer the most severe loss of ATP after METH injury, this may in turn produce further damage to the nearby neuronal terminals which are also under the toxic influence of METH.

CATH.a cells cocultured with mesencephalic astrocytes although showed an increased in the percentage of dead CATH.a cells, this increase was not significant and to a lesser extent when compared to striatal astrocytes. It may probably due to the fact that astrocytes from mesencephalon offer better protection to the neuronal cell bodies since mesencephalic astrocytes showed the earliest response (2 h) in increased HO-1 levels after METH treatment. This increase in HO-1 level may provide an earlier protection to nearby neurons to combat against METH-induced oxidative stress. Therefore, it is not surprising that although METH attack the dopaminergic system, mesencephalon is not as severely damaged when compared to the striatum.

In conclusion, the present study showed that astrocytes cultured from different regions of the brain showed differential responses to METH-induced oxidative and metabolic stress, in which, the striatal astrocytes were the most severely affected. Moreover, NO and ROS production are also shown to mediate METH-induced hyperthermic responses. It seems that if striatal astrocytes are more prone to oxidative and metabolic stress, this will make the neuronal environment in the striatum more susceptible to oxidative damage. The present findings showing an increase in the

percentage of dead CATH.a cells when cocultured with striatal astrocytes further confirmed this hypothesis. Striatal astrocytes seemed less adaptive in providing protection to nearby terminals against METH-induced oxidative stress. This study implied that astrocytes may play a key role in mediating METH-induced neurotoxicity.

## REFERENCES


Abekawa T, Ohmori T, Koyama T (1994) Effects of repeated administration of a high dose of methamphetamine on dopamine and glutamate release in rat striatum and nucleus accumbens. Brain Res 643: 276-281.

Abekawa T, Ohmori T, Koyama T (1996) Effects of nitric oxide synthesis inhibition on methamphetamine-induced dopaminergic and serotonergic neurotoxicity in the rat brain. J Neural Transm Gen Sect 103: 671-680.

Albers DS, Sonsalla PK (1995) Methamphetamine-induced hyperthermia and dopaminergic neurotoxicity in mice: pharmacological profile of protective and nonprotective agents. J Pharmacol Exp Ther 275: 1104-1114.

Ali SF, Itzhak Y (1998) Methamphetamine and MPTP-induced dopaminergic neurotoxicity in the inducible-NOS knockout mice. Society for Neuroscience Abstr 24: 2154.

Ali SF, David SN, Newport GD, Cadet JL, Slikker WJ (1994b) MPTP-induced oxidative stress and neurotoxicity are age-dependent: evidence from measures of reactive oxygen species and striatal dopamine levels. Synapse 18: 27-34.

Ali SF, Newport GD, Holson RR, Slikker WJ, Bowyer JF (1994a) Low environmental temperatures or pharmacologic agents that produce hypothermia decrease methamphetamine neurotoxicity in mice. Brain Res 658: 33-38.

Alzeer AH, Al Arifi A, Warsy AS, Ansari Z, Zhang H, Vincent JL (1999) Nitric oxide production is enhanced in patients with heat stroke. Intensive Care Med 25: 58-62.

Amador E, Dorfman LE, Wacker WEC (1963) Serum lactate dehydrogenase: An analytical assessment of current assays. Clin Chem 9: 391-398.

Anathan J, Goldberg AL, Voellmy R (1986) Abnormal proteins serve as eukaryotic stress signals and trigger the activation of heat shock genes. Science 232: 252-254.

Angrist BM, Gershon D (1972) Psychotic sequelae of amphetamine use. In: Psychiatric Complications of Medical Drugs (Shader R, ed), pp 175. New York: Raven Press.

Ansis SF, Smith RC (1979) Amphetamine abuse and its violence. In: Amphetamine use, misuse, and abuse. (Smith DE, ed), pp 205-217. Boston: G.K. Hall.

Applegate LA, Luscher P, Tyrrell RM (1991) Induction of heme oxygenase: a general response to oxidant stress in cultured mammalian cells. Cancer Res 51: 974-978.

Appleton I, Tomlinson A, Willoughby DA (1996) Induction of cyclo-oxygenase and nitric oxide synthase in inflammation. Adv Pharmacol 35: 27-78.

Asano T, Koide T, Gotoh O, Joshita H, Hanamura T, Shigeno T, Takakura K (1989) The role of free radicals and eicosanoids in the pathogenetic mechanism underlying ischemic brain edema. Mol Chem Neuropathol 10: 101-133.

Axt KJ, Molliver ME (1991) Immunocytochemical evidence for methamphetamine-induced serotonergic axon loss in the rat brain. Synapse 9: 302-313.

Backus KH, Kettenmann H, Schachner M (1989) Pharmacological characterization of the glutamate receptor in cultured astrocytes. J Neurosci Res 22: 274-282.

Bakhit C, Gibb JW (1981) Methamphetamine-induced depression of tryptophan hydroxylase: recovery following acute treatment. Eur J Pharmacol 76: 229-233.

Bakhit C, Morgan ME, Peat MA, Gibb JW (1981) Long-term effects of methamphetamine on the synthesis and metabolism of 5- hydroxytryptamine in various regions of the rat brain. Neuropharmacology 20: 1135-1140.

Baldwin HA, Colado MI, Murray TK, De SR, Green AR (1993) Striatal dopamine release in vivo following neurotoxic doses of methamphetamine and effect of the neuroprotective drugs, chlormethiazole and dizocilpine. Br J Pharmacol 108: 590-596.

Barbe MF, Tytell M, Gower DJ, Welch WJ (1988) Hyperthermia protects against light damage in the rat retina. Science 241: 1817-1820.

Barres BA (1991) New roles for glia. J Neurosci 11: 3685-3694.

Bauer I, Wanner GA, Rensing H, Alte C, Miescher EA, Wolf B, Pannen BH, Clemens MG, Bauer M (1998) Expression pattern of heme oxygenase isoenzymes 1 and 2 in normal and stress-exposed rat liver. Hepatology 27: 829-838.

Bazan NG, Rodriguez de Turco EB, Allan G (1995) Mediators of injury in neurotrauma: intracellular signal transduction and gene expression. J Neurotrauma 12: 791-814.

Beal MF, Hyman BT, Koroshetz W (1993) Do defects in mitochondrial energy metabolism underlie the pathology of neurodegenerative diseases? Trends Neurosci 16: 125-131.

Beasley TC, Bari F, Thore C, Thrikawala N, Louis T, Busija D (1998) Cerebral ischemia/reperfusion increases endothelial nitric oxide synthase levels by an indomethacin-sensitive mechanism. J Cereb Blood Flow Metab 18: 88-96.

Beckman JS, Beckman TW, Chen J, Marshall PA, Freeman BA (1990) Apparent hydroxyl radical production by peroxynitrite: implications for endothelial injury from nitric oxide and superoxide. Proc Natl Acad Sci U S A 87: 1620-1624.

Bell DS (1965) Comparison of amphetamine psychosis and schizophrenia. Br J Psychiatry 111: 701.

Bennett MVL, Barrio LC, Bargiello TA, Spray DC, Hertzberg E, Saez JC (1991) Gap junctions: New tools, new answers, new questions. Neuron 6: 305-320.

Bernheim HA, Gilbert TM, Stitt JT (1980) Prostaglandin E levels in third ventricular cerebrospinal fluid of rabbits during fever and changes in body temperature. J Physiol (Lond) 301: 69-78.

Bignami A, Dahl D (1974) Astrocyte-specific protein and neuroglial differentiation. An immunofluorescence study with antibodies to the glial fibrillary acidic protein. J Comp Neurol 153: 27-38.

Birnbaum G, Clark HB, Psihos D (1991) Expression of heat shock proteins in the brains of patients with multiple sclerosis and other neurological diseases. Ann Neurol 30: 305.

Boje KM, Arora PK (1992) Microglial-produced nitric oxide and reactive nitrogen oxides mediate neuronal cell death. Brain Res 587: 250-256.

Bolanos JP, Peuchen S, Heales SJ, Land JM, Clark JB (1994) Nitric oxide-mediated inhibition of the mitochondrial respiratory chain in cultured astrocytes. J Neurochem 63: 910-916.

Bondy SC, Lebel CP (1993) The relationship between excitotoxicty and oxidative stress in the central nervous system. Free Radic Biol Med 14: 633-642.

Boneh A, Shohami E, Brenner T (1993) Differential effects of phorbol myristate acetate and dexamethasone on protein kinase C activity and eicosanoids production in cultured rat astrocytes. J Neurosci Res 34: 629-634.

Borg DC (1993) Oxygen fred radicals and tissue injury. In: Oxygen Free Radicals in Tissue Damage (Tarr M, Samson FE, eds), pp 12-53. Boston: Birkhauser.

Bouchama A, Parhar RS, el-Yazigi A, Sheth K, al S (1991) Endotoxemia and release of tumor necrosis factor and interleukin 1 alpha in acute heatstroke. Journal of Applied Physiology 70: 2640-2644.

Boveris A, Cadenas E (1975) Mitochondrial production of superoxide anions and its relationship to the antimycin insensitive respiration. FEBS Lett 54: 311-314.

Boveris A, Chance B (1973) The mitochondrial generation of hydrogen peroxide. General properties and effect of hyperbaric oxygen. Biochem J 134: 707-726.

Bowyer JF, Clausing P, Gough B, Slikker WJ, Holson RR (1995) Nitric oxide regulation of methamphetamine-induced dopamine release in caudate/putamen. Brain Res 699: 62-70.

Bowyer JF, Davies DL, Schmued L, Broening HW, Newport GD, Slikker WJ, Holson RR (1994) Further studies of the role of hyperthermia in methamphetamine neurotoxicity. J Pharmacol Exp Ther 268: 1571-1580.

Bowyer JF, Tank AW, Newport GD, Slikker WJ, Ali SF, Holson RR (1992) The influence of environmental temperature on the transient effects of methamphetamine on dopamine levels and dopamine release in rat striatum. J Pharmacol Exp Ther 260: 817-824.

Brecher EM (1972) Licit and Illicit Drugs. Boston: Little Brown.

Breder CD, DeWitt D, Kraig RP (1995) Characterization of inducible cyclooxygenase in rat brain. J Comp Neurol 355: 296-315.

Brenner T, Boneh A, Shohami E, Abramsky O, Weidenfeld J (1992) Glucocorticoid regulation of eicosanoid production by glial cells under basal and stimulated conditions. J Neuroimmunol 40: 273-279.

Broening HW, Pu C, Vorhees CV (1997) Methamphetamine selectively damages dopaminergic innervation to the nucleus accumbens core while sparing the shell. Synapse 27: 153-160.

Brown IR, Rush SJ (1990) Expression of heat shock genes (hsp70) in the mammalian brain: distinguishing constitutively expressed and hyperthermia-inducible mRNA species. J Neurosci Res 25: 14.

Bruner G, Simmons ML (1993) Astrocyte: Targets and sources for purines, eicosanoids, and nitrosyl compounds. In: Astrocytes: Pharmacology and Function (Murphy S, ed), pp 89-108. San Diego: Academic Press.

Brunswick DJ, Benmansour S, Tejani-Butt SM, Hauptmann M (1992) Effects of high-dose methamphetamine on monoamine uptake sites in rat brain measured by quantitative autoradiography. Synapse 11: 287-293.

Brust JCM (1993) Amphetamine and Other Psychostimulants. In: Neurological aspects of substance abuse pp 61-81. Boston: Butterworth-Heinemann.

Buening MK, Gibb JW (1974) Influence of methamphetamine and neuroleptic drugs on tyrosine hydroxylase activity. Eur J Pharmacol 26: 30-34.

Bureau M, Laschet J, Bureau-Heeren M, Hennuy B, Minet A, Wins P, Grisar T (1995) Astroglial cells express large amounts of GABAA receptor proteins in mature brain. J Neurochem 65: 2006-2015.

Burrows KB, Meshul CK (1999) High-dose methamphetamine treatment alters presynaptic GABA and glutamate immunoreactivity. Neuroscience 90: 833-850.

Busija DW, Thore C (1997) Modulation of prostaglandin production by nitric oxide in astroglia. Prostaglandins Leukot Essent Fatty Acids 56: 355-359.

Cadenas E (1989) Biochemistry of oxygen toxicity. Annu Rev Biochem 58: 79-110.

Cadet JL, Ali S, Epstein C (1994b) Involvement of oxygen-based radicals in methamphetamine-induced neurotoxicity: evidence from the use of CuZnSOD transgenic mice. Ann N Y Acad Sci 738: 388-391.

Cadet JL, Ali SF, Rothman RB, Epstein CJ (1995) Neurotoxicity, drugs and abuse, and the CuZn-superoxide dismutase transgenic mice. Mol Neurobiol 11: 155-163.

Cadet JL, Brannock C (1998) Free radicals and the pathobiology of brain dopamine systems. Neurochem Int 32: 117-131.

Cadet JL, Ladenheim B, Baum I, Carlson E, Epstein C (1994a) CuZn-superoxide dismutase (CuZnSOD) transgenic mice show resistance to the lethal effects of methylenedioxyamphetamine (MDA) and of methylenedioxymethamphetamine (MDMA). Brain Res 655: 259-262.

Cadet JL, Ordonez SV, Ordonez JV (1997) Methamphetamine induces apoptosis in immortalized neural cells: protection by the proto-oncogene, bcl-2. Synapse 25: 176-184.

Caldwell.J. (1980) The metabolism of amphetamines an related stimulants in animals and man. In: Amphetamines and related stimulants: chemical, biological, clinical, and social aspects. (Caldwell J, ed), Boca Raton,FL.: CRC Press.

Cancilla PA, Bready J, Berliner J (1993) Astrocyte-endothelial cell interaction. In: Astrocytes: Pharmacology and Function (Murphy S, ed), pp 383-397. San Diego: Academic Press.

Canini F, Bourdon L, Cespuglio R, Buguet A (1997) Voltametric assessment of brain nitric oxide during heatstroke in rats. Neurosci Lett 231: 67-70.

Cao C, Matsumura K, Yamagata K, Watanabe Y (1997) Involvement of cyclooxygenase-2 in LPS-induced fever and regulation of its mRNA by LPS in the rat brain. Am J Physiol 272: R1712-R1725.

Cappon GD, Morford LL, Vorhees CV (1997) Ontogeny of methamphetamine-induced neurotoxicity and associated hyperthermic response. Brain Res Dev Brain Res 103: 155-162.

Carney JM, Floyd RA (1991) Protection against oxidative damage to CNS by alpha-phenyl-tert-butyl nitrone (PBN) and other spin-trapping agents: a novel series of nonlipid free radical scavengers. J Mol Neurosci 3: 47-57.

Carter EA, Derojas-Walker T, Tamir S, Tannenbaum SR, Yu YM, Tompkins RG (1994) Nitric oxide production is intensely and persistently increased in tissue by thermal injury. Biochemical Journal 304: 201-204.

Cataldo AM, Broadwell RD (1986b) Cytochemical identification of cerebral glycogen and glucose-6-phosphatase activity under normal and experimental conditions. II. Choroid plexeus and ependymal epithelia, endothelia and pericytes. J Neurol 15: 511-524.

Cataldo AM, Broadwell RD (1986a) Cytochemical identification of cerebral glycogen and glucose-6-phosphatase activity under normal and experimental conditions: Neurons and glia. J Elect Micros Tech 3: 413-437.

Catlin DH, Hatton CK (1991) Use and abuse of anabolic and other drugs for athletic enhancement. Adv Intern Med 36: 399-408.

Cervos-Navarro J, Sharma HS, Westman J, Bongcam-Rudloff E (1998) Glial reactions in the central nervous system following heat stress. Prog Brain Res 115: 241-274.

Chan P, Di Monte D, Luo JJ, DeLanney LE, Irwin I, Langston JW (1994) Rapid ATP loss caused by methamphetamine in the mouse striatum: relationship between energy impairment and dopaminergic neurotoxicity. J Neurochem 62: 2484-2487.

Chance B, Sies H, Boveris A (1979) Hydroperoxide metabolism in mammlian organs. Physiol Rev 59: 527-605.

Chao CC, Hu S, Molitor TW, Shaskan EG, Peterson PK (1992) Activated microglia mediate neuronal cell injury via a nitric oxide mechanism. J Immunol 149: 2736-2741.

Chesler M (1990) The regulation and modulation of pH in the nervous system. Prog Neurobiol 1990 34: 401-427.

Chesler M, Kraig RP (1987) Intracellular pH of astrocytes increases rapidly with cortical stimulation. Am J Physiol 253: R666-R670.

Chesler M, Kraig RP (1989) Intracellular pH transients of mammalian astrocytes. J Neurosci 9: 2011-2019.

Chiueh CC, Miyake H, Peng MT (1993) Role of dopamine autoxidation, hydroxyl radical generation, and calcium overload in underlying mechanisms involved in MPTP-induced parkinsonism. Adv Neurol 60: 251-258.

Cho AK (1990) Ice: A new dosage forom of an old drug. Science 249: 631-634.

Choi AM, Alam J (1996) Heme oxygenase-1: function, regulation, and implication of a novel stress-inducible protein in oxidant-induced lung injury. Am J Respir Cell Mol Biol 15: 9-19.

Choi DW, Rothman SM (1990) The role of glutamate neurotoxicity in hypoxic-ischemic neuronal death. Ann Rev Neurosci 13: 171-182.

Chopp M (1993) The roles of heat shock proteins and immediate early genes in central nervous system normal function and pathology. Curr Opin Neurol Neurosurg 6: 6-10.

Clark WC, Blackman HJ, Preston JE (1967) Certain factors in aggregated mice d-amphetamine toxicity. Arch Int Pharmacodyn Ther 170: 350-363.

Clarke AR, Purdie CA, Harrison DJ, Morris RG, Bird CC, Hooper ML, Wyllie AH (1993) Thymocyte apoptosis induced by p53-dependent and independent pathways. Nature 362: 849-852.

Coceani F, Lees J, Dinarello CA (1988) Occurrence of interleukin-1 in cerebrospinal fluid of the conscious cat. Brain Res 446: 245-250.

Commins DL, Seiden LS (1986) alpha-Methyltyrosine blocks methylamphetamine-induced degeneration in the rat somatosensory cortex. Brain Res 365: 15-20.

Cook CE, Jeffcoat AR, Perez-Reyes M, Sadler BM, Hill JM, White WR, McDonald S (1991) Plasma levels of methamphetamine after smoking of methamphetamine hydrochloride. NIDA Res Monogr 105: 578-579.

Cornell-Bell AH, Thomas PG, Smith SJ (1990) The excitatory neurotransmitter glutamate causes filopodia formation in cultured hippocampal astrocytes. Glia 3: 322-334.

Cox C, Smart RG, . (1970) The nature and extent of speed use in North America. Can Med Assoc J 102: 724-729.

Craig CG, White TD (1993) NMDA-evoked adenosine release from rat cortex does not require the intermediate formation of nitric oxide. Neurosci Lett 158: 167-169.

Crow JP, Spruell C, Chen J, Gunn C, Ischiropoulos H, Tsai M, Smith CD, Radi R, Koppenol WH, Beckman JS (1994) On the pH-dependent yield of hydroxyl radical products from peroxynitrite. Free Radic Biol Med 16: 331-338.

Cubells JF, Rayport S, Rajendran G, Sulzer D (1994) Methamphetamine neurotoxicity involves vacuolation of endocytic organelles and dopamine-dependent intracellular oxidative stress. J Neurosci 14: 2260-2271.

Cull-Candy SG, Wyllie DJ (1991) Glutamate-receptor channels in mammalian glial cells. Ann N Y Acad Sci 1991 633: 458-474.

Dahl D, Bignami A (1973) Glial fibrillary acidic protein from normal human brain. Purification and properties. Brain Res 57: 343-360.

Dalton TP, Li Q, Bittel D, Liang L, Andrews GK (1996) Oxidative stress activates metal-responsive transcription factor-1 binding activity. Occupancy in vivo of metal response elements in the metallothionein-I gene promoter. J Biol Chem 271: 26233-26241.

Dawson TM, Dawson VL, Snyder SH (1992) A novel neuronal messenger molecule in brain: the free radical, nitric oxide. Ann Neurol 32: 297-311.

Dawson TM, Snyder SH (1994) Gases as biological messengers: nitric oxide and carbon monoxide in the brain. J Neurosci 14: 5147-5159.

Denis-Donini S, Glowinski J, Prochiantz A (1984) Glial heterogeneity may define the three-dimensional shape of mouse mesencephalic dopaminergic neurones. Nature 307: 641-643.

Derlet RW, Heischober B (1990) Methamphetamine. Stimulant of the 1990s? West J Med 153: 625-628.

DeVito M, Wagner GC (1989b) Functional consequences following methamphetamine-induced neuronal damage. Psychopharmacology (Berl ) 97: 432-435.

DeVito M, Wagner GC (1989a) Methamphetamine-induced neuronal damage: a possible role for free radicals. Neuropharmacology 28: 1145-1150.

Di Monte D, Chan P, Sandy MS (1992) Glutathione in Parkinson's disease: a link between oxidative stress and mitonchondrial damage? Ann. Neurol. 32 Suppl:S111-S115

Di Monte D, Royland JE, Jakowec MW, Langston JW (1996) Role of nitric oxide in methamphetamine neurotoxicity: protection by 7-nitroindazole, an inhibitor of neuronal nitric oxide synthase. Journal of Neurochemistry 67: 2443-2450.

Di Rosa M, Ialenti A, Ianaro A, Sautebin L (1996) Interaction between nitric oxide and cyclooxygenase pathways. Prostaglandins Leukot Essent Fatty Acids 54: 229-238.

Donati YR, Slosman DO, Polla BS (1990) Oxidative injury and the heat shock response. Biochem Pharmacol 40: 2571-2577.

Dringen R, Hamprecht B (1992) Glucose, insulin, and insulin-like growth factor I regulate the glycogen content of astroglia-rich primary cultures. J Neurochem 58: 511-517.

Dwyer BE, Nishimura RN, De VJ, Yoshida T (1992) Heme oxygenase is a heat shock protein and PEST protein in rat astroglial cells. Glia 5: 300-305.

Dwyer BE, Nishimura RN, Lu SY (1995) Differential expression of heme oxygenase-1 in cultured cortical neurons and astrocytes determined by the aid of a new heme oxygenase antibody. Response to oxidative stress. Brain Res Mol Brain Res 30: 37-47.

Edison GR (1971) Amphetamines: a dangerous illusion. Ann Intern Med 74: 605-610.

Eisch AJ, Marshall JF (1998) Methamphetamine neurotoxicity: dissociation of striatal dopamine terminal damage from parietal cortical cell body injury. Synapse 30: 433-445.

Ellinwood EH, Cohen S (1971) Amphetamine abuse. Science 171: 420-421.

Ellis A, Wendon J (1996) Circulatory, respiratory, cerebral, and renal derangements in acute liver failure: pathophysiology and management. Semin Liver Dis 16: 379-388.

Ellis FP (1972) Mortality from heat illness and heat aggravated illness in the United State. Environ Res 5: 1-58.

Ellison G, Eison MS, Huberman HS, Daniel F (1978) Long-term changes in dopaminergic innervation of caudate nucleus after continuous amphetamine. Science 201: 276-278.

Eng LF (1988) Regulation of glial intermediate filaments in astrogliosis. In: Biochemical, Pathology of Astrocytes (Norenberg MD, Hertz L, Schousboe A, eds), pp 79-90. New Yrok: Liss.

Eng LF, Ghirnikar RS (1994) GFAP and astrogliosis. Brain Pathol 4: 229-237.

Eng LF, Shiurba RA (1988) Glial fibrillary acidic protein: A review of structure, function and clinical application. In: Neuronal and Glial Proteins: Structure, Function and Clinical Application. (Marangos PJ, Campbell I, Cohen RM, eds), pp 339-359. New York: Academic Press.

Eng LF, Vanderhaeghen JJ, Bignami A, Gerstl B (1971) An acidic protein isolated from fibrous astrocytes. Brain Res 28: 351-354.

Espelin DE, Done AK (1968) Amphetamine poisoning. Effectiveness of chlorpromazine. N Engl J Med 278: 1361-1365.

Ewing JF, Maines MD (1991) Rapid induction of heme oxygenase 1 mRNA and protein by hyperthermia in rat brain: heme oxygenase 2 is not a heat shock protein. Proc Natl Acad Sci U S A 88: 5364-5368.

Ewing JF, Maines MD (1993) Glutathione depletion induces heme oxygenase-1 (HSP32) mRNA and protein in rat brain. J Neurochem 60: 1512-1519.

Farfel GM, Seiden LS (1995) Role of hypothermia in the mechanism of protection against serotonergic toxicity. II. Experiments with methamphetamine, p-chloroamphetamine, fenfluramine, dizocilpine and dextromethorphan. J Pharmacol Exp Ther 272: 868-875.

Feng L, Xia Y, Seiffert D, Wilson CB (1995) Oxidative stress-inducible protein tyrosine phosphatase in glomerulonephritis. Kidney Int 48: 1920-1928.

Ferriero DM, Soberano HQ, Simon RP, Sharp FR (1990) Hypoxia-ischemia induces heat shock protein-like (HSP72) immunoreactivity in neonatal rat brain. Brain Res Dev Brain Res 53: 145-150.

Fibiger HC, McGeer EG (1971) Effect of acute and chronic methamphetamine treatment on tyrosine hydroxylase activity in brain and adrenal medulla. Eur J Pharmacol 16: 176-180.

Finnegan KT, Ricaurte G, Seiden LS, Schuster CR (1982) Altered sensitivity to d-methylamphetamine, apomorphine, and haloperidol in rhesus monkeys depleted of caudate dopamine by repeated administration of d- methylamphetamine. Psychopharmacology (Berl ) 77: 43-52.

Fleckenstein AE (1997) Effect of methamphetamine on tryptophan hydroxylase activity: role of hyperthermia. Eur J Pharmacol 332: 263-265.

Floyd RA (1991) Oxidative damage to behavior during aging. Science 254: 1597.

Floyd RA, Carney JM (1992) Free radical damage to protein and DNA: mechanisms involved and relevant observations on brain undergoing oxidative stress. Ann Neurol 32 Suppl: S22-S27.

Fonnum F (1984) Glutamate: a neurotransmitter in mammalian brain. J Neurochem 42: 1-11.

Fontana A, Erb P, Pircher H, Zinkernagel R, Weber E, Fierz W (1986) Astrocytes as antigen-presenting cells. Part II: Unlike H-2K-dependent cytotoxic T cells, H-2Ia-restricted T cells are only stimulated in the presence of interferon-gamma. J Neuroimmunol 12: 15-28.

Fontana A, Fierz W (1985) The endothelium--astrocyte immune control system of the brain. Springer Semin Immunopathol 8: 57-70.

Forstermann U, Pollock JS, Schmidt HH, Heller M, Murad F (1991) Calmodulin-dependent endothelium-derived relaxing factor/nitric oxide synthase activity is present in the particulate and cytosolic fractions of bovine aortic endothelial cells. Proc Natl Acad Sci U S A 88: 1788-1792.

Fraser DD, Mudrick-Donnon LA, MacVicar BA (1994) Astrocytic GABA receptors. Glia 11: 83-93.

Freeman BA, Crapo JD (1982) Biology of disease: free radicals and tissue injury. Lab Invest 47: 412-426.

Fridovich I (1986) Biological effects of the superoxide radical. Arch Biochem Biophys 247: 1-11.

Fridovich I (1995) Superoxide radical and superoxide dismutase. Annu Rev Biochem 64: 97-112.

Fukui K, Nakajima T, Kariyama H, Kashiba A, Kato N, Tohyama I, Kimura H (1989) Selective reduction of serotonin immunoreactivity in some forebrain regions of rats induced by acute methamphetamine treatment; quantitative morphometric analysis by serotonin immunocytochemistry. Brain Res 482: 198-203.

Fukui S, Wada K, Iyo M (1994) Epidemiology of Amphetamine Abuse in Japan and its Social Implications. In: Amphetamine and its Analogs: Psychopharmacology, Toxicology and Abuse (Cho AK, Segal DS, eds), pp 459-479. San Diego: Academic Press.

Fukumura M, Cappon GD, Broening HW, Vorhees CV (1998) Methamphetamine-induced dopamine and serotonin reductions in neostriatum are not gender specific in rats with comparable hyperthermic responses. Neurotoxicol Teratol 20: 441-448.

Funahashi M, Kohda H, Hori O, Hayashida H, Kimura H (1990) Potentiating effect of morphine upon d-methamphetamine-induced hyperthermia in mice. Effects of naloxone and haloperidol. Pharmacol Biochem Behav 36: 345-350.

Gaal J, Hermecz I (1993) Medicinal Chemistry of present and future MAO-B inhibitors. In: Inhibitors of Monoamine Oxidase B: Pharmacology and Clinical Use in Neurodegenerative Disorders (Szelenyi I, ed), pp 75-108. Basel: Birkhauser.

Geiger A (1958) Correlation of brain metabolism and function by the use of a brain perfusion method in situ. Physiol Rev 38: 1-20.

Gibb JW, Kogan FJ (1979) Influence of dopamine synthesis on methamphetamine-induced changes in striatal and adrenal tyrosine hydroxylase activity. Naunyn Schmiedebergs Arch Pharmacol 310: 185-187.

Giovanni A, Liang LP, Hastings TG, Zigmond MJ (1995) Estimating hydroxyl radical content in rat brain using systemic and intraventricular salicylate: impact of methamphetamine. J Neurochem 64: 1819-1825.

Goldberg MP, Weiss JH, Pham PC, Choi DW (1987) N-methyl-D-aspartate receptors mediate hypoxic neuronal injury in cortical culture. J Pharmacol Exp Ther 243: 784-791.

Goode HF, Cowley HC, Walker BE, Howdle PD, Webster NR (1995) Decreased antioxidant status and increased lipid peroxidation in patients with septic shock and secondary organ dysfunction. Critical Care Medicine 23: 646-651.

Goppelt-Struebe M (1995) Regulation of prostaglandin endoperoxide synthase (cyclooxygenase) isozyme expression. Prostaglandins Leukot Essent Fatty Acids 52: 213-222.

Goto S, Korematsu K, Oyama T, Yamada K, Hamada J, Inoue N, Nagahiro S, Ushio Y (1993) Neuronal induction of 72-kDa heat shock protein following methamphetamine-induced hyperthermia in the mouse hippocampus. Brain Res 626: 351-356.

Government Information Centre, Hong Kong Special Administrative Region. Central Registry of Drug Abuse 40th report. 1997.

Grootveld M, Halliwell B (1986) Aromatic hydroxylation as a potential measure of hydroxyl-radical formation in vivo. Biochem J 237: 499-504.

Gunasekar PG, Borowitz JL, Isom GE (1998) Cyanide-induced generation of oxidative species: involvement of nitric oxide synthase and cyclooxygenase-2. J Pharmacol Exp Ther 285: 236-241.

Guth L, Watson PK (1968) A correlated histochemical and quantitative study on cerebral glycogen after brain injury in the rat. Exp Neurol 22: 590-602.

Gutteridge JM, Halliwell B (1990) The measurement and mechanism of lipid peroxidation in biological systems. TIBS 15: 129-135.

Hall DM, Buettner GR, Matthes RD, Gisolfi CV (1994) Hyperthermia stimulates nitric oxide formation: electron paramagnetic resonance detection of .NO-heme in blood. Journal of Applied Physiology 77: 548-553.

Hallermayer K, Harmening C, Hamprecht B (1981) Cellular localization and regulation of glutamine synthetase in primary cultures of brain cells from newborn mice. J Neurochem 37: 43-52.

Halliwell B (1992) Reactive oxygen species and the central nervous system. J Neurochem 59: 1609-1623.

Halliwell B, Gutteridge JM (1985) The importance of free radicals and catalytic metal ions in human diseases. Mol Aspects Med 8: 89-193.

Hamprecht B, Dringen R (1995) Energy Metabolism. In: Neuroglia (Kettenmann H, Ransom BR, eds), pp 473-487. Oxford: Oxford University Press.

Hansson E, Sellstrom A, Persson LI, Ronnback L (1980) Brain primary culture - a characterization. Brain Res 188: 233-246.

Hara K, Kong DL, Sharp FR, Weinstein PR (1998) Effect of selective inhibition of cyclooxygenase 2 on temporary focal cerebral ischemia in rats. Neurosci Lett 256: 53-56.

Harrison PJ, Procter AW, Exworthy T, Roberts GW, Najlerahim A, Barton AJ, Pearson RC (1993) Heat shock protein (hsx70) mRNA expression in human brain: effects of neurodegenerative disease and agonal state. Neuropathol Appl Neurobiol 19: 10-21.

Hatten ME (1985) Neuronal regulation of astroglial morphology and proliferation in vitro. J Cell Biol 100: 384-396.

Hatton GI (1990) Emerging concepts of structure-function dynamics in adult brain: the hypothalamo- neurohypophysial system. Prog Neurobiol 34: 437-504.

Haymaker W, Miquel J, Ibrahim MZH (1970) Glycogen accumulation following brain trauma. Topical Probl Psychiat Neurol 10: 71-87.

Hermeking H, Eick D (1994) Mediation of c-Myc-induced apoptosis by p53. Science 265: 2091-2093.

Herschman HR (1996) Prostaglandin synthase 2. Biochim Biophys Acta 1299: 125-140.

Hertz L (1979) Functional interactions between neurons and astrocytes I. Turnover and metabolism of putative amino acid transmitters. Prog Neurobiol 13: 277-323.

Hess A, Desiderio C, McAuliffe WG (1990) Acute neuropathological changes in the caudate nucleus caused by MPTP and methamphetamine: immunohistochemical studies. J Neurocytol 19: 338-342.

Hevel JM, White KA, Marletta MA (1991) Purification of the inducible murine macrophage nitric oxide synthase. Identification as a flavoprotein. J Biol Chem 266: 22789-22791.

Higashi T, Takechi H, Uemura Y, Kikuchi H, Nagata K (1994) Differential induction of mRNA species encoding several classes of stress proteins following focal cerebral ischemia in rats. Brain Res 650: 239-248.

Hightower LE (1980) Cultured animal cells exposed to amino acid analogues or puromycin rapidly synthesize several polypeptides. J Cell Physiol 102: 407-427.

Hillered L, Ernster L (1983) Respiratory activity of isolated rat brain mitochondria following in vitro exposure to oxygen radicals. J Cereb Blood Flow Metab 3: 207-214.

Hirata H, Cadet JL (1997) p53-knockout mice are protected against the long-term effects of methamphetamine on dopaminergic terminals and cell bodies. J Neurochem 69: 780-790.

Hirata H, Ladenheim B, Carlson E, Epstein C, Cadet JL (1996) Autoradiographic evidence for methamphetamine-induced striatal dopaminergic loss in mouse brain: attenuation in CuZn-superoxide dismutase transgenic mice. Brain Res 714: 95-103.

Hirata H, Ladenheim B, Rothman RB, Epstein C, Cadet JL (1995) Methamphetamine-induced serotonin neurotoxicity is mediated by superoxide radicals. Brain Res 677: 345-347.

Hirsch EC (1992) Why are nigral catecholaminergic neurons more vulnerable than other cells in Parkinson's disease? Ann Neurol 32 Suppl: S88-S93.

Hockberger PE, Ahmed MS, Skimina TA, Lee C, Hung WY (1996) Imaging of hydrogen peroxide generation in cultured cells using dichlorofluorescein derivatives. In: Optical Diagnostics of Living Cells and Biofluids. (Asakura T, Farkas DL, Lief RC, Priezzhev AV, Tromberg B, eds), pp 129-140. Washingston: Bellingham.

Hockenbery D, Nunez G, Milliman C, Schreiber RD, Korsmeyer SJ (1990) Bcl-2 is an inner mitochondrial membrane protein that blocks programmed cell death. Nature 348: 334-336.

Hockenbery DM, Oltvai ZN, Yin XM, Milliman CL, Korsmeyer SJ (1993) Bcl-2 functions in an antioxidant pathway to prevent apoptosis. Cell 75: 241-251.

Hom DG, Jiang D, Hong EJ, Mo JQ, Andersen JK (1997) Elevated expression of glutathione peroxidase in PC12 cells results in protection against methamphetamine but not MPTP toxicity. Brain Res Mol Brain Res 46: 154-160.

Hosli E, Hosli L (1990) Evidence for GABAB-receptors on cultured astrocytes of rat CNS: autoradiographic binding studies. Exp Brain Res 1990 80: 621-625.

Hosli L, Hosli E (1987) Receptors for dopamine and serotonin on astrocytes of cultured rat central nervous system. J Physiol (Paris ) 1987 82: 191-195.

Hotchkiss AJ, Gibb JW (1980a) Blockade of methamphetamine-induced depression of tyrosine hydroxylase by GABA transaminase inhibitors. Eur J Pharmacol 66: 201-205.

Hotchkiss AJ, Gibb JW (1980b) Long-term effects of multiple doses of methamphetamine on tryptophan hydroxylase and tyrosine hydroxylase activity in rat brain. J Pharmacol Exp Ther 214: 257-262.

Hounsgaard J, Nicholson C (1983) Potassium accumulation around individual Purkinje cells in cerebellar slices from the guinea pig. J Physiol 340: 359-388.

Hyden H, McEwen B (1966) A glial protein specific for the nervous system. Proc Natl Acad Sci U S A 55: 354-358.

Imanishi M, Sakai T, Nishimura A, Konobu T, Nishio K, Murao Y, Tabuse H, Miyamoto S, Sakaki T, Nagaike C, Hatake K, Itou H (1997) [Cerebral infarction due to bacterial emboli associated with methamphetamine abuse]. No To Shinkei 49: 537-540.

Inghe G (1969) The present state of abuse and addiction to stimulant drugs in Sweden. In: Abuse of central stimulants (Sjoqvist F, Tottie M, eds), pp 19-27. Stockholm: Almqvist and Wiksell.

Itzhak Y, Ali SF (1996) The neuronal nitric oxide synthase inhibitor, 7-nitroindazole, protects against methamphetamine-induced neurotoxicity in vivo. J Neurochem 67: 1770-1773.

Itzhak Y, Gandia C, Huang PL, Ali SF (1998) Resistance of neuronal nitric oxide synthase-deficient mice to methamphetamine-induced dopaminergic neurotoxicity. J Pharmacol Exp Ther 284: 1040-1047.

Janssens SP, Shimouchi A, Quertermous T, Bloch DB, Bloch KD (1992) Cloning and expression of a cDNA encoding human endothelium-derived relaxing factor/nitric oxide synthase [published erratum appears in J Biol Chem 1992 Nov 5;267(31):22694]. J Biol Chem 267: 14519-14522.

Janzer RC, Raff MC (1987) Astrocytes induce blood-brain barrier properties in endothelial cells. Nature 325: 253-257.

Jesberger JA, Richardson JS (1991) Oxygen free radicals and brain dysfunction. Int J Neurosci 57: 1-17.

Johnson M, Hanson GR, Gibb JW (1988) Effects of dopaminergic and serotonergic receptor blockade on neurochemical changes induced by acute administration of methamphetamine and 3,4- methylenedioxymethamphetamine. Neuropharmacology 27: 1089-1096.

Johnson M; Hanson GR, Gibb JW (1991) Norepinephrine does not contribute to methamphetamine-induced changes in hippocampal serotonergic system. Neuropharmacology 30: 617-622.

Kalant O (1966) The amphetamines: toxicity abd addiction. Toronto: University of Toronto.

Kalant OJ (1973) The Amphetamines: Toxicity and Addiction.

Kane DJ, Sarafian TA, Anton R, Hahn H, Gralla EB, Valentine JS, Ord T, Bredesen DE (1993) Bcl-2 inhibition of neural death: decreased generation of reactive oxygen species. Science 262: 1274-1277.

Katzman R, Pappius HM (1973) Brain Electrolyres and Fluid Metabolism. Baltimore, Maryland: Williams & Wilkins.

Kaufmann SH (1992) Heat shock proteins in health and disease. Int J Clin Lab Res 21: 221-226.

Kaufmann WE, Worley PF, Pegg J, Bremer M, Isakson P (1996) COX-2, a synaptically induced enzyme, is expressed by excitatory neurons at postsynaptic sites in rat cerebral cortex. Proc Natl Acad Sci U S A 93: 2317-2321.

Keller M, Jackisch R, Seregi A, Hertting G (1985) Comparison of prostanoid forming capacity of neuronal and astroglial cells in primary cultures. Neurochem Int 7: 655-665.

Kettenmann H, Orkand RK, Schachner M (1983) Coupling among identified cells in mammalian nervous system cultures. J Neurosci 3: 506-516.

Keyse SM, Tyrrell RM (1989) Heme oxygenase is the major 32-kDa stress protein induced in human skin fibroblasts by UVA radiation, hydrogen peroxide, and sodium arsenite. Proc Natl Acad Sci U S A 86: 99-103.

Kiloh LG, Brandon S (1962) Habituation and addiction to amphetamines. Br Med J 40.

Kim YM, Bergonia HA, Muller C, Pitt BR, Watkins WD, Lancaster JR (1996) Loss and degradation of enzyme-bound heme induced by cellular nitric oxide synthesis. J Biol Chem 270: 5710-5713.

Kimelberg HK, Pelton EW (1983) High-affinity uptake of [3H]norepinephrine by primary astrocyte cultures and its inhibition by tricyclic antidepressants. J Neurochem 40: 1265-1270.

Kimelberg HK, Ransom BR (1986) Physiological and pathological aspects of astrocytic swelling. In: Astrocytes: Cell Biology and Pathology of Astrocytes (Fedoroff S, Vernadakis A, eds), pp 129-166. New York: Academic Press.

Kita T, Philbert MA, Wagner GC, Huang J, Lowndes HE (1998) Methamphetamine-induced modification of dopamine metabolism in cultured striatal astrocytes. Pharmacol Toxicol 83: 36-39.

Kitamura Y, Furukawa M, Matsuoka Y, Tooyama I, Kimura H, Nomura Y, Taniguchi T (1998) In vitro and in vivo induction of heme oxygenase-1 in rat glial cells: possible involvement of nitric oxide production from inducible nitric oxide synthase. Glia 22: 138-148.

Kluger MJ (1991) Fever: role of pyrogens and cryogens. Physiol Rev 71: 93-127.

Kogan FJ, Nichols WK, Gibb JW (1976) Influence of methamphetamine on nigral and striatal tyrosine hydroxylase activity and on striatal dopamine levels. Eur J Pharmacol 36: 363-371.

Kojima T, Une I, Yashiki M, Noda J, Sakai K, Yamamoto K (1984) A fatal methamphetamine poisoning associated with hyperpyrexia. Forensic Sci Int 24: 87-93.

Kondo T, Ito T, Sugita Y (1994) Bromocriptine scavenges methamphetamine-induced hydroxyl radicals and attenuates dopamine depletion in mouse striatum. Ann N Y Acad Sci 738: 222-229.

Konuma K (1997) Use and Abuse of Amphetamines in Japan. In: Amphetamine and its Analogs: Psychopharmacology, Toxicology and Abuse (Cho AK, Segal DS, eds), pp 415-433.

Kovachich GB, Aronson CE, Brunswick DJ (1989) Effects of high-dose methamphetamine administration on serotonin uptake sites in rat brain measured using [3H]cyanoimipramine autoradiography. Brain Res 505: 123-129.

Kramer JC, Fischman VS, Littlefield DC (1967) Amphetamine abuse. Pattern and effects of high doses taken intravenously. JAMA 201: 305-309.

Kuffler SW, Nicholls JG, Martin AR (1984) Physiology of neuroglial cells. In: From Neuron to Brain (Kuffler SW, Nicholls JG, Martin AR, eds), pp 323-360. Massachusetts: Sinauer.

Kujubu DA, Fletcher BS, Varnum BC, Lim RW, Herschman HR (1991) TIS10, a phorbol ester tumor promoter-inducible mRNA from Swiss 3T3 cells, encodes a novel prostaglandin synthase/cyclooxygenase homologue. J Biol Chem 266: 12866-12872.

Kuperman DI, Freyaldenhoven TE, Schmued LC, Ali SF (1997) Methamphetamine-induced hyperthermia in mice: examination of dopamine depletion and heat-shock protein induction. Brain Res 771: 221-227.

Lamas S, Marsden PA, Li GK, Tempst P, Michel T (1992) Endothelial nitric oxide synthase: molecular cloning and characterization of a distinct constitutive enzyme isoform. Proc Natl Acad Sci U S A 89: 6348-6352.

Lane DF (1992) Cancer. p53, guardian of the genome. Nature 358: 15-16.

Larsson OM, Hertz L, Schousboe A (1986) Uptake of GABA and nipecotic acid in astrocytes and neurons in primary cultures: Changes in sodium coupling ratio during differentiation. J Neurosci Res 16: 699-708.

LaVoie MJ, Hastings TG (1999) Dopamine quinone formation and protein modification associated with the striatal neurotoxicity of methamphetamine: evidence against a role for extracellular dopamine. J Neurosci 19: 1484-1491.

Lazaroff M, Dunlap K, Chikaraishi DM (1996) A CNS catecholaminergic cell line expresses voltage-gated currents. J Membr Biol 151: 279-291.

LeBel CP, Bondy SC (1990) Sensitive and rapid quantitation of oxygen reactive species formation in rat synaptosomes. Neurochem Int 17: 435-440.

LeBel CP, Ischiropoulos H, Bondy SC (1992) Evaluation of the probe 2',7'-dichlorofluorescin as an indicator of reactive oxygen species formation and oxidative stress. Chem Res Toxicol 5: 227-231.

Lemasters JJ, Hackenbrock CR (1979) Continuous measurement of adenosine triphosphate with firefly luciferase luminescence. Methods Enzymol 56: 530-544.

Levitt P, Pintar JE, Breakefield XO (1982) Immunocytochemical demonstration of monoamine oxidase B in brain astrocytes and serotonergic neurons. Proc Natl Acad Sci U S A 79: 6385-6389.

Lewis JJ, Van Petten GR (1962) The effect of amphetamine and related compounds on the concentration of adenine nucleotides, inorganic phosphate and creatine phosphate in the rat brain. J Pharmacol Exp Ther 136: 372-377.

Lorez H (1981) Fluorescence histochemistry indicates damage of striatal dopamine nerve terminals in rats after multiple doses of methamphetamine. Life Sci 28: 911-916.

Lowe SW, Ruley HE, Jacks T, Housman DE (1993) p53-dependent apoptosis modulates the cytotoxicity of anticancer agents. Cell 74: 957-967.

Lowenstein DH, Chan PH, Miles MF (1991) The stress protein response in cultured neurons: characterization and evidence for a protective role in excitotoxicity. Neuron 7: 1053-1060.

Lowry OH, Roseborough NJ, Farr AL, Randall RJ (1951) Protein measurement with the Folin phenol reagent. J Biol Chem 193: 265-275.

MacKenzie RG, Heischober B (1997) Methamphetamine. Pediatr Rev 18: 305-309.

Magistretti PJ (1988) Regulation of glycogenolysis by neurotransmitters in the central nervous system. Diabet Metab 14: 237-246.

Magistretti PJ, Hof PR, Martin JL (1986) Adenosine stimulates glycogenolysis in mouse cerebral cortex: a possible coupling mechanism between neuronal activity and energy metabolism. J Neurosci 6: 2558-2562.

Mailhos C, Howard MK, Latchman DS (1993) Heat shock protects neuronal cells from programmed cell death by apoptosis. Neuroscience 55: 621-627.

Maines MD (1988) Heme oxygenase: function, multiplicity, regulatory mechanisms, and clinical applications. FASEB J 2: 2557-2568.

Maines MD (1996) Carbon monoxide and nitric oxide homology: Differential modulation of heme oxygenase in brain and detection of protein and activity. Methods Enzymol 268: 473-488.

Makisumi T, Yoshida K, Watanabe T, Tan N, Murakami N, Morimoto A (1998) Sympatho-adrenal involvement in methamphetamine-induced hyperthermia through skeletal muscle hypermetabolism. Eur J Pharmacol 363: 107-112.

Marin P, Quignard JF, Lafon-Cazal M, Bockaert J (1993) Non-classical glutamate receptors, blocked by both NMDA and non-NMDA antagonists, stimulate nitric oxide production in neurons. Neuropharmacology 32: 29-36.

Marini AM, Kozuka M, Lipsky RH, Nowak TSJ (1990) 70-kilodalton heat shock protein induction in cerebellar astrocytes and cerebellar granule cells in vitro: comparison with immunocytochemical localization after hyperthermia in vivo. J Neurochem 54: 1509-1516.

Marklund SL, Westman NG, Lundgren E, Roos G (1982) Copper- and zinc-containing superoxide dismutase, manganese-containing superoxide dismutase,

catalase, and glutathione peroxidase in normal and neoplastic human cell lines and normal human tissues. Cancer Res 42: 1955-1961.

Marotta P, Sautebin L, Di Rosa M (1992) Modulation of the induction of nitric oxide synthase by eicosanoids in the murine macrophage cell line J774. Br J Pharmacol 107: 640-641.

Marriott DR, Wilkin GP, Wood JN (1991) Substance P-induced release of prostaglandins from astrocytes: regional specialisation and correlation with phosphoinositol metabolism. J Neurochem 56: 259-265.

Marshall JF, O'Dell SJ, Weihmuller FB (1993) Dopamine-glutamate interactions in methamphetamine-induced neurotoxicity. J Neural Transm Gen Sect 91: 241-254.

Martinez-Hernandez A, Bell KP, Norenberg MD (1977) Glutamine synthetase: glial localization in brain. Science 195: 1356-1358.

Matute C, Gutierrez-Igarza K, Rio C, Miledi R (1994) Glutamate receptors in astrocytic end-feet. Neuroreport 1994 Jun 2 5: 1205-1208.

Mayer B, Schmid M, Klatt P, Schmidt K (1993) Reversible inactivation of endothelial nitric oxide synthase by NG-nitro-L-arginine. FEBS Lett 333: 203-206.

Mayer B, Schmidt K, Humbert P, Bohme E (1989) Biosynthesis of endothelium-derived relaxing factor: a cytosolic enzyme in porcine aortic endothelial cells Ca2+-dependently converts L-arginine into an activator of soluble guanylyl cyclase. Biochem Biophys Res Commun 164: 678-685.

Mayer ML, Westbrook GL (1987) The physiology of excitatory amino acids in the vertebrate central nervous system. Prog Neurobiol 28: 197-276.

McCord JM (1985) Oxygen-derived free radicals in postischemic tissue injury. N Engl J Med 312: 159-163.

McCord JM, Fridovich I (1969) The utility of superoxide dismutase in studying free radical reactions. I. Radicals generated by the interaction of sulfite, dimethyl sulfoxide, and oxygen. J Biol Chem 244: 6056-6063.

Meister A, Anderson ME (1983) Glutathione. Annu Rev Biochem 52: 711-760.

Miller DB, O'Callaghan JP (1994) Environment-, drug- and stress-induced alterations in body temperature affect the neurotoxicity of substituted amphetamines in the C57BL/6J mouse. J Pharmacol Exp Ther 270: 752-760.

Miller DB, O'Callaghan JP (1995) The role of temperature, stress, and other factors in the neurotoxicity of the substituted amphetamines 3,4-methylenedioxymethamphetamine and fenfluramine. Mol Neurobiol 11: 177-192.

Miller MA, Hughes AL (1994) Epidemiology of Amphetamine Use in the United States. In: Amphetamine and its Analogs: Psychopharmacology, Toxicology and Abuse (Cho AK, Segal DS, eds), pp 439-458. San Diego: Academic Press.

Milton AS, Wendlandt S (1970) A possible role for prostaglandin E1 as a modulator for temperature regulation in the central nervous system of the cat. J Physiol (Lond) 207: 76P-77P.

Minghetti L, Polazzi E, Nicolini A, Creminon C, Levi G (1997) Up-regulation of cyclooxygenase-2 expression in cultured microglia by prostaglandin E2, cyclic AMP and non-steroidal anti-inflammatory drugs. Eur J Neurosci 9: 934-940.

Mitchell P (1966) Chemiosmotic coupling in oxidative and photosynthetic phosphorylation. Bio Rev Camb Philos Soc 41:445-502.

Mitchell P (1979) Keilin's respiratory chain concept and its chemiosmotic consequences. Science 206: 1148-1159.

Molina-Holgado F, Lledo A, Guaza C (1995) Evidence for cyclooxygenase activation by nitric oxide in astrocytes. Glia 15: 167-172.

Mollace V, Muscoli C, Rotiroti D, Nistico G (1997) Spontaneous induction of nitric oxide- and prostaglandin E2-release by hypoxic astroglial cells is modulated by interleukin 1 beta. Biochem Biophys Res Commun 238: 916-919.

Moncada S, Higgs EA (1991) Endogenous nitric oxide: physiology, pathology and clinical relevance. European Journal of Clinical Investigation 21: 361-374.

Moncada S, Palmer RM, Higgs EA (1991) Nitric oxide: physiology, pathophysiology, and pharmacology. Pharmacol Rev 43: 109-142.

Morgan ME, Gibb JW (1980) Short-term and long-term effects of methamphetamine on biogenic amine metabolism in extra-striatal dopaminergic nuclei. Neuropharmacology 19: 989-995.

Morgenbesser SD, Williams BO, Jacks T, DePinho RA (1994) p53-dependent apoptosis produced by Rb-deficiency in the developing mouse lens. Nature 371: 72-74.

Moszczynska A, Turenne S, Kish SJ (1998) Rat striatal levels of the antioxidant glutathione are decreased following binge administration of methamphetamine. Neurosci Lett 255: 49-52.

Murphy S, Pearce B, Jeremy J, Dandona P (1988) Astrocytes as eicosanoid-producing cells. Glia 1: 241-245.

Murphy S, Simmons ML, Agullo L, Garcia A, Feinstein DL, Galea E, Reis DJ, Minc-Golomb D, Schwartz JP (1993) Synthesis of nitric oxide in CNS glial cells [see comments]. Trends Neurosci 16: 323-328.

Nahorski SR, Rogers KJ (1973) In vivo effects of amphetamine on metabolites and metabolic rate in brain. J Neurochem 21: 679-686.

Nam MJ, Thore C, Busija D (1995) Rapid induction of prostaglandin synthesis in piglet astroglial cells by interleukin 1 alpha. Brain Res Bull 36: 215-218.

Narabayashi H, Takeshige K, Minakami S (1982) Alteration of inner-membrane components and damage to electron-transfer activities of bovine heart submitochondrial particles induced by NADPH- dependent lipid peroxidation. Biochem J 202: 97-105.

Narcotics Bureau of the Hong Kong Police, HKSAR. Enforcement action on illegal drugs. 1997.

Nash JF, Yamamoto BK (1992) Methamphetamine neurotoxicity and striatal glutamate release: comparison to 3,4- methylenedioxymethamphetamine. Brain Res 581: 237-243.

Nathaniel EJH, Nathaniel DR (1981) The reactive astrocyte. Adv Cell Neurobiol 2: 249-301.

Norenberg MD (1994) Astrocyte responses to CNS injury. J Neuropathol Exp Neurol 53: 213-220.

Nunez G, London L, Hockenbery D, Alexander M, McKearn JP, Korsmeyer SJ (1990) Deregulated Bcl-2 gene expression selectively prolongs survival of growth factor- deprived hemopoietic cell lines. J Immunol 144: 3602-3610.

Nwanze E, Jonsson G (1981) Amphetamine neurotoxicity on dopamine nerve terminals in the caudate nucleus of mice. Neurosci Lett 26: 163-168.

O'Banion MK, Miller JC, Chang JW, Kaplan MD, Coleman PD (1996) Interleukin-1 beta induces prostaglandin G/H synthase-2 (cyclooxygenase- 2) in primary murine astrocyte cultures. J Neurochem 66: 2532-2540.

O'Callaghan JP (1991) Assessment of neurotoxicity: use of glial fibrillary acidic protein as a biomarker. Biomed Environ Sci 4: 197-206.

O'Callaghan JP, Miller DB (1994) Neurotoxicity profiles of substituted amphetamines in the C57BL/6J mouse. J Pharmacol Exp Ther 270: 741-751.

O'Dell SJ, Weihmuller FB, Marshall JF (1993) Methamphetamine-induced dopamine overflow and injury to striatal dopamine terminals: attenuation by dopamine D1 or D2 antagonists. J Neurochem 60: 1792-1799.

Ohmori T, Abekawa T, Koyama T (1996) The role of glutamate in the neurotoxic effects of methamphetamine. Ann N Y Acad Sci 801: 315-326.

Okamoto H, Meng W, Ma J, Ayata C, Roman RJ, Bosnjak ZJ, Kampine JP, Huang PL, Moskowitz MA, Hudetz AG (1997) Isoflurane-induced cerebral hyperemia in neuronal nitric oxide synthase gene deficient mice. Anesthesiology 86: 875-884.

Olney JW (1969) Brain lesions, obesity and other disturbances in mice treated with monosodium glutamate. Science 164: 719-721.

Olney JW (1978) Neurotoxicity of excitatory amino acids. In: Kainic Acid as a Tool in Neurobiology (McGeer EG, Olney JW, McGeer PL, eds), pp 95-121. New York: Raven Press.

Olney JW (1994) Excitatory neurotransmitter neurotoxicity. Neurobiol Aging 15: 259-260.

Oswald I, Thacore VR (1963) Amphetamine and phenmetrazine addiction. Physiological abnormalities in the abstinence syndrome. Br Med J 2: 427.

Palmer RM, Moncada S (1989) A novel citrulline-forming enzyme implicated in the formation of nitric oxide by vascular endothelial cells. Biochemical & Biophysical Research Communications 158: 348-352.

Pannese E (1994) The neuroglial cell of the central nervous system. In: Neurocytology: Fine sturcture of neurons, nerve processes, and neuroglial cells (Pannese E, ed), pp 169-179. New York: Thieme Medical Publishers, Inc.

Park SK, Grzybicki D, Lin HL, Murphy S (1994) Modulation of inducible nitric oxide synthase expression in astroglial cells. Neuropharmacology 33: 1419-1423.

Pauli D, Tonka CH, Tissueres A, Arrigo AP (1990) Tissue-specific expression of heat shock protein HSP27 during *Drosophila melanogaster* development. Cell Biol 111: 817.

Peat MA, Warren PF, Bakhit C, Gibb JW (1985) The acute effects of methamphetamine, amphetamine and p-chloroamphetamine on the cortical serotonergic system of the rat brain: evidence for differences in the effects of methamphetamine and amphetamine. Eur J Pharmacol 116: 11-16.

Pelton EW, Kimelberg HK, Shipherd SV, Bourke RS (1981) Dopamine and norepinephrine uptake and metabolism by astroglial cells in cultures. Life Sci 28: 1655-1663.

Pontieri FE, Crane AM, Seiden LS, Kleven MS, Porrino LJ (1990) Metabolic mapping of the effects of intravenous methamphetamine administration in freely moving rats. Psychopharmacology (Berl ) 102: 175-182.

Pope A (1978) Dynamic properties of glial cells. In: Neuroglia: Quantataive aspects (Schoffeniels G, Franck L, Hertz L, Tower DB, eds), pp 13-20. London: Pergamon Press.

Porreca E, Reale M, Di Febbo C, Di Gioacchino M, Barbacane RC, Castellani ML, Baccante G, Conti P, Cuccurullo F (1996) Down-regulation of cyclooxygenase-2 (COX-2) by interleukin-1 receptor antagonist in human monocytes. Immunol 89: 424-429.

Porter JT, McCarthy KD (1997) Astrocytic neurotransmitter receptors in situ and in vivo. Prog Neurobiol 51: 439-455.

Prehn JH, Bindokas VP, Marcuccilli CJ, Krajewski S, Reed JC, Miller RJ (1994) Regulation of neuronal Bcl2 protein expression and calcium homeostasis by transforming growth factor type beta confers wide-ranging protection on rat hippocampal neurons. Proc Natl Acad Sci U S A 91: 12599-12603.

Preiser JC, Reper P, Vlasselaer D, Vray B, Zhang H, Metz G, Vanderkelen A, Vincent JL (1996) Nitric oxide production is increased in patients after burn injury. Journal of Trauma 40: 368-371.

Preston KL, Wagner GC, Schuster CR, Seiden LS (1985) Long-term effects of repeated methylamphetamine administration on monoamine neurons in the rhesus monkey brain. Brain Res 338: 243-248.

Prochiantz A, Mallat M (1988) Astrocyte diversity. Ann N Y Acad Sci 540: 52-63.

Pu C, Fisher JE, Cappon GD, Vorhees CV (1994) The effects of amfonelic acid, a dopamine uptake inhibitor, on methamphetamine- induced dopaminergic terminal degeneration and astrocytic response in rat striatum. Brain Res 649: 217-224.

Pu C, Vorhees CV (1993) Developmental dissociation of methamphetamine-induced depletion of dopaminergic terminals and astrocyte reaction in rat striatum. Brain Res Dev Brain Res 72: 325-328.

Pu C, Vorhees CV (1995) Protective effects of MK-801 on methamphetamine-induced depletion of dopaminergic and serotonergic terminals and striatal astrocytic response: an immunohistochemical study. Synapse 19: 97-104.

Raddassi K, Petit JF, Lemaire G (1993) LPS-induced activation of primed murine peritoneal macrophages is modulated by prostaglandins and cyclic nucleotides. Cell Immunol 149: 50-64.

Radi R, Beckman JS, Bush KM, Freeman BA (1991) Peroxynitrite-induced membrane lipid peroxidation: the cytotoxic potential of superoxide and nitric oxide. Arch Biochem Biophys 288: 481-487.

Raps SP, Lai JC, Hertz L, Cooper AJ (1989) Glutathione is present in high concentrations in cultured astrocytes but not in cultured neurons. Brain Res 493: 398-401.

Reier PJ (1986) Gliosis following CNS injury: the anatomy of astrocytic scars and their influences in axonal elongation. In: Astrocytes: Cell Biology and Pathology of Astrocytes (Fedoroff S, Vernadakis A, eds), pp 263-324. New York: Academic Press.

Reier PJ, Stensaas LJ, Guth L (1983) The astrocytic scar as an impediment to regeneration in the central nervous system. In: Spinal Cord Reconstruction (Kao CC, Budge RP, Reier PJ, eds), pp 163-196. New York: Raven Press.

Reif DW, Simmons RD (1990) Nitric oxide mediates iron release from ferritin. Arch Biochem Biophys 283: 537-541.

Reiter R, Tang L, Garcia JJ, Munoz-Hoyos A (1997) Pharmacological actions of melatonin in oxygen radical pathophysiology. Life Sci 60: 2255-2271.

Ricaurte GA, Guillery RW, Seiden LS, Schuster CR (1984b) Nerve terminal degeneration after a single injection of d-amphetamine in iprindole-treated rats: Relation to selective long-lasting dopamine depletion. Brain Res 291: 378-382.

Ricaurte GA, Guillery RW, Seiden LS, Schuster CR, Moore RY (1982) Dopamine nerve terminal degeneration produced by high doses of methylamphetamine in the rat brain. Brain Res 235: 93-103.

Ricaurte GA, Seiden LS, Schuster CR (1984a) Further evidence that amphetamines produce long-lasting dopamine neurochemical deficits by destroying dopamine nerve fibers. Brain Res 303: 359-364.

Richter C, Schlegel J (1993) Mitochondrial calcium release induced by prooxidants. Toxicol Lett 67: 119-127.

Rothman SM, Olney JW (1987) Excitotoxicity and the NMDA receptor. Trends Neurosci 10: 299-302.

Rothman SM, Olney JW (1995) Excitotoxicity and the NMDA receptor - Still lethal after eight years. Trends Neurosci 18: 57-58.

Rothwell NJ (1992) Eicosanoids, thermogenesis and thermoregulation. Prostaglandins Leukot Essent Fatty Acids 46: 1-7.

Salgo MG, Bermudez E, Squadrito GL, Pryor WA (1995) Peroxynitrite causes DNA damage and oxidation of thiols in rat thymocytes [corrected] [published erratum appears in Arch Biochem Biophys 1995 Dec 1;324(1):200]. Arch Biochem Biophys 322: 500-505.

Salvemini D, Masferrer JL (1996) Interactions of nitric oxide with cyclooxygenase: in vitro, ex vivo, and in vivo studies. Methods Enzymol 269: 12-25.

Sarge KD, Morimoto RI (1991) Surprising features of transcriptional regulation of heat shock genes. Gene Expr 1: 169-173.

Sarge KD, Murphy SP, Morimoto RI (1993) Activation of heat shock gene transcription by heat shock factor 1 involves oligomerization, acquisition of DNA-binding activity, and nuclear localization and can occur in the absence of stress [published errata appear in Mol Cell Biol 1993 May;13(5):3122-3 and 1993 Jun;13(6):3838-9]. Mol Cell Biol 13: 1392-1407.

Sasaki K, Suda H, Watanabe H, Kaneko S, Nomura Y, Nishino H, Ono T (1988) Habenular lesion attenuates methamphetamine-induced inhibition of dopamine neuronal activity in the substantia nigra pars compacta of rats. Neurosci Lett 86: 67-71.

Scarpino V, Arrigo A, Benzi G (1990) Evaluation and prevalence of "doping" among Italian athletes. Lancet 336: 399.

Schipper HM, Cisse S, Stopa EG (1995) Expression of heme oxygenase-1 in the senescent and Alzheimer-diseased brain. Ann Neurol 37: 758-768.

Schipper HM, Liberman A, Stopa EG (1998) Neural heme oxygenase-1 expression in idiopathic Parkinson's disease. Exp Neurol 150: 60-68.

Schmidt HH, Kelm M (1996) Determination of nitrite and nitrate by the Griess reaction. In: Methods in Nitric Oxide Research (Feelisch M, Stamler JS, eds), pp 491-497. Chichester: John Wiley & Sons.

Schousboe A (1981) Transport and metabolism of glutamate and GABA in neurons and glial cells. Int Rev Neurobiol 22: 1-45.

Schousboe A, Westergaard N, Sonnewald U, Petersen SB, Huang R, Peng L, Hertz L (1993) Glutamate and glutamine metabolism and compartmentation in astrocytes. Dev Neurosci 15: 359-366.

Seiden LS, Commins DL, Vosmer G, Axt K, Marek G (1988) Neurotoxicity in dopamine and 5-hydroxytryptamine terminal fields: a regional analysis in nigrostriatal and mesolimbic projections. Ann N Y Acad Sci 537: 161-172.

Seiden LS, Fischman MW, Schuster CR (1975) Changes in brain catecholamines induced by long-term methamphetamine administration in rhesus monkeys. In: Cocaine and other stimulants (Ellinwood EHJ, Kilbey MM, eds), pp 179-185. New York: Plenum Press.

Seiden LS, Fischman MW, Schuster CR (1976) Long-term methamphetamine induced changes in brain catecholamines in tolerant rhesus monkeys. Drug Alcohol Depend 1: 215-219.

Seiden LS, Vosmer G (1984) Formation of 6-hydroxydopamine in caudate nucleus of the rat brain after a single large dose of methylamphetamine. Pharmacol Biochem Behav 21: 29-31.

Sekine H, Nakahara Y (1987) Abuse of smoking methamphetamine mixed with tobacco: I. Inhalation efficiency and pyrolysis products of methamphetamine. J Forensic Sci 32: 1271-1280.

Semenoff D, Kimelberg HK (1985) Autoradiography of high affinity uptake of catecholamines by primary astrocyte cultures. Brain Res 1985 Nov 25 348: 125-136.

Seregi A, Keller M, Hertting G (1987) Are cerebral prostanoids of astroglial origin? Studies on the prostanoid forming system in developing rat brain and primary cultures of rat astrocytes. Brain Res 404: 113-120.

Sessa WC, Harrison JK, Barber CM, Zeng D, Durieux ME, D'Angelo DD, Lynch KR, Peach MJ (1992) Molecular cloning and expression of a cDNA encoding endothelial cell nitric oxide synthase. J Biol Chem 267: 15274-15276.

Sharma HS, Olsson Y, Persson S, Nyberg F (1995) Trauma-induced opening of the blood-spinal cord barrier is reduced by indomethacin, an inhibitor of prostaglandin biosynthesis. Experimental observations in the rat using [$^{131}$I]-sodium, evans blue and lanthanum as tracers. Neurol Neurosci 7: 207-215.

Sharma HS, Westman J, Alm P, Sjoquist PO, Cervos-Navarro J, Nyberg F (1997) Involvement of nitric oxide in the pathophysiology of acute heat stress in the rat. Influence of a new antioxidant compound H-290/51. Ann N Y Acad Sci 813:581-90: 581-590.

Sharma HS, Westman J, Nyberg F, Cervós-Navarro J, Dey PK (1994) Role of serotonin and prostaglandins in brain edema induced by heat stress. An experimental study in the rat. Acta Neurochir (Wien) Suppl. 60: 65-70.

Shaw PJ (1994) Excitotoxicity and motor neurone disease: A review of the evidence. J Neurol Sci 124: Suppl 6-13.

Sheng P, Cerruti C, Ali S, Cadet JL (1996) Nitric oxide is a mediator of methamphetamine (METH)-induced neurotoxicity. In vitro evidence from primary cultures of mesencephalic cells. Ann N Y Acad Sci 801: 174-186.

Sheng P, Cerruti C, Cadet JL (1994) Methamphetamine (METH) causes reactive gliosis in vitro: attenuation by the ADP- ribosylation (ADPR) inhibitor, benzamide. Life Sci 55: L51-L54.

Shibahara S, Muller RM, Taguchi H (1987) Transcriptional control of rat heme oxygenase by heat shock. J Biol Chem 262: 12889-12892.

Simonian NA, Coyle JT (1996) Oxidative stress in neurodegenerative diseases. Annu Rev Pharmacol Toxicol 36:83-106: 83-106.

Sinet PM, Heikkila RE, Cohen G (1980) Hydrogen peroxide production by rat brain in vivo. J Neurochem 34: 1421-1428.

Slivka A, Mytilineou C, Cohen G (1987) Histochemical evaluation of glutathione in brain. Brain Res 409: 275-284.

Sminia P, Van dZ, Wondergem J, Haveman J (1994) Effect of hyperthermia on the central nervous system: a review. Int J Hyperthermia 10: 1-30.

Smith CD, Carney JM, Starke-Reed PE, Oliver CN, Stadtman ER, Floyd RA, Markesbery WR (1991) Excess brain protein oxidation and enzyme dysfunction in normal aging and in Alzheimer disease. Proc Natl Acad Sci U S A 88: 10540-10543.

Smith EF, Kinter LB, Jugus M, Eckardt RD, Newton JF (1989) Concentration-dependent, stereoselective inhibition of the endotoxin- induced hemoconcentration in conscious rats with the peptidoleukotriene receptor antagonist SK & F 104353. Eicosanoids 2: 101-107.

Smith WL, Garavito RM, DeWitt DL (1996) Prostaglandin endoperoxide H synthases (cyclooxygenases)-1 and -2. J Biol Chem 271: 33157-33160.

Snyder SH (1986) Drugs and the Brain. New York: Scientific American Library.

Sonsalla PK, Albers DS, Zeevalk GD (1998) Role of glutamate in neurodegeneration of dopamine neurons in several animal models of parkinsonism. Amino Acids 14: 69-74.

Sonsalla PK, Nicklas WJ, Heikkila RE (1989) Role for excitatory amino acids in methamphetamine-induced nigrostriatal dopaminergic toxicity. Science 243: 398-400.

Sonsalla PK, Riordan DE, Heikkila RE (1991) Competitive and noncompetitive antagonists at N-methyl-D-aspartate receptors protect against methamphetamine-induced dopaminergic damage in mice. J Pharmacol Exp Ther 256: 506-512.

Sorger PK (1991) Heat shock factor and the heat shock response. Cell 65: 363-366.

Stadlin A, Lau JW, Szeto YK (1998) A selective regional response of cultured astrocytes to methamphetamine. Ann N Y Acad Sci 844: 108-121.

Steranka LR, Sanders-Bush E (1980) Long-term effects of continuous exposure to amphetamine on brain dopamine concentration and synaptosomal uptake in mice. Eur J Pharmacol 65: 439-443.

Stern GM (1995) Parkinson's disease: the apoptosis hypothesis. In: Advance in Neurology: Parkinson's Disease (Battistin L, Scarlato G, Caraceni T, Ruggieri S, eds), pp 101-110. Pheladephia: Lippincott-Raven.

Stuehr DJ, Cho HJ, Kwon NS, Weise MF, Nathan CF (1991) Purification and characterization of the cytokine-induced macrophage nitric oxide synthase: an FAD- and FMN-containing flavoprotein. Proc Natl Acad Sci U S A 88: 7773-7777.

Sugiyama K, Brunori A, Mayer ML (1989) Glial uptake of excitatory amino acids influences neuronal survival in cultures of mouse hippocampus. Neuroscience 32: 779-791.

Sulzer D, Pothos E, Sung HM, Maidment NT, Hoebel BG, Rayport S (1992) Weak base model of amphetamine action. Ann N Y Acad Sci 654: 525-528.

Sulzer D, Rayport S (1990) Amphetamine and other psychostimulants reduce pH gradients in midbrain dopaminergic neurons and chromaffin granules: a mechanism of action. Neuron 5: 797-808.

Suri C, Fung BP, Tischler AS, Chikaraishi DM (1993) Catecholaminergic cell lines from the brain and adrenal glands of tyrosine hydroxylase - SV40 T antigen transgenic mice. J Neurosci 13: 1280-1291.

Swierkosz TA, Mitchell JA, Warner TD, Botting RM, Vane JR (1995) Co-induction of nitric oxide synthase and cyclo-oxygenase: interactions between nitric oxide and prostanoids. Br J Pharmacol 114: 1335-1342.

Sylvia AL, LaManna JC, Rosenthal M, Jobbis FF (1977) Metabolite studies of methamphetamine effects based upon mitochondrial respiratiory state in rat brain. J Pharmacol Exp Ther 201: 117-125.

Szabo C, Zingarelli B, O'Connor M, Salzman AL (1996) DNA strand breakage, activation of poly (ADP-ribose) synthetase, and cellular energy depletion are involved in the cytotoxicity of macrophages and smooth muscle cells exposed to peroxynitrite. Proc Natl Acad Sci U S A 93: 1753-1758.

Takahashi K, Hara E, Suzuki H, Sasano H, Shibahara S (1996) Expression of heme oxygenase isozyme mRNAs in the human brain and induction of heme oxygenase-1 by nitric oxide donors. J Neurochem 67: 482-489.

Taraska T, Finnegan KT (1997) Nitric oxide and the neurotoxic effects of methamphetamine and 3,4-methylenedioxymethamphetamine. Journal of Pharmacology & Experimental Therapeutics 280: 941-947.

Trocino RA, Akazawa S, Ishibashi M, Matsumoto K, Matsuo H, Yamamoto H, Goto S, Urata Y, Kondo T, Nagataki S (1995) Significance of glutathione depletion and oxidative stress in early embryogenesis in glucose-induced rat embryo culture. Diabetes 44: 992-998.

Tsujimoto Y, Finger LR, Yunis J, Nowell PC, Croce CM (1984) Cloning of the chromosome breakpoint of neoplastic B cells with the t(14;18) chromosome translocation. Science 226: 1097-1099.

Turrens JF, Boveris A (1980) Generation of superoxide anion by the NADH-dehydrogenase of bovine heart mitochondria. Biochem J 191: 421-427.

Vane JR, Bakhle YS, Botting RM (1998) Cyclooxygenases 1 and 2. Annu Rev Pharmacol Toxicol 38: 97-120.

Vass K, Welch WJ, Nowak TSJ (1988) Localization of 70-kDa stress protein induction in gerbil brain after ischemia. Acta Neuropathol 77: 128.

Villemagne V, Yuan J, Wong DF, Dannals RF, Hatzidimitriou G, Mathews WB, Ravert HT, Musachio J, McCann UD, Ricaurte GA (1998) Brain dopamine neurotoxicity in baboons treated with doses of methamphetamine comparable to those recreationally abused by humans: evidence from [11C] WIN-35,428 positron emission tomography studies and direct in vitro determinations. J Neurosci 18: 419-427.

Vincent SR, Das S, Maines MD (1994) Brain heme oxygenase isoenzymes and nitric oxide synthase are co-localized in select neurons. Neuroscience 63: 223-231.

Wagner AJ, Kokontis JM, Hay N (1994) Myc-mediated apoptosis requires wild-type p53 in a manner independent of cell cycle arrest and the ability of p53 to induce p21waf1/cip1. Genes Dev 8: 2817-2830.

Wagner GC, Carelli RM, Jarvis MF (1985) Pretreatment with ascorbic acid attenuates the neurotoxic effects of methamphetamine in rats. Res Commun Chem Pathol Pharmacol 47: 221-228.

Wagner GC, Ricaurte GA, Seiden LS, Schuster CR, Miller RJ, Westley J (1980) Long-lasting depletions of striatal dopamine and loss of dopamine uptake sites following repeated administration of methamphetamine. Brain Res 181: 151-160.

Walicke P, Varon S, Manthrope M (1986) Purification of a human red blood cell protein supporting the survival of cultured CNS neurons, and its identification as catalase. J Neurosci 6: 1114-1121.

Wallace DC (1992) Diseases of the mitochondrial DNA. Annu Rev Biochem 61: 1175-1212.

Walsh D, Li K, Wass J, Dolnikov A, Zeng F, Zhe L, Edwards M (1993) Heat-shock gene expression and cell cycle changes during mammalian embryonic development. Dev Genet 14: 127-136.

Walsh DA, Li K, Speirs J, Crowther CE, Edwards MJ (1989) Regulation of the inducible heat shock 71 genes in early neural development of cultured rat embryos. Teratology 40: 321-334.

Walz W (1989) Role of glail cells in the regulation of hte brain ion microenvironment. Prog Neurobiol 33: 309-333.

Watkins JC, Evans RH (1981) Excitatory amino acid transmitters. Annu Rev Pharmacol Toxicol 21: 165-204.

Welch WJ (1992) Mammalian stress response: cell physiology, structure/function of stress proteins, and implications for medicine and disease. Physiol Rev 72: 1063-1081.

Westman J, Sharma HS (1999) Heat shock protein response in central nervous system following hyperthermia. Prog Brain Res 115: 207-240.

Whitaker-Azmitia PM, Murphy R, Azmitia EC (1990) Stimulation of astroglial 5-HT1A receptors releases the serotonergic growth factor, protein S-100, and alters astroglial morphology. Brain Res 528: 155-158.

Wilkin GP, Marriott DR (1993) Biochemical responses of astrocytes to neuroprotective peptides. In: Astrocytes: Pharmacology and Function (Murphy S, ed), pp 67-87. San Diego: Academic Press.

Wilson JM, Kalasinsky KS, Levey AI, Bergeron C, Reiber G, Anthony RM, Schmunk GA, Shannak K, Haycock JW, Kish SJ (1996) Striatal dopamine nerve terminal markers in human, chronic methamphetamine users. Nat Med 2: 699-703.

Winger G, Hoffmann FG, Woods JH (1992) Central Nervous System Stimulants: Amphetamines, Caffeine, and Related Drugs. In: A Handbook on Drug and Alcohol Abuse: The Biomedical Aspects pp 132-140. New York: Oxford University Press.

Wrona MZ, Yang Z, McAdams M, O'Connor-Coates S, Dryhurst G (1995) Hydroxyl radical-mediated oxidation of serotonin: potential insights into the neurotoxicity of methamphetamine. J Neurochem 64: 1390-1400.

Xue ZY, Grossfeld RM (1993) Stress protein synthesis and accumulation after traumatic injury of crayfish CNS. Neurochem Res 18: 209-218.

Yamada S, Yokoo H, Nishi S (1994) Effects of N-ethylmaleimide on dopamine release in the rat striatum after repeated treatment with methamphetamine. Eur J Pharmacol 257: 243-248.

Yamagata K, Andreasson KI, Kaufmann WE, Barnes CA, Worley PF (1993) Expression of a mitogen-inducible cyclooxygenase in brain neurons: regulation by synaptic activity and glucocorticoids. Neuron 11: 371-386.

Yamamoto BK, Zhu W (1998) The effects of methamphetamine on the production of free radicals and oxidative stress. J Pharmacol Exp Ther 287: 107-114.

Yang Z, Wrona MZ, Dryhurst G (1997) 5-hydroxy-3-ethylamino-2-oxindole is not formed in rat brain following a neurotoxic dose of methamphetamine: evidence that methamphetamine does not induce the hydroxyl radical-mediated oxidation of serotonin. J Neurochem 68: 1929-1941.

Yonetani T, Yamamoto H, Erman JE, Leigh JSJ, Reed GH (1972) Electromagnetic properties of hemoproteins: Optical and electron paramagnetic resonance characteristics of nitric oxide derivatives of metalloporphyrin-apohemoprotein complexes. J Biol Chem 247: 2447-2455.

Yu X, Imam SZ, Newport GD, Slikker W, Jr., Ali SF (1999) Ibogaine blocked methamphetamine-induced hyperthermia and induction of heat shock protein in mice. Brain Res 823: 213-216.

Yui Y, Hattori R, Kosuga K, Eizawa H, Hiki K, Kawai C (1991) Purification of nitric oxide synthase from rat macrophages. J Biol Chem 266: 12544-12547.

Zakhary R, Miller JAJ, Miller FS (1967) Hypothermia, asphyxia and brain carbohydrates in newborn puppies. Biol Neonat 11: 36-49.

Zalis EG, Lundberg GD, Knutson RA (1967) The pathophysiology of acute amphetamine poisoning with pathologic correlation. J Pharmacol Exp Ther 158: 115-127.

Zalis EG, Parmley LF (1963) Fatal amphetamine poisoning. Arch Intern Med 112: 822.

Zhang Y, Marcillat O, Giulivi C, Ernster L, Davies KJ (1990) The oxidative inactivation of mitochondrial electron transport chain components and ATPase. J Biol Chem 265: 16330-16336.